Signaling and Feedback Networks Underlying Senstivity and Resistance to Kinase Inhibitors in Oncogene Addicted Cancers

Dr. Jeffrey A. Engelman   Alexa Betzig Schrock

Signaling and Feedback Networks Underlying
Sensitivity and Resistance to Kinase Inhibitors in
Oncogene Addicted Cancers

Abstract

Targeted therapies have begun to be developed and approved in the clinic

over the past several decades to treat cancers with specific genetic alterations. In

non-small cell lung cancer (NSCLC), patients harboring *EGFR* activating mutations

often respond to the EGFR inhibitors gefitinib/erlotinib, exhibiting down-regulation of

central oncogenic pathways and dramatic tumor regressions. Despite initially

promising results, the vast majority of patients develop resistance to targeted

therapies. Thus far, several mechanisms of resistance including T790M mutation in

EGFR, amplification of the MET receptor tyrosine kinase (RTK), activating mutations

in downstream signaling molecules, and loss of negative regulators have been

identified. As a result, next generation inhibitors and combination therapies continue

to be developed and tested in the clinic.

There are still many cases in which the cause of resistance to a particular

targeted therapy is unknown, or the subset of patients most likely to benefit has not

been identified. This thesis describes the ability of the MET ligand, HGF, to activate

PI3K signaling and cause gefitinib resistance in EGFR-driven cancers. In addition,

detection of a preexisting subpopulation of *MET* amplified cells (present before

treatment with an EGFR inhibitor) is shown to successfully predict the development

of *MET* amplification as a resistance mechanism. These results suggest that it may

be possible to prospectively identify patients who will benefit from combined

MET/HGF and EGFR inhibitors as initial therapies. Further, this thesis highlights the

importance of both PI3K/AKT and MEK/ERK signaling as drivers of cell proliferation and viability, and describes a novel feedback network regulating these pathways. In multiple cancer models, treatment with a single agent MEK inhibitor leads to feedback up-regulation of ERBB3/PI3K/AKT signaling. The mechanism for this feedback involves loss of an inhibitory threonine phosphorylation in the conserved juxtamembrane domains of EGFR and HER2 following MEK inhibition, which leads to increased ERBB receptor activation. These results further elucidate the complex feedback networks that regulate signaling in cancer cells, and suggest possible limitations for the efficacy of single agent RAF/MEK pathway inhibitors. Collectively, this work describes multiple resistance mechanisms to kinase inhibitors, and suggests new biomarkers to define those patients who are likely to benefit from specific targeted therapies.

Table of Contents

List of Tables and Figures

Chapter 5

Dedication

I dedicate this thesis to my parents. They have advised me, inspired me, challenged me, and most importantly given me constant and unconditional love and encouragement. Without them I would not be where I am today, and I will forever be extremely grateful for everything they have done for me.

Acknowledgements

Jeffrey Engelman has been an excellent mentor and scientific advisor. I thank him for his encouragement, ideas, and advice; as well as his inspiration and support over the past several years. Without Jeff, my work would not have been nearly as exciting, successful, or enjoyable. It has been a wonderful opportunity to have been able to work with him, and I am extremely grateful.

I would also like to thank the members of my advisory committee, Pasi Jänne, Lewis Cantley, Jeffrey Settleman and David Fisher. Together with Jeff Engelman, Pasi and Lew published the *Science* paper that helped make my decision to come to Harvard for graduate school and ultimately to work with Jeff. My committee members have also made many of the seminal discoveries that laid the framework for this thesis, and they have continued to provide me with helpful guidance over the past several years.

All of the members of the Engelman Lab have contributed to my progress and have made positive impressions on me as a scientist and as a person. Tony Faber has been my colleague, ally, co-conspirator and friend since my first day in the Engelman Lab, and I may not have made it through without his humor and support. I am also very grateful to Tony for his scientific observations concerning the effects of MEK inhibition on AKT signaling, which launched my feedback project, and for his work on the H1975 resistant cell line model, which he allowed me to use to develop the EMT story. Youngchul Song has provided an enormous amount of technical assistance, and I thank Young sincerely for his constant help and positive attitude. I am grateful to Eugene Lifshits for invaluable technical assistance with mouse experiments, and for making sure I made time for lunch as often as possible. I am also grateful to Adam Crystal for his enthusiasm, which is often contagious, and to all of our clinical fellows for helpful discussions, both scientific and otherwise. I would

Chapter 1- Background

1.1 History of Cancer

Cancer is a disease characterized by abnormal growth of cells in the body. These malignant cells exhibit uncontrolled proliferation and resistance to cell death signals, and are capable of invasion and metastasis. There are hundreds of cancer types listed by the National Cancer Institute, traditionally characterized by the location in the body where the primary malignancy originated. In the past decade cancer has surpassed heart disease as the leading cause of death in the United States (Jemal et al., 2010). In 2010 there were approximately 1.5 million new cases of cancer diagnosed in the United States and over 500,000 deaths. Of these, lung cancer is by far the leading cause of cancer death in both men and women (Jemal et al., 2010).

In approximately 2500 BC, an Egyptian physician gave the first known description of cancer, writing of a patient with "bulging tumors of the breast…swellings on the breast, large, spreading and hard". Under a section titled "Therapy", the physician wrote, "There is none". Two thousand years later in 400 BC, the first word for cancer, karkinos (the Greek word for "crab") appeared in the medical literature. These early cancers were mostly large superficial tumors and were initially treated with crude surgical techniques often leading to massive infections. During this period Hippocrates noted that cancer was "best left untreated, since patients live longer that way" (Mukherjee, 2010).

Unfortunately, unlike other widespread diseases including heart disease, progress in the development of effective cancer therapies has thus far been markedly slow. In many cases, particularly if the disease is not detected early, the long-term prognosis remains poor. Current therapies typically offer only short-term remissions, and these treatments are commonly associated with significant side

effects. Just in the last few decades have we begun to understand cancer at the genetic level. We have started to develop promising therapies that target these genetic lesions, which demonstrate improved specificity and less toxicity, and we are moving in the direction of personalized cancer medicine.

1.2 Evolution of Cancer Therapies

Surgical removal of cancerous tumors was the first treatment developed in an attempt to cure patients of this disease, and it has remained one of the most effective cancer therapies, particularly for localized solid tumors. However, for non-solid tumors or in cases where the cancer has already metastasized or is difficult to remove, surgery is relatively ineffective.   In the late 19th century, cancer researchers discovered the ability of X-rays to selectively kill rapidly dividing cells and began to test radiation therapies in cancer patients. Today radiation is also still used in the clinic, despite toxic side effects. In 1948 Sidney Farber treated children with acute lymphoblastic leukemia with derivatives of a new drug compound called an antifolate, a chemical that blocks the growth of white blood cells, and achieved the first cancer remissions in response to a chemotherapeutic (Farber and Diamond, 1948). At the same time, scientists began using DNA damaging agents, initially designed as war gasses, to target and destroy rapidly dividing cancer cells. Successful trials using multiple combinations of new chemotherapeutics continued into the 1950s, and in fact, several of these drugs are still used as the standard of care for cancer patients today. However, these therapies are often incredibly toxic, and some patients are forced to withdraw from treatment due to the severity of the side effects (Mukherjee, 2010).

In addition to the discovery of radiation and chemotherapy, significant progress has also been made in terms of cancer prevention. Numerous clinical trials

have been carried out over the past century to identify environmental causes of cancer. In 1948 two independent groups reached the same clear conclusion following from their respective trials: cigarette smokers are significantly more likely to develop lung cancer (Doll and Hill, 1950; Wynder and Graham, 1950). In the following decades, these studies were repeated on larger scales and eventually led to increased public awareness of smoking-associated cancer risk. Today, these efforts are finally contributing to a decreased incidence of lung cancer in men and similar trends are projected to follow in women (Jemal et al., 2010).

We began to understand the biology and signaling within the cancer cell in the late 20th century. In the 1970s, Michael Bishop and Harold Varmus at UCSF began to look for variations of the viral oncogene *v-src* in normal cells (Stehelin et al., 1976), and in 1989 they won the Nobel Prize for their discovery of the cellular origin of retroviral oncogenes. Soon after the characterization of *src*, the *ras* oncogene was discovered in the Weinberg laboratory in Cambridge, MA and the results were published with two other groups in 1982 (Der et al., 1982; Parada et al., 1982; Shih and Weinberg, 1982). These seminal discoveries provided the first real understanding of the proteins and pathways that are often deregulated in cancer, and lead to the identification of new cellular targets.

Once specific oncogenes began to be identified, pharmaceutical companies started to develop drugs that could inhibit these proteins directly, thus targeting the growth and proliferation of cancer cells much more specifically while causing relatively few off-target effects in normal tissues. The first targeted cancer therapy was developed at Genentech in collaboration with Dennis Slamon, an oncologist at UCSF. Herceptin (Trastuzumab) is a humanized monoclonal antibody against the HER2 receptor tyrosine kinase, which is amplified in a subset of breast cancers (Bazell, 1998). Trials using this new targeted therapy were first performed in breast

3

cancer patients (with tumors expressing high levels of *HER2*) in the early 1990s with very promising results. The first tyrosine kinase inhibitor (TKI), imatinib (Gleevec), was developed by Novartis in collaboration with Brian Druker and Charles Sawyers to target the hyper-activated BCR-ABL fusion protein, as well as c-KIT and PDGFR kinases. Gleevec gained FDA approval in 2001 for treatment of patients with chronic myelogenous leukemia (CML) and gastrointestinal stromal tumors (GIST), and remains one of the greatest success stories for targeted cancer therapy (Demetri et al., 2002; Druker et al., 2001). Over the past twenty years, dozens of new targeted therapies, including monoclonal antibodies and small molecule kinase inhibitors, have been developed and tested in the clinic. However, there are still many cancers in which the target or targets driving oncogenesis are unidentified, or in which there are currently no effective drugs available to block the target. Furthermore, numerous challenges involving specificity, drug delivery and pharmacokinetics, and drug resistance remain unsolved.

1.3 The PI3K/AKT and RAF/MEK/ERK Signaling Pathways

The phosphatidylinositol 3-kinase (PI3K) and RAF/MEK/ERK mitogen-activated protein kinase (MAPK) signaling pathways have been identified as central oncogenic drivers in a wide range of cancers. These signaling cascades are made up of kinases, enzymes that transfer phosphate groups from high-energy donors such as ATP to specific substrates, and converge on downstream effectors that regulate apoptosis, cell growth, metabolism, proliferation, and metastasis.

Upstream of both the PI3K/AKT and RAF/MEK/ERK signaling pathways are trans-membrane receptor tyrosine kinases (RTKs), which receive extra-cellular signals and transmit these signals into the cell, activating downstream pathways through phosphorylation cascades. The ERBB family of receptors is comprised of

four members; EGFR (ERBB1), HER2 (ERBB2, neu), HER3 (ERBB3), and HER4 (ERBB4) (Zhang et al., 2007) (Figure 1). Each of these receptors, with the exception of HER2, binds extracellular ligands and undergoes a conformational change to form asymmetric dimers. Within these active dimers, the kinase domain of one of the receptors trans- and auto-phosphorylates tyrosine residues on the C-terminal tails of both receptors. Adaptors and signaling molecules are then recruited to bind these phosphorylated tyrosine residues, leading to activation of downstream pathways. The ERBB3 receptor is unique in that it is kinase-dead and serves only as an inactive binding partner for other RTKs; however, ERBB3 contains several PI3K binding sites and is commonly used as an adaptor to directly activate PI3K/AKT signaling (Engelman et al., 2005).
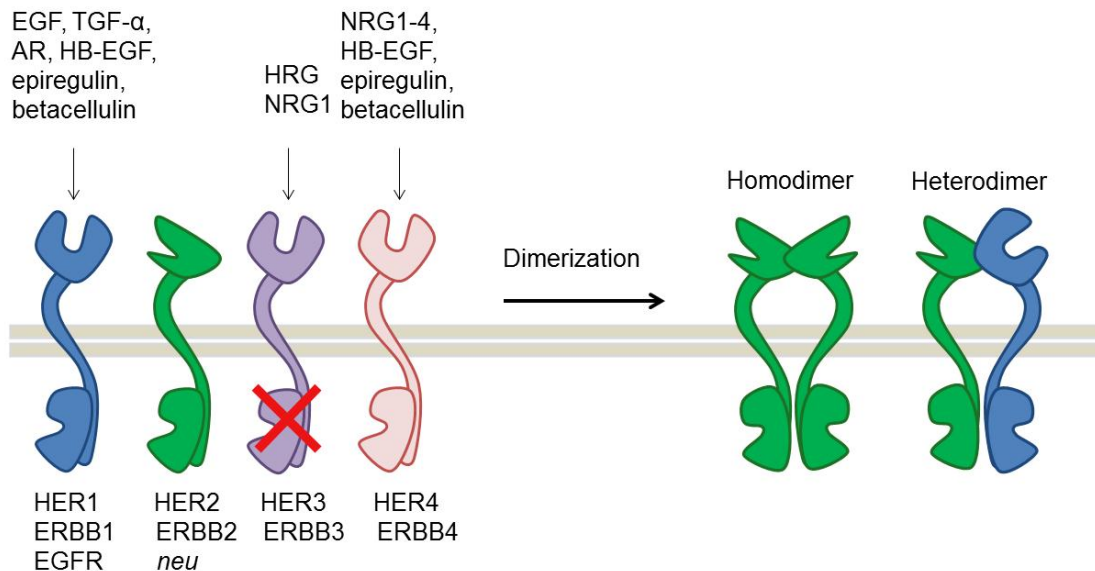
Figure 1. The ERBB family of receptors. The ERBB family is made up of four receptor tyrosine kinases (RTKs). ERBB2 (HER2) is the only receptor that does not bind a ligand, and ERBB3 is kinase dead. Upon dimerization receptors become activated. Adapted from Zhang, H et al., *JCI* 2007.

5

The PI3K pathway has been shown in the laboratory and in the clinic to be critical for the viability of many cancers (Cantley, 2002; Engelman, 2009; Lee et al., 2007). The class I phosphoinositide 3-kinase (PI3K) is a heterodimer composed of a p110α catalytic subunit and a p85 regulatory subunit. In unstimulated cells, PI3K exists in the cytoplasm in an inactive conformation. However, when receptors or adaptor proteins become activated, two p85 Src homology 2 (SH2) domains bind to phosphorylated tyrosine residues at the cell membrane. As a result, PI3K is recruited to the cell membrane and p110α is released from p85 inhibition, allowing for the phosphorylation of the membrane lipid phosphatidylinositol 4,5-bisphosphate (PIP_2) to produce phosphatidylinositol 3,4,5-trisphosphate (PIP_3) (Figure 2). This leads to the recruitment and activation of several downstream signaling effectors,
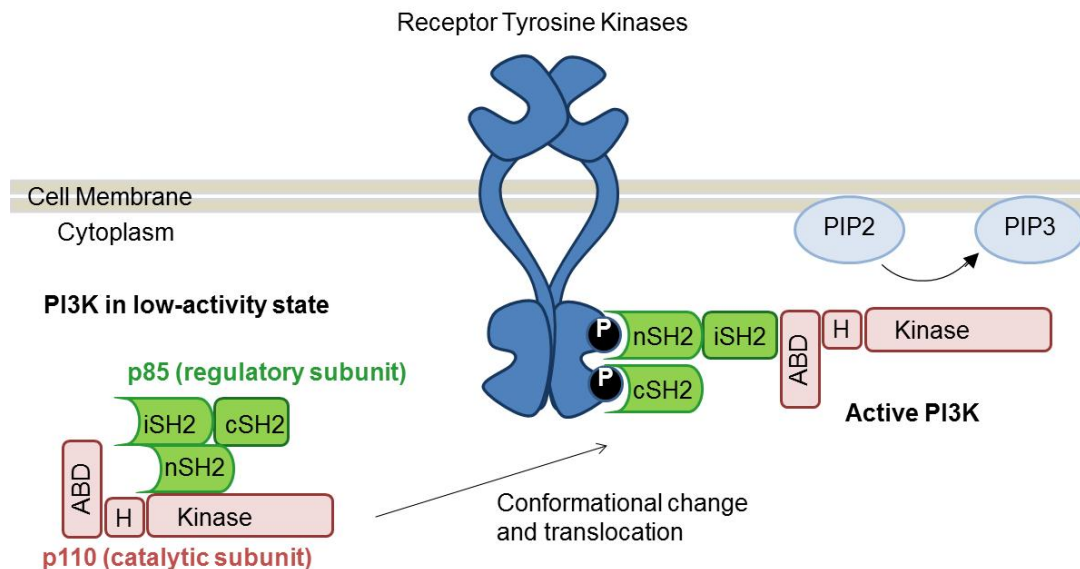
Figure 2. The phosphoinositide 3-kinase pathway. PI3K is a heterodimer composed of a p85 regulatory subunit and a p110 catalytic subunit. p85 SH2 domains bind to phospho-tyrosine residues at the cell membrane leading to de-repression of p110 and membrane recruitment. Adapted from Lee et al., *Science* 2007.

6

including AKT, which is activated through phosphorylation at two serine/threonine

sites, S473 and T308. AKT itself is a serine/threonine kinase that has been widely

implicated in cancers and regulates multiple pathways that control cell growth,

proliferation, and survival (Brugge et al., 2007; Carpten et al., 2007; Engelman et al.,

2006a) (Figure 3).

The RAF/MEK/ERK signaling pathway has also been shown to be aberrantly

activated in a wide range of human cancers (Davies et al., 2002; Malumbres and

Barbacid, 2003; Montagut and Settleman, 2009). Signaling through this pathway is
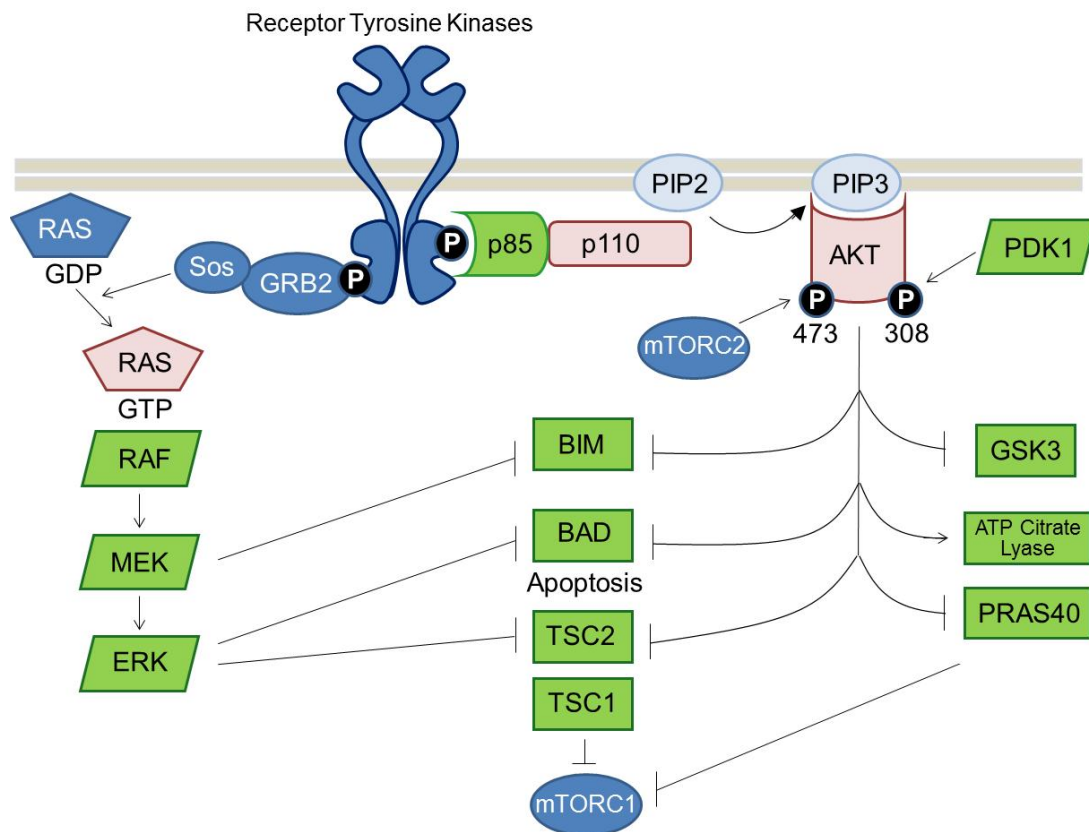
Figure 3. PI3K/AKT and RAF/MEK/ERK signaling pathways. PI3K phosphorylates PIP_2 at the cell membrane to produce PIP_3, which recruits AKT. AKT is activated at the cell membrane through serine/threonine phopshorylated by mTORC2 and PDK1, and leads to the activation of downstream effectors. The RAF/MEK/ERK or MAPK pathway begins with the conversion of inactive RAS-GDP to active RAS-GTP. This leads to a phosphorylation cascade activating RAF (MAPKKK), MEK (MAPKK) and ERK (MAPK). Each of these pathways converge on mTORC1, apoptotic proteins, and pathways affecting cell cycle, growth, and proliferation. Adapted from Engelman, JA et al., *Nat Rev Cancer* 2009.

initiated through activation of RAS family GTPases, by RTKs or through direct mutation, at the cell membrane. Active RAS then initiates a signaling cascade in which RAF kinases phosphorylate MEK kinases, which in turn phosphorylate extracellular related kinases (ERK1 and ERK2), leading to activation of multiple downstream effectors including those regulating cell proliferation and apoptosis.

One of the major effectors of both PI3K/AKT and RAF/MEK/ERK signaling is the mammalian target of rapamycin complex 1 (mTORC1), which includes the the serine/threonine kinase mTOR. Depending on the particular cancer type, the mTORC1 complex integrates signals from a combination of the PI3K/AKT and MEK/ERK pathways, as well as nutrient, growth factor, and energy sensing inputs; and controls numerous protein synthesis and cell growth pathways (Huang and Manning, 2008; Kim et al., 2002; Manning and Cantley, 2007) (Figure 3).

Multiple negative regulators are in place to control these central oncogenic pathways regulating cell cycle, growth, and survival. The PTEN phosphatase terminates PI3K signaling by dephosphorylating PIP_3 (Li et al., 1997; Maehama and Dixon, 1998). A collection of additional phosphatases de-phosphorylate RTKs, adaptor molecules, and kinases—including AKT and RAF—in order to abrogate signaling and minimalize flux through a particular pathway. The ubiquitin proteasome system mediates protein degradation and thus can regulate protein expression levels. Finally, there are multiple feedback loops that have evolved to actively control cellular signaling, and these complex feedbacks can complicate the effects of specific inhibitors in certain cancer models.

1.4 Targeted Cancer Therapies

Over the past few decades, specific mutation, over-expression, or deletion of key components of the PI3K/AKT and MAPK signaling pathways have been identified and linked to tumorigenesis. Activating mutations in *EGFR* have been shown to drive central oncogenic pathways in non-small cell lung cancer (NSCLC) (Lynch et al., 2004; Paez et al., 2004; Rusch et al., 1993), and amplification of the HER2 and MET receptor tyrosine kinases has been associated with certain forms of cancer including breast, gastric, and NSCLC (Engelman et al., 2007b; Slamon et al., 1987; Smolen et al., 2006). Mutations in *AKT* and the *PIK3CA* gene encoding the p110α subunit of PI3K have also been found to occur frequently in cancers (Brugge et al., 2007; Huang et al., 2007; Samuels et al., 2004). Activating *RAS* mutations are the most common mutations observed thus far in human cancers (Malumbres and Barbacid, 2003), and oncogenic mutations and amplifications of RAF and MEK are also common (Davies et al., 2002; Montagut and Settleman, 2009). Finally, loss of negative regulators, including *PTEN* deletions, has been shown to occur frequently (Li et al., 1997). Identification of the central pathways regulating tumorgenesis and the key oncogenic events responsible for transformation has allowed for the development of specific targeted cancer therapies. Since Herceptin was first used in patients with HER2-positive breast cancer in the early 1990s, many additional targets have been identified and validated, and dozens of new drugs have been developed and tested in the clinic.

Kinases are relatively accessible targets; a number of therapeutics including small molecule ATP mimetics have been successfully developed to inhibit kinase activity. Notable examples include the clinically approved EGFR inhibitors gefitinib (Iressa) and erlotinib (Tarceva), and the BCR-ABL kinase inhibitor imatinib (Gleevec). Numerous drugs targeting additional RTKs—as well as inhibitors of PI3K,

mTOR, AKT, MEK, and RAF—are currently under clinical development and are being tested both as mono-therapies and in combinations.

Therapies targeting non-kinases are also being explored in the clinic. Therapeutic monoclonal antibodies that target extracellular proteins represent a growing class of drugs. As discussed above, Herceptin is a HER2 monoclonal antibody effective in *HER2*-positive breast cancers (Baselga, 2001a). The EGFR monoclonal antibody Cetuximab has also been approved clinically (Baselga, 2001a; Baselga, 2001b). Antibodies targeting the kinase dead ERBB3 receptor scaffold are actively undergoing pre-clinical development (Schoeberl et al., 2010). Finally, subsets of drugs targeting additional pathways upon which cancer cells depend heavily are being explored for the inhibition of central processes including angiogenesis, metastasis, and apoptosis.

Most targeted therapies already provide a significant advantage over the traditional, relatively toxic chemotherapy and radiation therapies; however, despite their successful clinical development thus far, there are still a number of challenges that remain. First, limiting the number and severity of dose-limiting side effects incurred by normal cells is essential, and these challenges will only increase as more patients require treatment with multiple drug combinations. Second, substantial efforts are being made to achieve optimal pharmacokinetic and pharmakodynamic properties for new drugs, including designing drugs that are orally available, and determining which dosing schedules are most effective. Third, there are still several cancers in which the oncogenic driver or drivers have not yet been identified or in which there is not yet a drug available to reliably and selectively hit a particular target. Finally, despite often dramatic initial responses following treatment with targeted therapies, patients develop resistance almost universally. Efforts to further

elucidate the signaling pathways and feedback networks that are active in cancers

with acquired resistance will be a focal point of this thesis.

1.5 Resistance to EGFR Targeted Therapies

Non-small cell lung cancer (NSCLC) patients with *EGFR* activating mutations

often exhibit exquisite sensitivity to the EGFR tyrosine kinase inhibitors gefitinib and

erlotinib (Asahina et al., 2006; Inoue et al., 2006; Sequist et al., 2008) (Figure 4A).

However, the vast majority of these patients develop resistance despite promising

initial responses (Figure 4B), typically within 12 months (Engelman and Settleman,

2008; Sharma et al., 2007). In *EGFR* mutant NSCLC, a secondary T790M mutation

in the ATP binding pocket of EGFR occurs in about 50% of resistance cases,
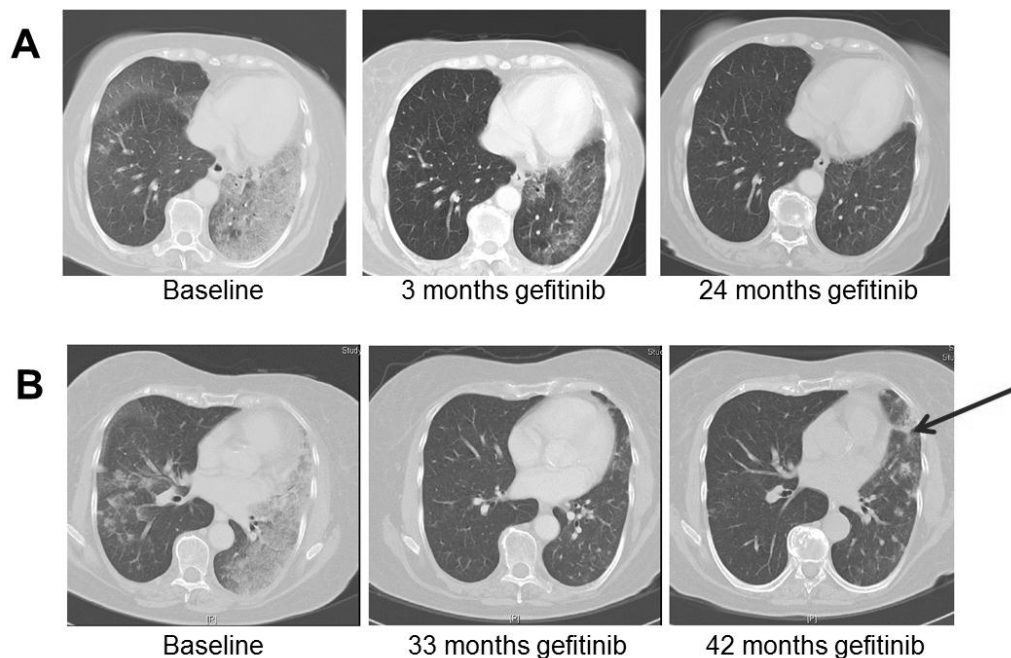
Figure 4. Clinical response to gefitinib in NSCLC. NSCLC patients with *EGFR* activating mutations were treated and monitored at Massachusetts General Hospital. (A) Dramatic and sustained tumor regression in response to treatment with the EGFR inhibitor gefitnib. (B) Dramatic response to gefitinib followed by the development of resistance and tumor re-growth (arrow).

allowing the EGFR kinase to remain active in the presence of drug (Balak et al., 2006; Kobayashi et al., 2005; Pao et al., 2005). Recently, irreversible EGFR inhibitors have been developed that bind covalently to the ATP binding pocket and are effective in inhibiting T790M mutant *EGFR* (Zhou et al., 2009; Zhou et al., 2011). Similar secondary mutations in the target kinase, often affecting this "gatekeeper" residue, are also common in other forms of cancer (Katayama et al., 2011; O'Hare et al., 2009). In addition to direct mutation of the target kinase, activation of parallel RTKs has also been shown to cause resistance to EGFR targeted therapies. For example, amplification of the MET receptor occurs in approximately 20% of NSCLC patients with acquired gefitinib resistance (Engelman et al., 2007b). Activation of IGFR signaling through loss of IGF binding proteins has also been shown to cause resistance to EGFR targeted therapies (Guix et al., 2008).

In the majority of cases, resistant cancers re-activate downstream oncogenic pathways including PI3K/AKT and RAF/MEK/ERK. Combinations of PI3K inhibitors, mTOR inhibitors, BRAF inhibitors, and MEK inhibitors are currently being tested in a variety of human cancers including NSCLC. However, the ultimate success of these combination therapies may be limited by toxicity and resistance. There is a pressing need for the development of more effective diagnostic tools and the identification of new biomarkers will allow for more efficient clinical trials. The discovery of novel therapeutics and a more complete understanding of the signaling pathways and feedback networks that become re-activated in resistant cancers will ultimately encourage the shift towards more effective and lasting personalized targeted cancer therapies.

Chapter 2- Ligand mediated resistance[1]

2.1 Abstract

MET amplification activates ERBB3/PI3K/AKT signaling in *EGFR* mutant lung cancers, and causes resistance to EGFR kinase inhibitors. My colleagues and I demonstrate that activation of MET by its ligand, hepatocyte growth factor (HGF), also activates downstream signaling pathways and rescues several EGFR-driven cancer cell lines from TKI sensitivity in a dose dependent manner. However, when MET is activated via ligand cells use GAB1 to activate PI3K. This is in contrast to *MET* amplified cancers, which use ERBB3 to activate PI3K. Further, we show that HGF does not activate PI3K signaling in HER2-driven cell line models, and that IGF ligand is less potent than HGF in promoting resistance. In non-small cell lung cancer (NSCLC) patient samples, high levels of HGF expression correlated significantly with resistance to EGFR inhibitors. These results suggest that an additional subset of patients, those with high HGF expression but normal *MET* copy number, may benefit from treatment with combined MET and EGFR inhibitors. This study also highlights the need for the development of anti-HGF targeted therapies.

2.2 Introduction

The epidermal growth factor receptor (EGFR) tyrosine kinase inhibitors (TKIs) gefitinib and erlotinib are effective clinical therapies for advanced non-small cell lung cancer (NSCLC) patients with *EGFR* activating mutations (Asahina et al., 2006; Inoue et al., 2006; Paz-Ares et al., 2006; Sequist et al., 2008; Tamura et al., 2008). A recent phase III clinical trial demonstrated that patients with *EGFR* mutant NSCLC had superior outcomes with gefitinib treatment compared to standard first line

---

[1] Excerpts and figures from this chapter were published in Turke at al., *Cancer Cell*, January 2010.

cytotoxic chemotherapy (Mok et al., 2008). However, despite dramatic benefits from EGFR TKIs in this genetically defined cohort, all of these patients ultimately develop resistance (referred to as acquired resistance herein) to gefitinib and erlotinib.

In *EGFR* mutant lung cancers over 50% of resistance cases are due to the occurrence of a secondary T790M mutation in EGFR. Amplification of the MET receptor has also been shown to maintain ERBB3/PI3K/AKT signaling in the presence of gefitinib (reviewed in (Engelman and Janne, 2008)) and cause resistance to EGFR targeted therapies in approximately 20% of NSCLC patients (Engelman et al., 2007b). In fact, clinical trials using combined EGFR and MET inhibitors in NSCLC patients with acquired resistance to gefitinib/erlotinib are currently underway. Activation of IGF-1Rβ/IRS-1 signaling through loss of IGF binding proteins also drives gefitinib resistance in *EGFR* wild-type cancer cell lines (Guix et al., 2008). Additionally, a recent study suggested that the MET ligand, HGF, can promote short-term resistance in two *EGFR* mutated cancer cell lines (Yano et al., 2008). Both ligand-dependent resistance mechanisms maintain PI3K/AKT activation despite EGFR inhibition. However, differences between IGF and HGF ligand-driven resistance in terms of potency and activation of downstream signaling pathways have yet to be thoroughly examined.

MET encodes a trans-membrane RTK for the hepatocyte growth factor (HGF) and is capable of activating ERBB receptors to drive cell migration, invasion, proliferation, survival and angiogenesis (Christensen et al., 2003). *MET* amplification has been detected in gastric and esophageal cancers (Christensen et al., 2003; Miller et al., 2006) and cell lines derived from such tumors display ligand-independent dependence on MET (Smolen et al., 2006). However, it remains unknown whether activation of MET by its ligand, HGF, is a mechanism utilized by human tumors to develop resistance to ERBB-targeted therapies.

14

In the current study, we evaluated the potency of the MET ligand, HGF, to activate downstream PI3K/AKT and MEK/ERK signaling pathways, and promote resistance to EGFR TKIs *in vitro* and *in vivo*. We also assessed the potential of the IGF ligand to promote resistance. Finally, we analyzed tumor samples from NSCLC patients with acquired resistance to gefitinib and compared HGF expression levels in paired pre- and post-treatment tumor samples. The findings from these analyses highlight a new cohort of patients, those with high HGF expression but without *MET* amplification, that may benefit from combined EGFR and HGF/MET targeted therapies.

2.3 Materials and Methods

Cell culture and reagents

The *EGFR* mutant NSCLC cell lines HCC827 (del E746_A750), PC-9 (del E746_A750) and H1975 (L858R/T790M) have been previously characterized (Amann et al., 2005; Engelman et al., 2007a; Engelman et al., 2007b; Mukohara et al., 2005; Ono et al., 2004). The *EGFR* wild type epidermoid carcinoma cell line A431 and head and neck cancer cell line HN11 have been described previously (Guix et al., 2008). The *HER2* amplified breast cancer cell lines BT-474 and SKBR3 cells were kind gifts from Dr. Carlos L. Arteaga (Vanderbilt University School of Medicine, Nashville, Tennessee). HCC827 cells were maintained in RPMI 1640 (Cellgro; Mediatech Inc., Herndon, CA) supplemented with 5% FBS; H1975, PC-9, A431 and HN11 cell lines were maintained in RPMI 1640 supplemented with 10% FBS. BT-474 cells were maintained in Dulbecco's Modification of Eagle's Medium (DMEM) (Cellgro; Mediatech Inc., Herndon, CA) and SKBR3 cells were maintained in McCoy's 5A Medium (Invitrogen, Carlsbad, CA), both supplemented with 10% FBS.

Recombinant human HGF and the Quantikine ELISA Kit for quantification of HGF in cell culture medium were purchased from R&D Systems (Minneapolis, MN). Recombinant human IGF-1 was purchased from Austral Biologicals (San Ramon, CA). Gefitinib and lapatinib were obtained from commercial sources (American Custom Chemical Corporation and LC Laboratories Woburn, MA). PF00299804, PHA-665,752 and PF2341066 were provided by Pfizer (La Jolla, CA).

Cell viability assays

Growth and inhibition of growth was assessed by Syto60 staining (Invitrogen). Cells were fixed with 4% formaldehyde for 20 min at 37°C and incubated with a 1:5000 dilution of Syto60 stain for 60 min. Cell density in each well was determined with an Odyssey Infrared Imager (LiCor Biosciences), corrected for background fluorescence from empty wells and normalized to untreated wells, as described previously (Rothenberg et al., 2008).

For 72 hour viability assays, cells were seeded in 96-well plates and exposed to the indicated TKIs (3.3 nM to 10 µM) alone or in combination with the indicated concentrations of HGF or IGF ligand. The number of cells used per experiment was determined empirically and has been previously established (Mukohara et al., 2005). All experimental points were set up in six to twelve wells and all experiments were repeated at least three times. The data was graphically displayed using GraphPad Prism version 5.0, (GraphPad Software; www.graphpad.com). The curves were fitted using a non-linear regression model with a sigmoidal dose response.

Antibodies and Western Blotting

Cells grown under the previously specified conditions were lysed in the following lysis buffer: 20 mM Tris, pH 7.4/150 mM NaCl/1% Nonidet P-40/ 10%

glycerol/1 mM EDTA/1 mM EGTA/5 mM sodium pyrophosphate/50 mM NaF/10 nM β

-glycerophosphate/1 mM sodium vanadate/0.5 mM DTT/4 µg/ml leupeptin/4 µg/ml

pepstatin/4 µg/ml apoprotein/1 mM PMSF. Lysates were centrifuged at 16,000 × g

for 5 min at 4℃. The supernatant was used for subsequen t procedures. Western

blot analyses were conducted after separation by SDS/PAGE electrophoresis and

transfer to nitrocellulose or PVDF membranes. Immunoblotting was performed

according to the antibody manufacturer's recommendations. Antibody binding was

detected using an enhanced chemiluminescence system (PerkinElmer, Waltham,

MA). Anti-phospho-Akt (Ser 473), anti-phospho-ERBB-3 (Tyr-1289), anti-phospho-

p42/44 MAP kinase (Thr 202 Tyr 204), anti-p42/44 MAP kinase, anti-phospho-S6

ribosomal protein (Ser 335/236), anti-S6 ribosomal protein, anti-phospho MET (Tyr

1234/1235), anti-MET (25H2), anti-phospho HER2 (Tyr 1211/1222), anti-phospho

IGF-I receptor (Try 1135/1136), anti-IGFR, and anti-phospho-Tyr-100 antibodies

were from Cell Signaling Technology (Beverly, MA). Anti-ERBB3, anti-AKT, anti-

GAB1, and anti-EGFR antibodies were purchased from Santa Cruz Biotechnology

(Santa Cruz, CA). The phospho-specific EGFR (Tyr1068) antibody was from AbCam

(Cambridge, MA). The anti-HER2 antibody was from Oncogene Research Products

now Calbiochem (SanDiego, CA). The anti-p85 antibody used for

immunoprecipitations was from Millipore (Billerica, MA). Western blots images were

captured using GeneSnap image acquisition software and analyzed using

GeneTools manual band quantification (SynGene: www.syngene.com).

In vivo treatment studies

All xenograft studies were performed in accordance with the standards of the

Institutional Animal Care and Use Committee (IACUC) under a protocol approved by

the Animal Care and Use Committee of Massachusetts General Hospital. Nude mice

(nu/nu; 6-8 weeks old; Charles River Laboratories) were anesthetized using a 2% Isoflurane (Baxter) inhalation oxygen mixture. A suspension of 5×10^6 HCC827-HGF cells (in 0.2 ml of PBS) was inoculated subcutaneously into the lower-left quadrant of the flank of each mouse. Mice were randomized to 4 treatment groups (n=5 per group) once the mean tumor volume reached ~500 mm^3. PF2341066 was dissolved in sterile water and administered at 25mg/kg/day. Gefitinib was dissolved in polysorbite vehile and administered at 150mg/kg/day. For combination studies oral administration of the two agents was separated by 1 hour. Tumors were measured twice weekly using calipers, and volume was calculated using the formula (length x width^2 x 0.52). Mice were monitored daily for body weight and general condition. The experiment was terminated when the mean size of either the treated or control groups reached 2000 mm^3.

Tumor volume was analyzed by a mixed linear model, assuming an unstructured covariance matrix for the random effects and an AR(1) structure for the within-mouse correlation. Volume measurements were transformed into the log scale for analysis in order to approximate a linear fit, reflecting the exponential growth of tumors. A quadratic effect was included in the model for the HCC827-HGF xenografts to account for the initial tumor shrinkage followed by subsequent re-growth in the treatment group with gefitinib alone.

sRNA transfections and Lentiviral Infections

Hs_GAB1_6 HP validated siRNA and AllStars Negative Control siRNA were obtained from Qiagen (Valencia, CA). HCC827 cells were seeded 200K cells/well on a 6-well plate in RPMI media without penicillin or streptomycin. Cells were transfected with 50nM siRNA with using 18µL HiPerFect Transfection Reagent (Qiagen) in Opti-MEM Reduced Serum Media from Gibco Invitrogen (Frederick, MD)

and incubated at 37°C for 48 hours. HGF cDNA was obtained from Open Biosystems and cloned into a lentiviral destination vector, pWPI, using the Gateway cloning system (Invitrogen), and infections were performed as previously described (Rothenberg et al., 2008).

NSCLC patients

Tumor specimens from gefitinib or erlotinib treated patients were obtained from the Dana Farber Cancer Institute/Brigham and Women's Hospital (Boston, MA), Massachusetts General Hospital (Boston, MA), the Chinese University (Hong Kong, China) and from Guangdong Provincial People's Hospital (Guangzhou, China) under Institutional Review Board approved studies. All patients provided written informed consent. The presence of an *EGFR* mutation in each specimen was confirmed by exon-specific amplification (exons 18-21), followed by direct sequencing, or using the Surveyor™ endonuclease coupled with denaturing HPLC (DHPLC), fractionation and sequencing (Janne et al., 2006). The *EGFR* T790M mutation was detected using Surveyor™ endonuclease coupled with DHPLC or an allele specific PCR (Janne et al., 2006; Maheswaran et al., 2008). Both methods are capable of detecting the *EGFR* T790M mutation at an allele frequency of 1-5%. HGF immunohistochemistry was performed using an anti-HGF 7.2 antibody kindly provided by Dr. George Vander Woude at the Van Andel Institute.

HGF immunohistochemistry

Immunohistochemistry for HGF protein was performed on positively charged glass slides containing 5-micron sections of formalin-fixed, paraffin-embedded tissue. Slides were deparaffinized in Hemo-De for 10 min and rinsed (6 washes) into absolute ethanol, before endogenous peroxidase was blocked with 1.05% hydrogen

peroxide in ethanol for 30 min. Blocked slides were rinsed in water and microwave

antigen retrieval was performed in citrate buffer (pH 6.0). The sections were

incubated overnight, at room temperature, with primary antibody (mouse monoclonal

anti-HGF, generously contributed by Dr. George Vander Woude) diluted 1:300 in

TBS. After incubation, excess primary antibody was rinsed off with TBS, and the

sample was washed in TBS with 0.02% BRIJ for 10 min. Signal was amplified by

secondary incubation with EnvisionPlus (DAKO, Carpinteria, CA), for 30 min. Bound

antibodies were detected by DAB chromogenic (brown) reaction, after 5 min

incubation.

Slides were interpreted by a board-certified anatomic pathologist (NIL), who

evaluated the percentage of cancer cells with positive cytoplasmic and/or

membranous staining (0 – 100%), and the modal intensity of the positively-staining

cells on a scale from 0 to 4+ (Figure 9). The percentage and the intensity were

multiplied to give a scoring index ranging from 0 – 400. For comparison of HGF

immunohistochemistry results, the HGF scores in paired NSCLC patient specimens

were compared using the Wilcoxon signed rank test. A one sided p-value was used

to test the hypothesis that HGF scores were higher in the drug resistant compared to

the pre-treatment specimens.

2.4 Results

HGF activates PI3K/AKT signaling and mediates resistance to EGFR targeted
therapies

MET amplification was previously shown to cause gefitinib resistance in

HCC827 GR cells (Engelman et al., 2007b). Here we investigated whether activation

of MET signaling by its ligand, HGF, could also cause resistance to gefitinib and

other ERBB-targeted therapies. In a 72 hour survival assay, HGF induced substantial

gefitinib resistance in HCC827 cells that was abolished by the addition of the MET

inhibitor PHA-665,752 (Figure 5A). Furthermore, HGF maintained PI3K/AKT,

mTORC1 and ERK activation in the presence of gefitinib in a dose-dependent

manner that mirrored its capacity to maintain cell viability (Figures 5B, C).
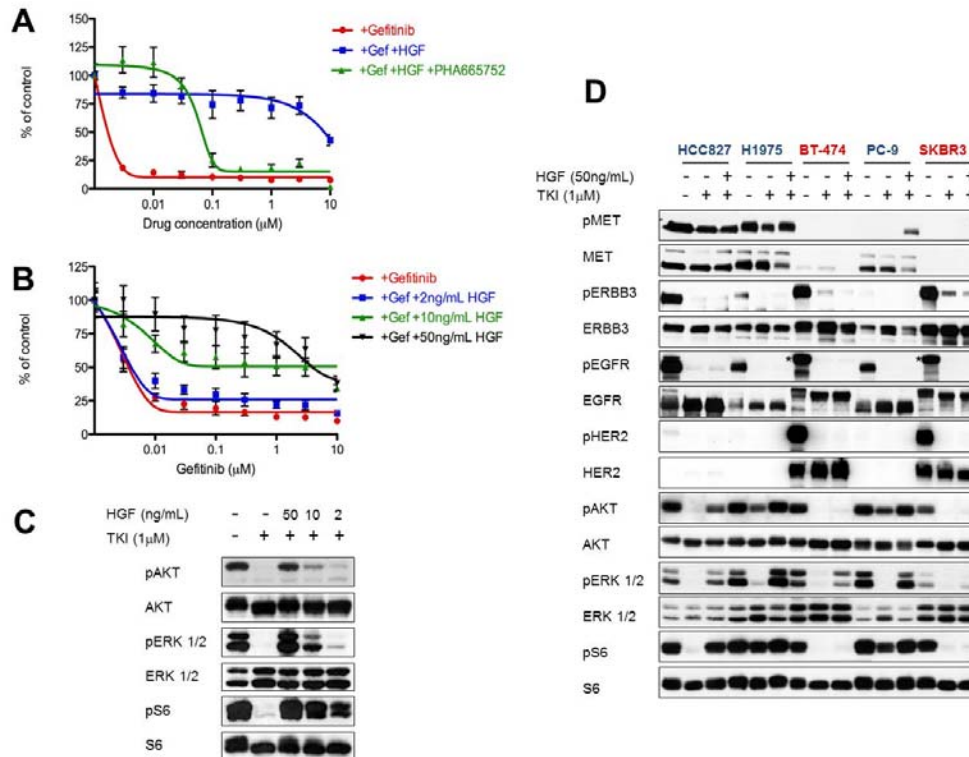
Figure 5. HGF induces MET dependent resistance only in cell lines in which it activates PI3K/AKT, ERK and mTORC1 signaling. (A, B) HCC827 cells treated with (A) increasing concentrations of gefitinib alone or in combination with PHA-665,752, in the absence or presence of HGF (50ng/mL), or (B) increasing concentrations of gefitinib alone or in combination with the indicated concentrations of HGF. Cell viability relative to untreated controls measured after 72 hours. Each data point represents the mean ±SD of 6 wells. (C) HCC827 cells were treated for 6 hours with 1μM gefitinib alone or in combination with the indicated concentrations of HGF. Cell lysates were immunoblotted to detect indicated proteins. (D) Cells were treated for 6 hours with gefitinib (HCC827, PC-9), PF00299804 (H1975), or lapatinib (BT-474, SKBR3), alone or in combination with HGF (50ng/mL). All drugs were used at 1μM. Cell lysates were immunoblotted to detect indicated proteins. *indicates cross-reaction by the p-EGFR antibody against p-HER2. Cell lines in which HGF rescued viability are labeled in blue, and cell lines in which HGF did not rescue viability are labeled in red.

We also determined the capacity for HGF to maintain downstream signaling

and cell viability in other EGFR and HER2 addicted cancers. In cell lines with *EGFR*

exon 19 deletions (HCC827 and PC-9), and an EGFR-driven lung cancer cell line

carrying the T790M resistance mutation (H1975), HGF restored PI3K/AKT, mTORC1

and ERK signaling, despite continued EGFR inhibition in the presence of 1µM

gefitinib or the irreversible EGFR inhibitor PF00299804 (Figure 5D). HGF also
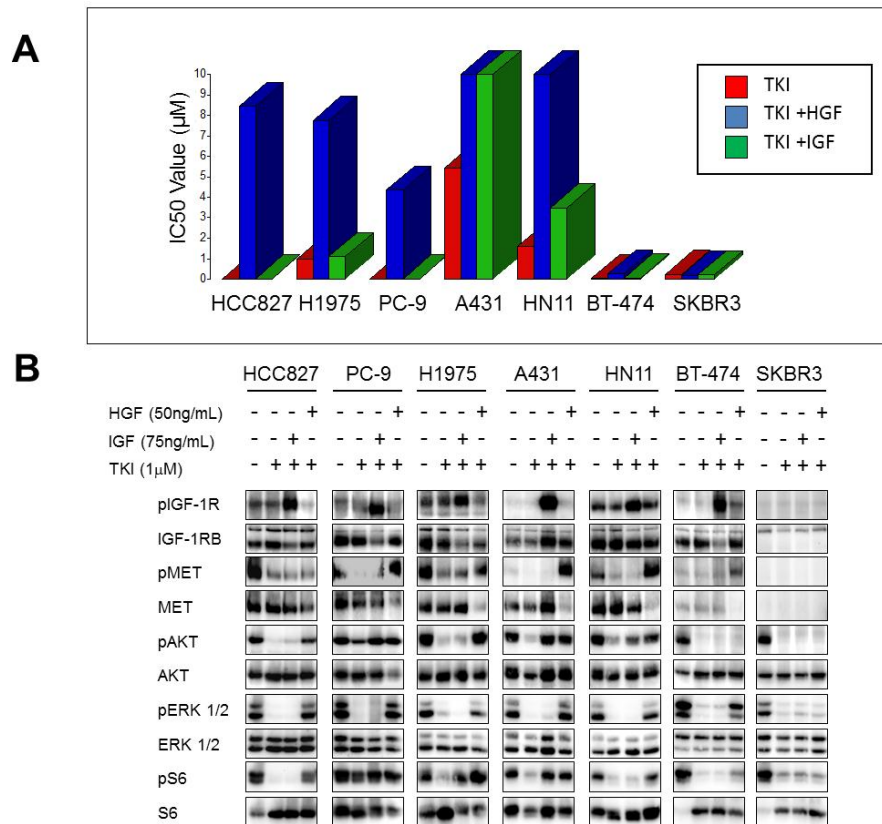
Figure 6. IGF rescues PI3K/AKT and mTORC1 signaling in some cell lines, but fails to activate ERK. (A) IC$_{50}$ values for viability curves (see Turke et al. *Cancer Cell,* 2010. SF 1) in the presence or absence of HGF and IGF. Cells were treated with increasing concentrations of the appropriate TKI alone (red) or in combination with 50ng/mL HGF (blue) or 75ng/mL IGF (green). **(B)** Cells were treated for 6 hours with gefitinib (HCC827, PC-9, A431, HN11), PF00299804 (H1975) or lapatinib (BT-474, SKBR3) alone or in combination with HGF (50ng/mL) or IGF (75ng/mL). All drugs were used at 1µM. Cell lysates immunoblotted to detect indicated proteins. BT-474 and SKBR3 cell lysates were run on the same gel, and no MET or IGF-1Rβ was detected in SKBR3 cells relative to BT-474 cells.

rescued each of these cell lines from TKI-induced cell death after 72 hours (Figure

6A). In contrast to the EGFR addicted cancers, HGF did not rescue HER2 amplified

breast cancer cell lines from the effects of the HER2 TKI lapatinib (Figure 6A), nor

did it rescue AKT or mTORC1 signaling in either HER2 driven cell line (Figure 5D).

Thus, the capacity to rescue cell viability appears to strongly correlate with capacity

to restore downstream signaling, especially along the PI3K/AKT pathway. We

suspect that HGF had a minimal effect in BT-474 and SKBR3 cells because these

cell lines have lower levels of MET expression compared to the other EGFR-driven

cell lines that were tested.
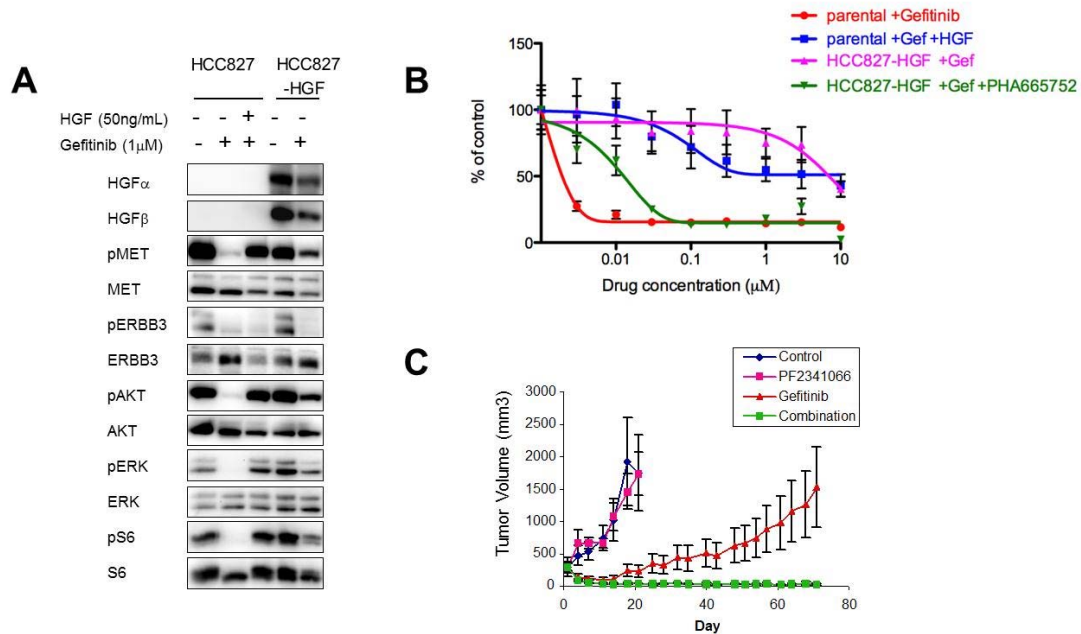
Figure 7. HGF expression in HCC827 cells maintains signaling and induces gefitinib resistance. (A) HCC827 cells were infected with a lentivirus engineered to express HGF (HCC827-HGF). Parenal HCC827 and HCC827-HGF cells were treated for 6 hours with gefitinib (1μM) alone or in combination with HGF (50ng/mL) where indicaed. Cell lysates were immunoblotted to detect indicated proteins. **(B)** Parental HCC827 cells were treated with increasing concentrations of gefitinib, alone or in combination with HGF (50ng/mL) for 72 hours. HCC827-HGF cells were treated increasing concentrations of gefitinib, alone or in combination with the MET inhibitor PHA665752 for 72 hours. Cell viability was measured relative to untreated controls. Each data point represents the mean ±SD of 6 wells. **(C)** HCC827-HGF xenografts in *nu/nu* mice treated with PF2341066, gefitinib, or their combination and tumors measured twice weekly. Some growth inhibiton was observed with gefitinib alone, however only combination treatment led to complete tumor shrinkage (p = 0.002). Each data point represents the mean ±SD for 5 mice.

To confirm the ability of HGF to induce resistance to EGFR TKIs, we introduced the human HGF gene into HCC827 cells (HCC827-HGF). Parental HCC827 cells secrete undetectable levels of HGF; however, HCC827-HGF cells express HGF protein (Figure 7A) and secrete approximately 70ng/mL HGF into the culture medium (data not shown). Further, HCC827-HGF cells are gefitinib resistant (Figure 7B) and maintain PI3K/AKT, ERK and mTOR signaling in the presence of gefitinib (Figure 7A); however gefitinib sensitivity is restored with the addition of a MET inhibitor (Figure 7B).

We also evaluated the capacity of HGF to induce gefitinib resistance *in vivo* using an HCC827-HGF xenograft model. We have previously shown that parental HCC827 cells demonstrate complete responses to gefitinib in vivo (Engelman et al., 2006b; Engelman et al., 2007a). However, the HCC827-HGF xenografts demonstrated resistance (Figure 7C). Treatment with gefitinib alone was slightly more effective than no treatment or treatment with the MET inhibitor PF2341066 alone, but only the combination of gefitinib and PF2341066 completely inhibited tumor growth (p < 0.001; gefitinib vs. gefitinib/PF2341066; Figure 7C). Indeed, 3 out of 4 mice were cured after 70 days of combined treatment with no evidence of re-growth 70 days after stopping treatment.

IGF is much less potent than HGF in promoting resistance to EGFR TKIs

Since HGF ligand appeared to be a potent inducer of resistance to RTK inhibitors, we compared its efficacy to that of IGF ligand, which we had previously found to cause gefitinib resistance in A431 cells (Guix et al., 2008). Although IGF exposure led to significant rescue from gefitinib-induced cell death in A431 cells, and partial rescue in HN11 *EGFR* wild-type cells, the other five cell lines tested remained sensitive to ERBB inhibition despite the presence of IGF (Figure 6A). Interestingly, in

three of those cell lines (BT-474, HCC827 and H1975), IGF was unable to maintain

PI3K/AKT signaling despite potent activation of IGR-1Rβ (Figure 6B). Of note, IGF

did not restore ERK phosphorylation in any of the six cell lines examined, including

those in which it induced IGF-1Rβ and/or PI3K/AKT activation (Figure 6B). Thus,

unlike IGF, HGF may be more potent at promoting resistance because it leads to

activation of both the PI3K/AKT and ERK pathways. Unexpectedly, IGF restored

PI3K/AKT signaling in PC-9 cells, but these cells still remained highly sensitive to

EGFR-inhibition after 72 hours (Figure 6A, B). This disconnect between maintenance

of PI3K/AKT signaling and lack of an effect on cell viability is not due to a brief,

transient restoration of downstream signaling, as we observed that IGF maintained

PI3K signaling in PC-9 cells for at least 24 hours in the presence of gefitinib (data not

shown).

HGF rescue of PI3K signaling is mediated though GAB1 instead of ERBB3

   MET amplified gefitinib resistant HCC827 GR cells utilize ERBB3 as the

primary adaptor to activate PI3K/AKT signaling (Engelman et al., 2007b). Although

HGF treatment was sufficient to rescue AKT phosphorylation in several EGFR-driven

cell lines in the presence of TKIs, ERBB3 phosphorylation was not restored (Figure

5D). This suggests that HGF-induced MET activation utilizes an adaptor other than

ERBB3 to activate PI3K signaling. To determine which PI3K adaptors were being

utilized to maintain HGF-mediated PI3K signaling, we immunoprecipitated the p85

regulatory subunit of PI3K and examined co-precipitating phosphotyrosine proteins

(Engelman et al., 2005; Engelman et al., 2007b; Guix et al., 2008). As expected,

treatment with a TKI disrupted the association of ERBB3 (and other phosphotyrosine

proteins) with p85, and the addition of HGF did not restore the interaction (Figure

8A). However, we observed that HGF potently induced the association between p85

and Grb2 associated binder 1 (GAB1), which runs as a broad, highly tyrosine-

phophorylated band at approximately 110kDa.
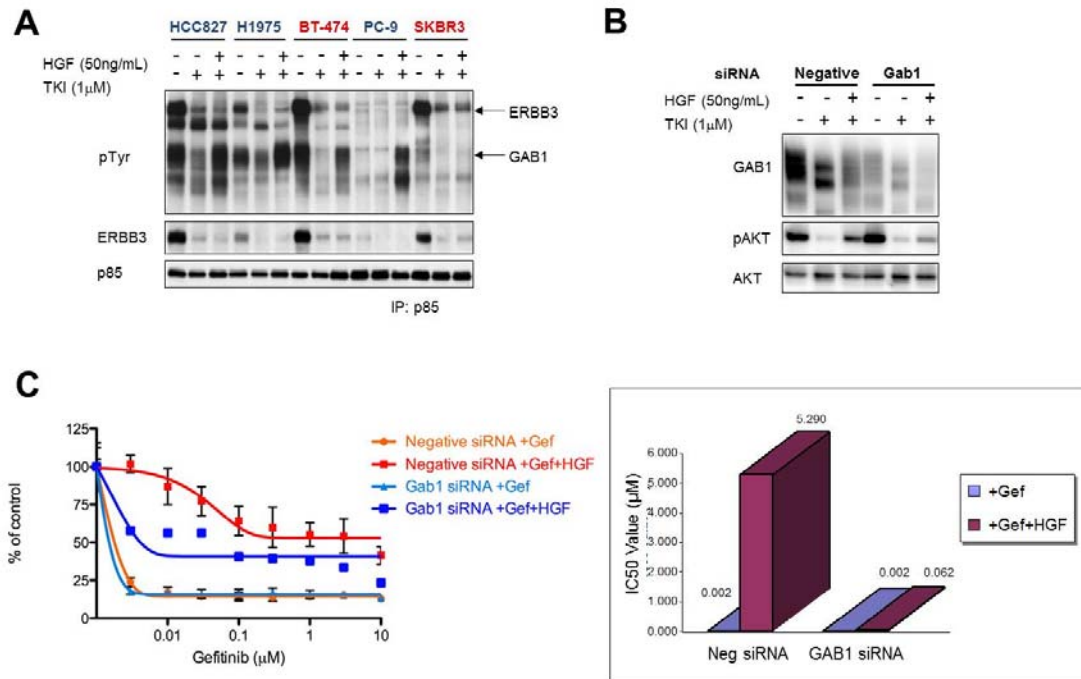
Figure 8. HGF rescue of PI3K/AKT signaling is mediated though GAB1 instead of ERBB3.
(A) Cells treated for 6 hours with gefitinib (HCC827, PC-9), PF00299804 (H1975), or lapatinib (BT-474, SKBR3), alone or in combination with HGF (50ng/mL). All drugs were used at 1μM. Cell extracts were immunoprecipitated with an anti-p85 antibody followed by Western blot with anti-p-Tyr, anti-ERBB3 and anti-p85 antibodies. **(B)** HCC827 cells were transfected with a negative control or GAB1 siRNA for 48 hours. Transfected cells were treated for 6 hours with gefitinib (1μM) alone or in combination with HGF (50ng/mL). Cell lysates were immunoblotted to detect indicated proteins. See also Figure S3. **(C)** HCC827 cells were transfected with GAB1 siRNA or a negative control siRNA for 48 hours, then treated with increasing concentrations of gefitinib, alone or in combination with 50ng/mL HGF. *Left,* cell viability relative to untreated controls measured after 72 hours. Each data point represents the mean ±SD of 6 wells. *Right*, plot of IC_{50} values corresponding to cell viability curves.

To more directly assess if GAB1 mediates HGF-mediated activation of

PI3K/AKT signaling and cell viability, we used small interfering RNA (siRNA) to

knockdown GAB1 expression in the HCC827 cells. Knockdown of GAB1 reduced

HGF-mediated rescue of PI3K/AKT signaling (Figure 8B), and inhibited the ability of

HGF to rescue HCC827 cells from gefitinib induced cell death (Figure 8C). Of note, although the addition of HGF leads to substantial loss of GAB1 protein (Figure 8B), the amount of tyrosine phosphorylated GAB1 is dramatically increased (data not shown, see Turke et al, *Cancer Cell* 2010, Supplemental Figure 3), and this facilitates the efficient coupling to PI3K (Figure 8A). Thus, activation of HGF/MET signaling can lead to gefitinib resistance in EGFR mutant cancers by activating PI3K/AKT signaling through two different adaptors: ERBB3 when MET is activated by genomic amplification or GAB1 when MET is activated by HGF.

Analyses of tumors with acquired resistance to gefitinib/erlotinib reveal increased HGF expression in resistant cancers

To determine the clinical implications of these *in vitro* and *in vivo* observations, we examined tumor specimens from gefitinib or erlotinib treated *EGFR* mutant NSCLC patients (Table 1). All patients had a clinical partial tumor response to gefitinib or erlotinib treatment and subsequently developed clinical drug resistance. We evaluated 27 patients, 16 with paired pre and post geftinib/erlotinib treatment specimens and 11 with drug resistance specimens alone. All specimens, when feasible, were evaluated for *MET* amplification, HGF expression by immunohistochemistry (IHC), and presence of *EGFR* T790M (Table 1, Figure 9). We observed *EGFR* T790M in 55 % (15/27) and *MET* amplification in 4/27 (15%) of resistant tumor specimens. In patients with paired tumor specimens, HGF expression was higher in the drug resistant specimens compared to pre-treatment specimens (p = 0.025; Wilcoxon signed-rank test). In patients with drug resistant specimens alone, HGF expression was similar to that of drug resistant specimens in patients with

Table 1. HGF expression and pre-existing *MET* in tumor specimens from NSCLC patients.

#	Paired Specimines						
	Pre-Treatment			*Drug Resistant*			
#	EGFR mutation	MET Amp	HGF Score	EGFR mutation	T790M	MET Amp	HGF Score
1	Exon 19 del	No	30	Exon 19 del	No	No	200
2	Exon 19 del	No	50	Exon 19 del	No	No	120
3	Exon 19 del	No	N/A	Exon 19 del	Yes	No	300
				Exon 19 del	Yes	No	200
4	Exon 19 del	Yes (< 1%)	200	Exon 19 del	No	Yes	300
5	Exon 19 del	Yes (< 1%)	120	Exon 19 del	Yes	No	200
6	Exon 19 del	No	200	Exon 19 del	No	No	200
7	Exon 19 del	N/A	400	Exon 19 del	Yes	No	350
				Exon 19 del	Yes	No	350
8	L858R	N/A	N/A	L858R	Yes	No	90
9	G719S, S768I	No	95	None*	N/A	No	60
10	L858R	Yes (< 1%)	60	L858R	No	Yes	400
11	Exon 19 del	N/A	70	Exon 19 del	Yes	No	300
12	L858R	N/A	100	L858R	No	No	50
13	Exon 19 del	No	300	Exon 19 del	Yes	No	145
14	L858R	No	40	L858R	No	No	180
15	Exon 19 del	Yes (< 1%)	0	Exon 19 del	Yes	Yes	100
16	Exon 19 del	Yes (< 1%)	100	Exon 19 del	Yes	Yes**	150
	Resistant Only						
17				Exon 19 del	Yes	No	180
18				Exon 19 del	Yes	No	200
19				L858R	Yes	No	200
20				Exon 19 del	Yes	No	300
21				Exon 19 del	Yes	No	200
22				Exon 19 del	Yes	No	80
23				Exon 19 del	No	No	30
24				L858R	No	No	400
25				Exon 19 del	No	No	N/A
26				Exon 19 del	No	No	N/A
27				Exon 19 del	Yes	No	0

*Specimen contained less < 30% tumor cells. **MET* amplification defined by qPCR as previously described (Engelman et al., *Science* 2007). Data on *EGFR* T790M and *MET* amplification in resistant specimens only from patients 1-4 and 17-19 has been previously published (Engelman et al., *Science* 2007). N/A; not available.

paired tumor specimens. Together these findings support our *in vitro* and *in vivo* studies on HGF mediating resistance to EGFR TKIs.
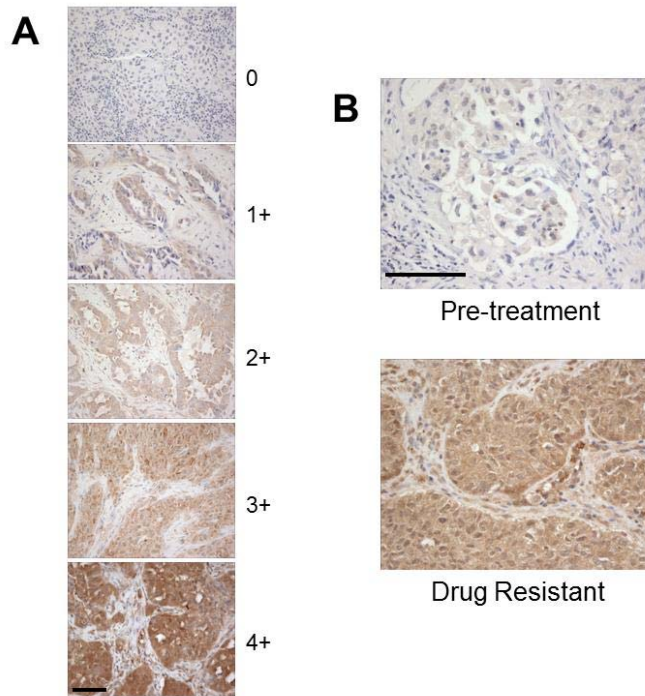
Figure 9. High HGF expression correlates with resistance to EGFR TKIs in NSCLC patient samples. (A) Patient samples were analyzed for HGF expression using immunohistochemistry. Samples were scored from 0 (no detectable HGF) to 4+ (high HGF expression) and a scoring system was developed (see Materials and Methods). Results are shown in Table 1. Scale bars represent 100μm. **(B)** Pre-treatment *(upper)* and drug resistant *(lower)* tumor samples from patient 1 show low HGF expression before treatment but high HGF expression after relapse and development of resistance to the EGFR TKI. There was no *EGFR* T790M or *MET* amplification detected from the drug resistant specimen. Scale bars represent 100μm.

2.5 Discussion

EGFR targeted therapies have shown promising results in cancers with EGFR activating mutations. However, resistance frequently occurs within 12 months. Previously, resistance mechanisms have focused on RTK mutations or amplifications, including the T790M mutation in EGFR kinase and amplification of the MET receptor (Engelman et al., 2007b; Kobayashi et al., 2005; Kosaka et al., 2006; Pao et al., 2005). Recent studies highlight examples of ligand over expression, or de-repression, leading to activation of parallel signaling pathways (Guix et al., 2008; Yano et al., 2008) and resistance to targeted therapies.

In this study, we show that HGF can independently rescue bothPI3K/AKT and ERK signaling in the presence of gefitinib and lead to drug resistance both *in vitro* and *in vivo*. Interestingly, cells that use HGF to maintain MET signaling utilize GAB1 to activate PI3K and are slightly less sensitive to combined MET and EGFR inhibition compared to *MET* amplified gefitinib resistant cells that maintain PI3K signaling through ERBB3. Thus, it may be useful to investigate the signaling advantages and disadvantages conferred by GAB1 versus ERBB3 as activators of PI3K. Of note, we also observed that although HGF restores the association of GAB1 with p85 in BT-474 cells (Figure 8A), this is insufficient to restore PI3K/AKT signaling or cell viability in the presence of lapatinib.

Higher levels HGF can be detected in tumor specimens from NSCLC patients that are clinically resistant to gefitinib or erlotinib compared to pre-treatment tumor specimens (Table 1, Figure 9). Notably in some patients without evidence of *EGFR* T790M or *MET* amplification, HGF expression is greater in the resistant specimen (patients 1 (Figure 9B) and 14) than in the pre-treatment specimen, supporting a role for HGF alone in promoting drug resistance. This is consistent with prior observations (Yano et al., 2008). Ligand mediated drug resistance is unique to HGF as IGF does not rescue TKI-induced cell death in the majority of cell lines tested. Surprisingly, IGF did not restore P13K/AKT signaling in most *EGFR* mutant cancers, despite substantial levels of IGF-1Rβ expression and tyrosine phosphorylation. Furthermore, unlike HGF, IGF did not restore ERK signaling even in cell lines in which it restored PI3K/AKT signaling in the presence of a TKI. These signaling differences between HGF and IGF may underlie the lack of drug resistance induced by IGF.

Our current findings provide insight into future therapeutic strategies for the treatment of *EGFR* mutant NSCLC. Although *MET* amplification has been detected

in up to 20% of *EGFR* mutant patients that develop acquired resistance to gefitinib or erlotinib, activation of MET signaling (by both amplification and mediated by HGF) may in fact account for a larger fraction of gefitinib/erlotinib resistant tumors. It is tempting to speculate that HGF production by the stroma may also partially explain why clinical resistance emerges discordantly in some tissues like the liver, bone and brain, while pulmonary disease continues to respond to erlotinib treatment (Dr. Jeffrey Engelman, personal observation).   These results highlight a new cohort of patients, beyond those with *MET* amplification, who may benefit from combined HGF/MET and EGFR targeted therapies.

Chapter 3- Preexistence and clonal selection of *MET* amplified cells[2]

3.1 Abstract

The therapeutic success of EGFR tyrosine kinase inhibitors (TKIs) in *EGFR* mutant lung cancers is limited by the development of drug resistance, mediated by *MET* amplification in a subset of patients. Our group has previously shown that the EGFR-driven cell line, HCC827, develops *MET* amplification as a resistance mechanism to the EGFR inhibitor gefitinib (Engelman et al., 2007b). In this study, my colleagues and I developed a second resistance model using the HCC827 cell line and showed that these cells also develop *MET* amplification in response to treatment with an irreversible EGFR inhibitor. Using high-throughput FISH analyses we determined that parental HCC827 cells harbor a small (<1%) preexisting population of *MET* amplified cells, making them uniquely poised to develop *MET* amplification as a resistance mechanism. In non-small cell lung cancer (NSCLC) patient samples, detection of pre-existing *MET* amplified cells before treatment accurately predicted the development of *MET* amplification as a resistance mechanism. Surprisingly, expression of the MET ligand, HGF, dramatically accelerated the development of *MET* amplification both in vitro and in vivo. These findings provide insight into the origins of drug resistance in *EGFR* mutant cancers, and highlight the potential to prospectively identify treatment naïve *EGFR* mutant lung cancer patients who will benefit from initial combination therapy.

3.2 Introduction

Non-small cell lung cancers (NSCLCs) with EGFR activating mutations have been shown to respond to EGFR targeted therapies including the kinase inhibitors

---

[2] Excerpts and figures from this chapter were published in Turke, et al., *Cancer Cell,* January 2010.

32

gefitinib and erlotinib (Mok 2008, Sequist 2008). However, despite dramatic initial responses, patients often develop resistance within 12 months (Engelman and Settleman, 2008; Sharma et al., 2007). Thus far, two mechanisms of acquired resistance have been validated in patients. The first involves a secondary mutation in *EGFR* itself, including the *EGFR* T790M "gatekeeper" mutation, which is observed in 50% of resistance cases (Balak et al., 2006; Kobayashi et al., 2005; Pao et al., 2005). Second, activation of MET signaling via amplification of the MET receptor occurs in at least 20% of resistance cases (Balak et al., 2006; Bean et al., 2007; Engelman et al., 2007b; Kosaka et al., 2006). In the previous chapter, we described a novel mechanism of resistance in which MET signaling is activated by the HGF ligand, leading to maintenance of PI3K/AKT signaling and cell viability in the presence of an EGFR inhibitor (Turke et al., 2010).

Strategies for overcoming acquired resistance to gefitinib are now undergoing clinical evaluation. In preclinical studies, the T790M mutant *EGFR* can be effectively inhibited by second-generation, irreversible EGFR inhibitors (Engelman et al., 2007a; Kobayashi et al., 2005; Riely, 2008). Indeed, there are now clinical trials assessing both irreversible EGFR inhibitors and a combination of MET and EGFR inhibitors in patients with acquired resistance to gefitinib/erlotinib. Further, clinical activity of the irreversible EGFR inhibitor, PF00299804, has been observed in NSCLC patients that have developed acquired resistance to gefitinib/erlotinib (Janne et al., 2008). As an alternative strategy, to delay or avoid the emergence of resistance, there is increased enthusiasm to utilize agents effective against specific resistance mechanisms as initial systemic therapies. However, methods to determine which resistance mechanism will develop, diagnostic tests to detect these changes, and factors influencing the kinetics of resistance are still largely unknown.

In this study, we modeled in vitro resistance to PF00299804 in the TKI sensitive *EGFR* mutant NSCLC cell line HCC827 (Engelman et al., 2007b; Ogino et al., 2007). We also examined HCC827 cells exposed transiently to HGF ligand in the presence of an EGFR inhibitor. Surprisingly, the results from both of these avenues of investigation led us to determine that *MET* amplification pre-exists in a subpopulation of cells prior to treatment with a TKI, and that HGF dramatically accelerates the selection of these cells. The findings from these analyses suggest that assessment of treatment naïve cancers can inform more effective clinical therapeutic strategies for *EGFR* mutant lung cancer patients.

3.3 Materials and Methods

Cell culture reagents, viability studies and Western analyses

HCC827 GR (del E746_A750/*MET* amplified) cells were maintained in RPMI 1640 (Cellgro; Mediatech Inc., Herndon, CA) supplemented with 5% FBS and have been described previously (Engelman et al., 2007b). H3255 cells were maintained in ACL-4 media (Invitrogen, Carlsbad, CA) supplemented with 5% FBS. All growth medium was supplemented with 100 units/mL penicillin, 100 units/mL streptomycin, and 2 mM glutamine. Cell lines and growth conditions for HCC827 and PC-9 cells, as well as EGFR and MET inhibitors are described in Chapter 2 Materials and Methods. Cell viability was assessed 72 hours following drug exposure by Syto60 staining (Invitrogen) as described in Chapter 2. Cells were lysed in an NP-40 containing lysis buffer, separated by SDS/PAGE electrophoresis and transferred to PVDF membranes. Immunoblotting was performed according to the antibody manufacturer's recommendations. Antibody binding was detected using enhanced chemiluminescence (PerkinElmer, Waltham, MA) and antibodies are described in detail in Chapter 2.

Generation of in vitro drug resistant HCC827 cells

To generate a resistant cell line, HCC827 cells were exposed to increasing concentrations of PF00299804 similar to our previously described methods (Engelman et al., 2006b; Engelman et al., 2007b). PF00299804 concentrations were increased stepwise from 1 nM to 1 µM when the cells resumed growth kinetics similar to untreated parental cells. To confirm the emergence of a resistant clone, MTS assays were performed following growth at each concentration.

Xenograft Studies

HCC827 PFR6 xenograft studies were performed in accordance with the standards of the Institutional Animal Care and Use Committee (IACUC) under a protocol approved by the Animal Care and Use Committee of Massachusetts General Hospital as described in Chapter 2 Materials and Methods. PF2341066 was dissolved in sterile water and administered at 25mg/kg/day. PF00299804 was dissolved in a 0.05N lactate buffer and administered at 10 mg/kg/day.

SNP analyses

SNP analyses to evaluate genome wide copy number changes were performed as previously described (Engelman et al., 2007b). Comparison of gene copy number between HCC827 and the PFR clones was performed using dChip software according to previously established methods (Engelman et al., 2007b; Zhao and Vogt, 2008). SNP data is available from the ncbi gene expression omnibus database (accession number: GSE18797).

EGFR and MET genomic analyses

The *EGFR* tyrosine kinase domain (exons 18-21) from the HCC827 PFR clones were examined for genetic alterations using a modification of previously described sensitive gene scanning methods (Engelman et al., 2006b; Janne et al., 2006). The PCR primers and conditions are available upon request. The relative copy number for *MET* was determined using quantitative real time PCR using a PRISM 7500 sequence detection kit (Applied Biosystems) and a QuantiTect SYBR Green PCR Kit (Qiagen, Inc., Valencia, CA) and as previously described (Engelman et al., 2007b).

FISH probes and hybridization

Bacterial artificial chromosome (BAC) clones CTD-2257H21 (*EGFR* (7p11.2)) and RP11-95I20 (*MET* (7q31.2)) were purchased from Children's Hospital Oakland Research Institute (CHORI; Oakland, CA). DNA was extracted using a Qiagen kit (Valencia, CA) and labeled with Spectrum Green- or Spectrum Orange-conjugated dUTP by nick translation (Vysis/Abbott Molecular, Des Plaines, IL). The CEP7 probe (Vysis/Abbott Molecular, Des Plaines, Il) was used according to manufacturer's instructions. Chromosomal mapping and hybridization efficiency for each probe set were verified in normal metaphase spreads (data not shown). Three color FISH assays were performed as previously described (Engelman et al., 2007b).

High throughput fluorescence in situ hybridization

A Bioview work station with Duet^TM software (Bioview Ltd, Rehovot, Israel) was used to screen for rare *MET* amplified cells. Automatic scans were performed according to manufacturer's suggested guidelines after setting classification criteria for each FISH probe. Images were captured and classified in an automated fashion and manually reviewed to ensure accuracy. Any unclassified images were manually reviewed and

scored. Any cells that could not be scored were excluded from the analysis. Paraffin embedded specimens derived from NSCLC patients or from xenografts were manually scanned for evidence of *MET* amplification.

FACS analysis for GFP positive cells

Cells were harvested, resuspended in 0.5% FBS in phosphate buffered saline, and stained with 1µg/mL Propidium Iodide (PI) Staining Solution (BD Biosciences, San Jose, CA). Cells were analyzed on a FACSAria flow cytometer (BD Biosciences, San Jose, CA) equipped with a 30mW Argon air-cooled laser and signals were detected through a 530/30 bandpass filter for GFP and 575/26 bandpass for PI.

NSCLC Patients

Tumor specimens from gefitinib or erlotinib treated patients analyzed for *MET* copy number, *EGFR* mutational status and HGF expression level are described in detail in Chapter 2 Material and Methods.

3.4 Results

MET amplification causes resistance to the irreversible EGFR inhibitor PF00299804 by activating ERBB3 signaling.

We generated *in vitro* resistant clones of HCC827 cells to the irreversible pan-ERBB kinase inhibitor, PF00299804, using previously described methods (Engelman et al., 2006b; Engelman et al., 2007b). HCC827 cells were exposed to increasing concentrations of PF00299804, starting with 1nM, until they were able to proliferate freely in 1µM PF00299804, which occurred after 6 months of drug selection. This concentration was chosen because it is ~1000 fold greater than the
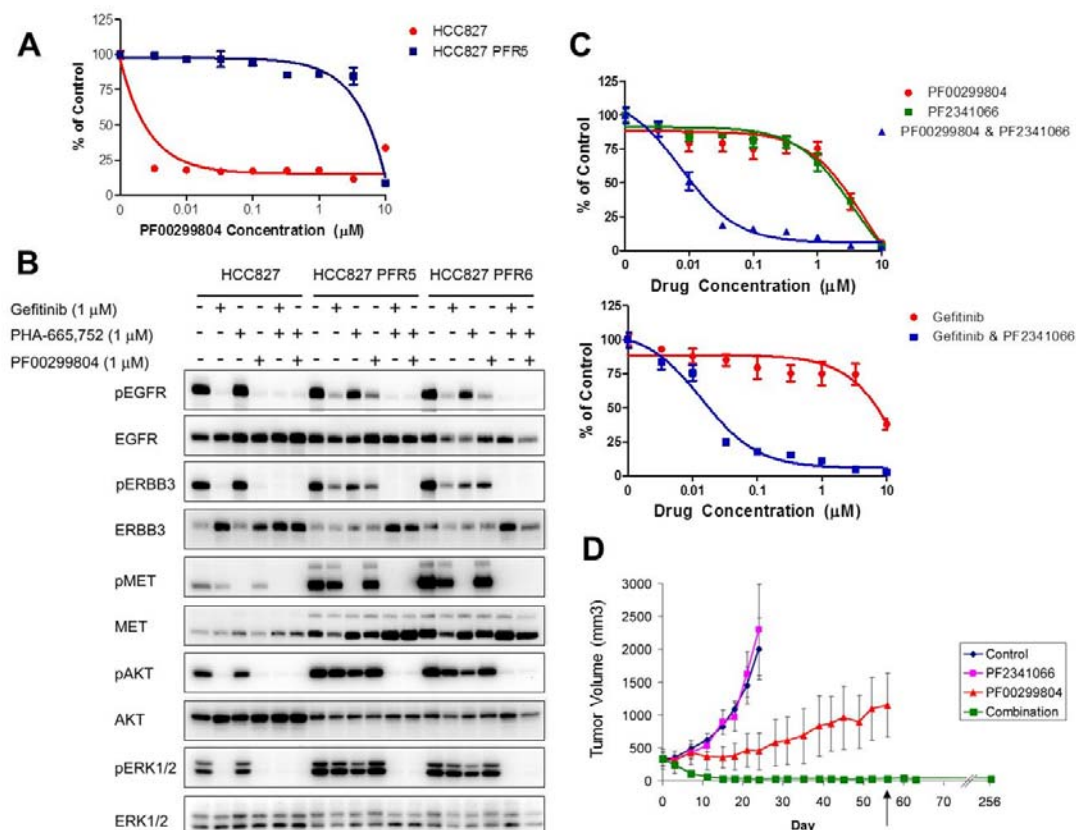
Figure 10. HCC827 PFR cells are resistant to PF00299804, but combined MET and EGFR inhibition blocks PI3K/AKT and ERK signaling and restores sensitivity *in vitro* and *in vivo*. (A) Parental and resistant HCC827 PFR5 cells treated with increasing concentrations of PF00299804. Cell viability relative to untreated controls measured after 72 hours. Each data point represents the mean ±SD of 6 wells. **(B)** HCC827 and HCC827 PFR5 and PFR6 cells were treated for 6 hours with 1 mM PF00299804 or gefitinib, PHA-665,752, or their combination. Cell lysates were immunoblotted to detect indicated proteins. **(C)** *Upper,* HCC827 PFR6 cells treated with increasing concentrations of PF00299804, PF2341066, or their combination. *Lower,* HCC827 PFR6 cells treated with increasing concentrations of gefitinib alone or in combination with PF2341066. Cell viability relative to untreated controls measured after 72 hours. Each data point represents the mean ±SD of 6 wells. **(D)** HCC827 PFR xenogafts in *nu/nu* mice were treated with PF2341066, PF00299804, or their combination. Tumors measured twice weekly. Only combination treatment led to tumor shrinkage and was the most effective treatment in vivo (p < 0.0001). Treatment was stopped after 56 days (arrow) and no tumor re-growth was observed in 35 weeks. Each data point represents the mean ±SD for 5 mice.

IC_{50} for growth inhibition of HCC827 cells and approximately 5 times greater than the serum concentration of PF00299804 observed in NSCLC patients in the phase I clinical trial (Janne et al., 2008; Schellens et al., 2007). Five independent clones were isolated and expanded for further studies. All five HCC827 <u>PF</u>00299804 <u>R</u>esistant (PFR) clones were resistant to PF00299804 *in vitro* (Figure 10A and data

not shown). No secondary EGFR mutations (e.g. T790M) were detected in any of the clones (data not shown).

We next examined the effects of PF00299804 on EGFR, ERBB3, AKT and ERK phosphorylation in the HCC827 PFR clones. Unlike in parental HCC827 cells, ERBB3 activation as well as downstream PI3K/AKT and ERK signaling is maintained in the presence of PF00299804 in HCC827 PFR cells (Figure 10B). We also observed increased total MET protein in the HCC827 PFR cells, and combined MET and EGFR inhibition down-regulated ERBB3, AKT and ERK phosphorylation as well as the modest EGFR phosphorylation that was maintained in the presence of PF00299804 alone (Figure 10B). This behavior following treatment with PF00299804 alone or in combination with a MET inhibitor is similar to that observed in gefitinib resistant HCC827 cells (HCC827 GR cells), which were generated in an analogous manner and contained a focal amplification in chromosome 7 harboring the *MET* oncogene (Engelman et al., 2007b).

Given the similarities in the HCC827 PFR and GR cells following treatment with either PF00299804 or gefitinib, respectively, we determined whether the addition of a MET inhibitor would overcome resistance to PF00299804. We used both a tool compound PHA-665,752 and the MET inhibitor PF2341066 currently undergoing clinical development (Figure 10C**,** *upper* and data not shown) (Zou et al., 2007). The combination of PF00299804 and a MET inhibitor effectively inhibited the growth of HCC827 PFR cells while neither agent alone led to growth inhibition (Figure 10C**,** *upper* and data not shown). In addition, the combination of gefitinib and PF2341066 also effectively inhibited the growth of HCC827 PFR cells (Figure 10C**,** *lower*). These findings further suggest that the resistance mechanism in the HCC827 PFR cells is not unique or dependent on the differences between reversible (gefitinib) or irreversible (PF00299804) EGFR inhibitors but rather due solely to *MET*

amplification. We also evaluated the effects of the irreversible EGFR inhibitor PF00299804 and the MET inhibitor PF2341066 in an HCC827 PFR xenograft model. Treatment with PF00299804 alone was modestly more effective than treatment with PF2341066 alone, but the tumors demonstrated resistance to PF00299804. However, combined MET and EGFR inhibition completely inhibited tumor growth and produced complete responses (p<0.0001; Figure 10D). In fact, the combination treatment was discontinued after 56 days (Figure 10D; arrow) and no tumor re-growth has been observed to date in any of the xenografts (after more than 35 weeks off therapy) (Figure 10D), suggesting that the mice have been cured.

We next determined whether the increase in MET protein expression was due to *MET* amplification in the HCC827 PFR cells (Figure 11A). All of the PFR clones contained at least a four fold amplification of *MET*, similar to the amplification previously observed in the gefitinib resistant HCC827 (HCC827 GR) cells ((Engelman et al., 2007b) and Figure 11A). All of the PFR clones also had higher levels of MET protein expression (Figure 11B). Genome-wide SNP analysis revealed that the only area of significant copy number gain in HCC827 PFR cells is on distal chromosome 7, similar to that observed in HCC827 GR cells, and contains the *MET* oncogene (Figure 11C, D). Furthermore, HCC827 PFR and GR cells share single copy losses of 4p, 5q, 14p, 14q and 19p, but only HCC827 PFR cells have a single copy loss of 16q. Intriguingly, further examination of the region of *MET* amplification on distal chromosome 7 in both set of clones showed that, although the copy number changes within the amplicons are not identical in the HCC827 GR and PFR cells, the size and the proximal borders of the amplicons are very similar (Figure 11D). Together these findings, along with the multiple shared regions of single copy genomic loss between the HCC827 PFR and GR cells, suggest that the resistant clones may have arisen from a common origin.
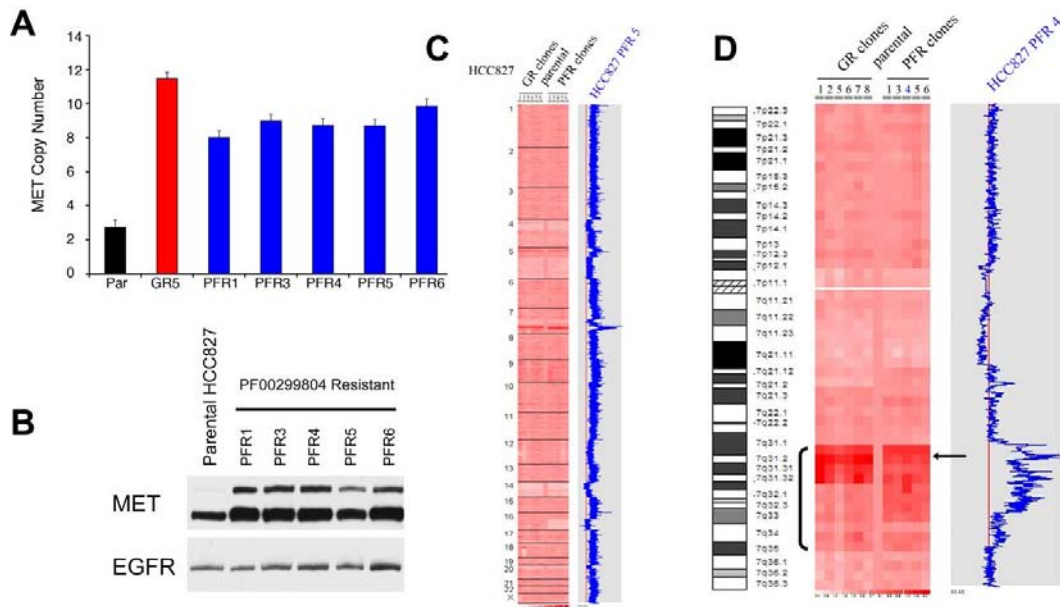
Figure 11. HCC827 PFR cells have a focal amplification in *MET* that is similar to HCC827 GR cells. (A) *MET* copy number determined by quantitative PCR. Parental (Par) HCC827 and *MET* amplified HCC827 GR (GR5) cells were used as negative and positive controls, respectively. Each column represents the mean ±SD for 3 independent experiments. **(B)** Parental HCC827 cells and PFR clones were immunoblotted to detect indicated proteins. **(C)** Genome wide view of copy number changes generated using Human Mapping 250K Sty single nucleotide polymorphism (SNP) array and analyzed using the dChip program (see Materials and Methods). HCC827 GR clones were compared with HCC827 PFR and HCC827 parental clones. Blue curve indicates degree of amplification of each SNP from 0 (left) to 8 (right). **(D)** Chromosome 7 view of copy number changes in HCC827 parental, GR and PFR cells. Arrow indicates *MET* oncogene.

Transient HGF exposure leads to the development of MET amplification and stable ligand-independent gefitinib resistance in HCC827-50GR cells

As described in the previous chapter, HGF ligand potently activates PI3K/AKT and MEK/ERK signaling in EGFR driven cell lines and causes resistance to gefitinib. However, because HGF-induced resistance to EGFR TKIs appears intimately linked to ligand-induced activation of downstream signaling, we hypothesized that long-term resistance would require continuous exposure to HGF. We observed that by replenishing cells with HGF in combination with the EGFR TKI every 3 days, cells continue to be highly resistant indefinitely (data not shown). Thus, we treated each cell line with HGF in the presence of an EGFR inhibitor for 14 days,

and then removed HGF, but maintained the cells in the EGFR TKI. Surprisingly,

HCC827 cells treated transiently with HGF remained permanently resistant to

gefitinib after HGF withdrawal (Figure 12A, B).
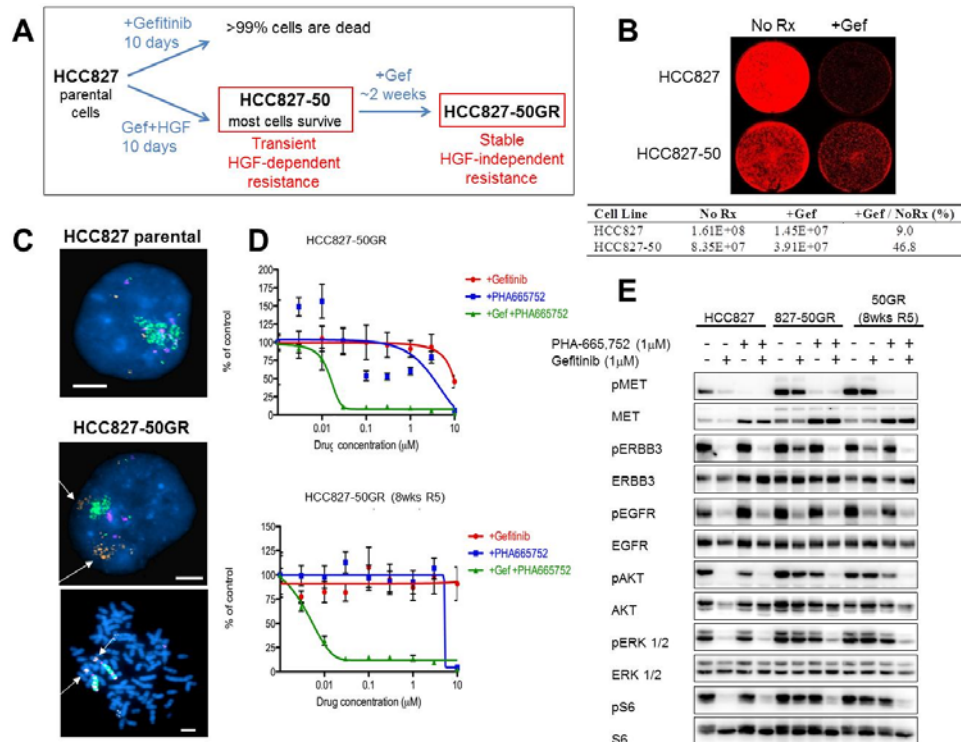
Figure 12. Transient HGF exposure leads to *MET* amplification and stable ligand-independent gefitinib resistance in HCC827 cells. (A) HCC827 cells treated with HGF (50ng/mL) and 1μM gefitinib are resistant to gefitinib (HCC827-50 cells). After the removal of HGF, stably resistant HGF-independent HCC827-50GR cells survive in 1μM gefitinib alone. In contrast, parental HCC827 cells do not survive when treated with 1μM gefitinib. **(B)** Parental HCC827 cells and HCC827-50 cells (pre-treated with gefitinib in combination with HGF (50ng/mL) for 14 days) were grown in media alone (No Rx) or media treated with 1μM gefitinib (+Gef) for 7 days. Viable cells were visualized and quantified using Syto60 staining. **(C)** Fluorescence in situ hybridization (FISH) of *MET/EGFR/CEP7* probe set with HCC827 and HCC827-50GR cells. *MET* (orange) *EGFR* (green) *CEP7* (aqua). Metaphase spread (*bottom*) shows multiple copies of *EGFR* and *MET* (arrow) on individual chromosomes. Scale bars represent 10μm. **(D)** HCC827-50GR cells (*upper*) and HCC827-50GR cells grown in media alone (without gefitinib) for 8 weeks, 50GR 8wks R5 (*lower*), were treated with increasing concentrations of gefitinib or PHA-665,752 or their combination for 72 hours. Cell viability was measured relative to untreated controls. Each data point represents the mean ±SD of 6 wells. **(E)** HCC827 cells and stably resistant HCC827-50GR cells were treated for 6 hours with gefitinib, PHA-665,752, or their combination. All drugs were used at 1μM. Cell lysates were immunoblotted to detect indicated proteins.

These stably resistant cells were termed HCC827-50GR (50ng HGF Gefitinib

Resistant) cells (Figure 12A). In contrast, HCC827 cells that are not pretreated with

HGF, develop gefitinib resistance only after 6 months of gradually increasing

concentrations of drug exposure (Engelman et al., 2007b). In addition, when

HCC827-50GR cells were grown in media alone (without gefitinib) for eight weeks,

these cells (HCC827-50GR (8wksR5)) maintained their resistance (Figure 12D).

Treatment with HGF alone (without gefitinib) for 14 days did not yield stably resistant

cells (Figure 13). Thus, lasting resistance conferred by transient HGF requires the

selective pressure of gefitinib during ligand exposure.

Cell Line	No Rx	+TKI	+TKI / NoRx (%)
HCC827	2.21E+08	1.42E+07	6.4
HCC827 +HGF14d	1.84E+08	1.41E+07	7.7
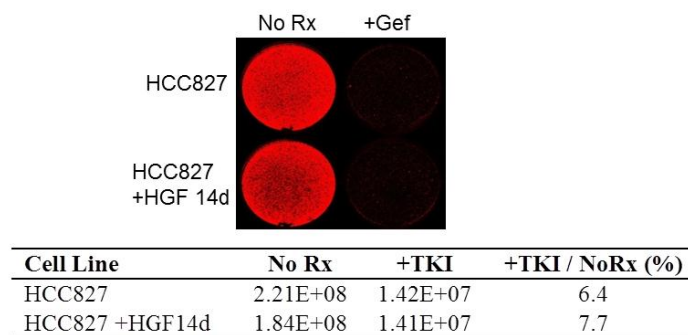
Figure 13. Selective pressure is necessary for HGF-mediated gefitinib resistance in HCC827 cells. Parental HCC827 cells, and HCC827 cells pre-treated with HGF (50ng/mL) in the absence of gefitinib for 14 days (HCC827 +HGF 14d), were seeded on a 6-well plate and grown in media alone (No Rx) or treated with 1μM gefitinib for 9 days. Viable cells were visualized using Syto60 staining.

Stably resistant HCC827-50GR cells maintained PI3K/AKT, mTORC1 and

ERK activation in the presence of gefitinib. Surprisingly, ERBB3 also remained

phosphorylated in HCC827-50GR cells treated with gefitinib (Figure 12E), which

suggests that although initial HGF-mediated resistance mechanisms utilized GAB1 to

activate PI3K/AKT signaling, the ligand-independent HCC827-50GR cells utilize

ERBB3 to activate PI3K/AKT signaling. This observation suggests that short-term

exposure to HGF may lead HCC827 cells to develop or select the same mechanism

of stable resistance, through activation of ERBB3/PI3K signaling, as was observed in

MET amplified HCC827 GR cells (Engelman et al., 2007b). Unlike the HCC827 cells,

several other EGFR-driven cancer cell lines that were made resistant to EGFR TKIs

by HGF treatment did not maintain stable ligand-independent resistance after the withdrawal of HGF (data not shown, see Turke at al., *Cancer Cell* 2010, Supplemental Figure 4). These findings suggest that HCC827 cells are uniquely poised to develop stable ligand-independent resistance.

Stably-resistant HCC827-50GR cells had increased total MET protein levels compared to parental cells and maintained MET phosphorylation in the presence of gefitinib (Figure 12E), mimicking *MET* amplified HCC827 GR cells. Therefore, we examined *MET* copy number using fluorescent in situ hybridization (FISH), and found significant *MET* copy number gains in HCC827-50GR cells compared to parental cells (Figure 12C). Quantitative PCR demonstrated a three to four fold amplification of *MET*, similar to the HCC827 GR and PFR cells (data not shown). These results suggest that *MET* amplification may be driving ERBB3/PI3K/AKT signaling and gefitinib resistance in HCC827-50GR cells.

To examine this hypothesis, we exposed HCC827-50GR cells to PHA-665,752 alone or in combination with gefitinib. Only the combination of gefitinib and PHA-665,752 resulted in a substantial reduction in the number of viable cells (Figure 12D, *upper*). In addition, the HCC827-50GR (8wks R5) cells (grown in media without gefitinib for eight weeks) also remained sensitive only to the combination of MET and EGFR inhibition (Figure 12D, *lower*). Further, treatment with gefitinib in combination with PHA-665,752 completely blocked ERBB3 phosphorylation as well as downstream PI3K/AKT, mTORC1 and ERK signaling in HCC827-50GR and HCC827-50GR(8wks R5) cells (Figure 12E). Taken together, these results suggest that MET inhibition restores EGFR dependence and gefitinib sensitivity in HCC827-50GR cells.

These results led us to examine tissue sections from HCC827-HGF xenograft models treated with gefitinib (Figure 7C). Of three tumors that developed gefitinib

resistance, one exhibited significant *MET* amplification (Figure 14A). Thus, *MET*

amplification is also facilitated by HGF *in vivo*.

Cell Line	No of Cells Analyzed	No of Positive Cells
HCC827	4237	6 (0.14%)
HCC827 N1	4812	4 (0.08%)
HCC827 C1	5057	7 (0.14%)
HCC827 C2	6670	2 (0.06%)
H3255	1164	0 (0%)
PC-9	5630	0 (0%)

		Day 0 (%GFP)	Day 19 (%GFP)	fold
Gef+HGF	827-GFP	0.02	.004 ±0.006	<1
NoRx	827-GFP	0.02	0.02	1.0
	GR6-GFP	0.10	32.9 ±7.30	329
	GR6-GFP	0.10	1.21	12.1
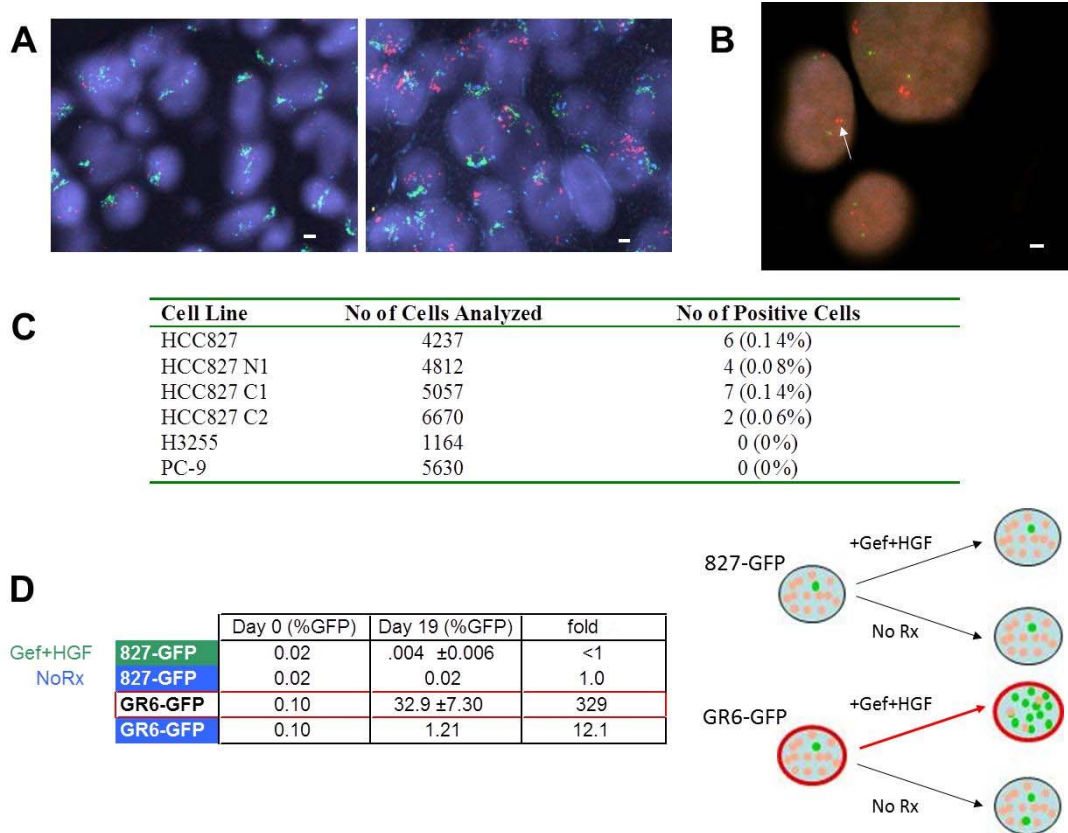
Figure 14. HGF treatment selects out a small pre-existing population of *MET* amplified HCC827 cells from the parental population *in vitro* and *in vivo*. (A) Fluorescence in situ hybridization (FISH) of *MET/EGFR/CEP7* probe set. *MET* (red) *EGFR* (green) CEP7 (aqua). *Left*, tumor sections from control HCC827 xenograft models that do not express HGF showed normal *MET* copy number. *Right,* tumor sections from one of three HCC827-HGF xenografts treated with gefitinib (Figure 7C) showed significant *MET* amplification. **(B)** High-throughput FISH analysis of HCC827 cells identifies a subpopulation harboring *MET* amplification *(arrow)*. *MET* (RP-11-95I120; red); 7qter (RP-11-6903; green). All scale bars represent 10μm. **(C)** Parental HCC827 cells and three independent clones harbor a small percentage of *MET* amplified cells. No pre-existing *MET* amplification was detected in H3255 or PC-9 cell populations. **(D)** *Left*, HCC827 cells were spiked with approximately 0.1% of GFP labeled HCC827 cells or GFP labeled *MET* amplified HCC827 GR6 cells. Each population was grown in either media alone or media treated with gefitinib (1μM) with HGF (50ng/mL). Cells were collected after 19 days and GFP levels were quantified using FACS. Each data point for cells treated with gefitinib+HGF represents the mean ±SD for 3 independent wells. Fold change is the ratio of Day 19 to Day 0 (%GFP). *Right*, diagrammatic depiction of results.

HCC827 cells harbor a small subpopulation of preexisting MET amplified cells and

HGF dramatically accelerates the selection of these cells

Because HCC827 GR, PFR and 50GR cells all eventually develop focal *MET* amplification as a resistance mechanism, we hypothesized that parental HCC827 cells may harbor a pre-existing *MET* amplified clone. We analyzed 4237 individual HCC827 cell nuclei using high-throughput fluorescence in situ hybridization (FISH) (see Materials and Methods) and identified 6 cells (0.14%; 6/4237) that harbored significant *MET* copy number gains (Figure 14B, C). These results were confirmed in an independent experiment using a second gefitinib sensitive parental HCC827 cell line (HCC827 N1; Figure 14C). We also generated two subclones derived from single cells from the gefitinib sensitive parental HCC827 cell line (HCC827 C1 and C2). Both subclones were sensitive to gefitinib *in vitro* (data not shown), and each also contained a low frequency population of *MET* amplified cells (Figure 14C). We further examined the gefitinib sensitive H3255 and PC-9 cells using FISH. Gefitinib resistant clones of both H3255 and PC-9 have been isolated and reported to contain the *EGFR* secondary resistance mutation T790M but not *MET* amplification (Engelman et al., 2006b; Ogino et al., 2007). We did not detect a subpopulation of *MET* amplified cells in the H3255 or the PC-9 cells (Figure 14C).

We hypothesized that the mechanism by which transient treatment with HGF and gefitinib leads to the generation of *MET* amplified HCC827-50GR cells is by selecting out this small population of preexisting *MET* amplified cells from the parental HCC827 cell population. To test this hypothesis, we spiked unlabeled HCC827 parental cells with 0.1% of either GFP labeled HCC827 cells or GFP labeled *MET* amplified HCC827 GR6 cells. We treated these two populations with either media alone (no selection) or with gefitinib in combination with HGF. Media was changed and fresh HGF was added every 72 hours, and cells were collected after 19 days for FACS to quantify the percent of cells with GFP expression. As expected, there was no significant change in the percentage of GFP labeled

46

HCC827 cells at the end of 19 days. However, the percentage of GFP labeled *MET* amplified HCC827 GR6 cells increased over 300 fold to almost 33% in just over two weeks (Figure 14D). Taken together, these results suggest that HGF exposure in the presence of an EGFR inhibitor leads to the rapid selection of a pre-existing *MET* amplified clone in the HCC827 cells (Figure 15).
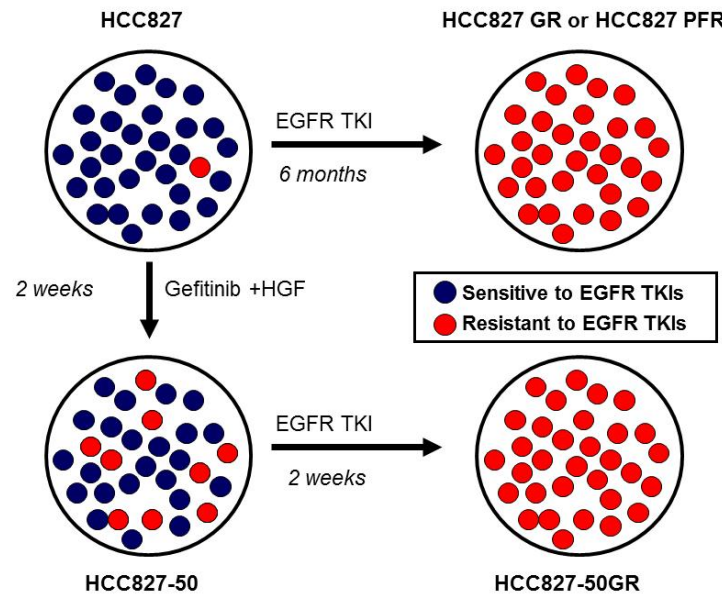
Figure 15. A model for *MET* amplification in HCC827 cells. *MET* amplification preexists at low frequency in the parental HCC827 cells. These *MET* amplified clones can be selected by exposure to an EGFR TKI (either gefitinib or PF00299804) to generate resistant (HCC827 GR or HCC827 PFR) cell lines. Concomitant exposure of HCC827 cells to gefitinib HGF dramatically increases the appearance of the *MET* amplified clones.

Analyses of tumors with acquired resistance to gefitinib/erlotinib reveal evidence of
pre-treatment MET amplification in resistant cancers.

To determine the clinical implications of these observations, we further examined tumor specimens from the panel of paired pre and post treatment samples from NSCLC patients previously described in chapter two (Table 1). Each of these patients had a clinical partial tumor response to gefitinib or erlotinib treatment and subsequently developed clinical drug resistance. We observed *EGFR* T790M in

47

15/27 (55%) and *MET* amplification in 4/27 (15%) of resistant tumor specimens. We

evaluated each of the16 pre-treatment specimens for evidence of *MET* amplification.

In all 4 patients with *MET* amplification in the drug resistant specimens, we observed

rare (<1%) tumor cells with *MET* amplification in the corresponding pre-treatment

specimens (Table 1, Figure 16). In contrast, of 8 cases that had resistant cancers

without *MET* amplification, we observed rare *MET* amplified tumor cells in only 1 of

the corresponding pre-treatment tumor specimens. These findings are consistent

with cell line data (Figure 14B, C) where we observed evidence of pre-existing *MET*

amplification only in the cell line that subsequently develops *MET* amplification as its

resistance mechanism.
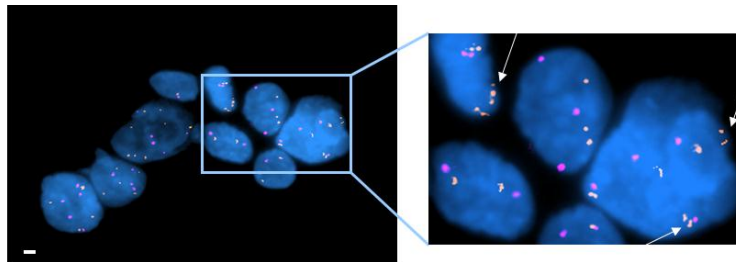
Figure 16. Pre-existing *MET* amplified cells correlate with the development of *MET* amplification as a resistance mechanism to EGFR TKIs in NSCLC patient samples. FISH analysis of the pre-treatment sample from patient 10 (Table 1) shows evidence of a small subset of *MET* amplified cells *(arrows)* before exposure to an EGFR TKI. *MET* (RP-11-95I120; orange); *CEP 7* (aqua). FISH analysis of the post-treatment drug resistant sample from patient 10 (Table 1) showed evidence of *MET* amplification (Table 1, not shown).

3.5 Discussion

Kinase inhibitors have emerged as effective clinical therapies for cancers that

exhibit oncogene addiction to a particular kinase (Demetri et al., 2002; Druker et al.,

2001; Inoue et al., 2006; Mok et al., 2008; Sequist et al., 2008). However, the clinical

success of kinase inhibitor therapies is uniformly limited by the development of drug

resistance. To date, resistance mechanisms have predominately involved secondary

genomic alterations in the target kinase that alter either the physical (such as steric hindrance) or biochemical (change in ATP affinity) properties of the receptor and result in drug resistance (Gorre et al., 2001; Shah et al., 2002; Yun et al., 2008). We have previously described *MET* amplification as a mechanism of gefitinib resistance in *EGFR* mutant cancers (Engelman et al., 2007b), leading to persistent activation of both PI3K/AKT and ERK signaling in the presence of the EGFR TKI (Engelman et al., 2007b).

A critical question for all resistance mechanisms to kinase inhibitors is whether they occur as a result of treatment or whether they preexist prior to treatment and are selected out during the course of therapy. At least some imatinib resistant CML clones are thought to be present at low levels *prior* to treatment and undergo clonal selection during imatinib exposure (Hofmann et al., 2003; Roche-Lestienne et al., 2003; Roche-Lestienne et al., 2002; Shah et al., 2002). Similarly, *EGFR* T790M can be detected at low levels in *EGFR* mutant NSCLC patients prior to gefitinib or erlotinib treatment (Maheswaran et al., 2008). Our current findings provide support that this may also be the case for *MET* amplification both in HCC827 cells (Figure 15) and in NSCLC patients that subsequently develop *MET* amplification at the time of clinical gefitinib or erlotinib resistance (Table 1). The identification of a drug resistance mechanism from a pre-treatment tumor specimen provides the opportunity to specifically target that resistance mechanism prior to its emergence. This approach is clinically appealing as combined treatment with an EGFR and MET inhibitor, specifically in patients with evidence of *MET* amplification at baseline, may lead to a longer time to progression than is currently observed with gefitinib or erlotinib alone (Asahina et al., 2006; Inoue et al., 2006; Mok et al., 2008; Paz-Ares et al., 2006; Sequist et al., 2008; Tamura et al., 2008). In fact, combined EGFR and MET inhibition in HCC827 cells extinguishes the emergence of *MET*

amplified drug resistant clones (data not shown). However, it will be critical to learn whether upfront treatment with combination therapy is tolerable (toxicity) and/or will provide more clinical benefit than treatment at the time of relapse.

Intriguingly, HCC827 cells appear to be pre-disposed to the development of low level *MET* amplification as subclones of cells expanded from single cell clones derived from parental HCC827 cells (HCC827 N1 and N2) also are found to contain low levels of *MET* amplification (Figure 14C). *MET* is located at a fragile site in chromosome 7, which facilitates its amplification, and subsequently a selection for clones harboring *MET* amplification can occur under drug pressure (Hellman et al., 2002). Why this occurs only in the HCC827 cells and a subset of lung cancers, and not in other *EGFR* mutant cell lines and cancers, is currently unknown. Collectively, these studies suggest, but do not prove that the specific mechanisms of resistance that will develop as a result of drug exposure may be pre-determined and occur as a result of drug selection. Understanding why some *EGFR* mutant cancers are pre-disposed to develop *MET* amplification will help further refine the clinical development of EGFR and MET inhibitor combinations.

In this study, we demonstrate that in addition to its ability to activate downstream signaling pathways and mediate short-term resistance in multiple EGFR-driven cell line models, HGF also accelerates the emergence of *MET* amplification in HCC827 cells both *in vitro* and *in vivo*. Intriguingly, this process requires concomitant EGFR inhibition, as HGF exposure alone does not lead to emergence of *MET* amplified clones. It is possible that in the presence of EGFR inhibition, HGF provides a unique proliferative advantage to a subset of cells with high MET expression (those with amplification) thus facilitating their rapid clonal expansion. Activation of MET signaling is a unique resistance mechanism to kinase inhibitors as it can occur through multiple independent mechanisms, amplification

and/or ligand mediated, and when combined can lead to rapid evolution of drug resistance.

Our current findings suggest further therapeutic strategies for EGFR mutant NSCLC. First, this study implies that the therapeutic combination of an irreversible EGFR inhibitor (effective against *EGFR* T790M) and a MET inhibitor is an attractive treatment combination for a significant portion of gefitinib/erlotinib resistant *EGFR* mutant NSCLC patients. In addition, these findings highlight the potential to prospectively identify treatment naïve *EGFR* mutant lung cancer patients who are likely to develop *MET* amplification and may benefit from initial combination therapy with a MET inhibitor. Finally, our results suggest that in patients with high levels of HGF expression, the kinetics of selection of preexisting *MET* amplified cells and the development of resistance to single agent EGFR inhibitors will be accelerated.

Chapter 4- MEK feedback activation of PI3K/AKT signaling[3]

4.1 Abstract

The PI3K/AKT and RAF/MEK/ERK signaling pathways are critically activated in a wide range of human cancers. In many cases, inhibition of both pathways is necessary to block proliferation and induce cell death and tumor shrinkage. Several feedback systems have been described in which inhibition of one intracellular pathway leads to activation of a parallel signaling pathway, thereby decreasing the effectiveness of single-agent targeted therapies. In this study we describe a feedback mechanism in which MEK inhibition leads to activation of PI3K/AKT signaling in EGFR and HER2 driven cancers. We find that MEK inhibitor-induced activation of PI3K/AKT results from hyperactivation of ERBB3. This is caused by loss of an inhibitory threonine phosphorylation in the conserved juxtamembrane (JM) domains of EGFR and HER2. Mutation of this amino acid leads to increased ERBB receptor activation and up-regulation of ERBB3/PI3K/AKT signaling, that is no longer responsive to MEK inhibition. These results further characterize the important feedback networks regulating central oncogenic pathways in human cancer and support the use of combination therapies in the clinic.

4.2 Introduction

The phosphatidylinositol 3-kinase (PI3K), RAF/MEK/ERK mitogen-activated protein kinase (MAPK), and mammalian target of rapamycin complex 1 (mTORC1) signaling pathways transmit signals from membrane bound receptor tyrosine kinases (RTKs) to multiple downstream effector networks regulating cell growth, metabolism,

---

[3] Excerpts and figures from this chapter are in preparation for submission (Turke et al. MEK inhibition relieves a negative feedback on ERBB receptors activating PI3K/AKT signaling. 2011 *(in preparation)*).

survival, and proliferation (Engelman, 2009; Guertin and Sabatini, 2007; Montagut

and Settleman, 2009). Numerous feedback systems regulating these central

oncogenic pathways have been described, and these feedbacks can impact the

sensitivity of cancers to specific kinase inhibitors. For example, inhibition of

mTORC1 relieves proteasomal degradation of IRS-1 leading to feedback up-

regulation of IRS-1/PI3K/AKT signaling, reducing the efficacy of mTORC1 inhibitors

as single agents and prompting the use of combination therapies (Carracedo et al.,

2008; O'Reilly et al., 2006). PI3K and AKT inhibitors have been shown to relieve a

negative feedback on ERBB receptors and other RTKs through de-repression of

forkhead transcription factors, leading to increased transcription of these receptors.

Increased RTK expression correlates with partial re-activation of PI3K/AKT signaling,

MEK/ERK signaling, and other downstream pathways, potentially limiting the utility of

PI3K inhibitors as single agents (Chakrabarty et al., 2011; Chandarlapaty et al.,

2011; Serra et al., 2011). Similarly, we and others have shown that MEK inhibition

leads to increased AKT activation, often resulting in reduced efficacy of MEK

inhibitors as single agents (Faber et al., 2009; Hoeflich et al., 2009; Mirzoeva et al.,

2009). However, the mechanism by which MEK inhibition leads to increased AKT

signaling has not yet been resolved.

Targeted therapies such as the EGFR inhibitors gefintinib and erlotinib are

extremely effective when cells are "addicted" to EGFR. Inhibition of the driving RTK

leads to down-regulation of critical growth and survival signaling pathways,

especially PI3K/AKT and MEK/ERK (Engelman and Settleman, 2008; Faber et al.,

2009; Ono et al., 2004). We recently determined that treatment with a combination of

a MEK inhibitor and a PI3K inhibitor led to significant apoptosis in EGFR-driven

cancers, similar to that induced by an EGFR TKI, whereas treatment with either

pathway inhibitor alone was not sufficient to induce marked cell death (Faber et al.,

2009). In those studies, we observed that treatment with a single-agent MEK inhibitor led to increased activation of AKT phosphorylation. Currently, there are multiple MEK and BRAF inhibitors, including the highly selective allosteric MEK1/2 inhibitor, AZD6244 (Yeh et al., 2007), being developed as cancer treatments. However, the feedbacks induced by MEK inhibitors that may ultimately impact their utility are poorly understood.

In cancers that are addicted to receptor tyrosine kinases, such as *EGFR* mutant lung cancers and *HER2* amplified breast cancers, receptor dimerization leads to tyrosine phosphorylation and recruitment of adaptor proteins to the cell membrane, which in turn lead to activation of downstream effectors including PI3K/AKT and RAF/MEK/ERK signaling pathways. The ERBB3 receptor is a kinase dead member of the ERBB family that commonly serves as a scaffold in EGFR and HER2 driven cancers. ERBB3 directly binds to PI3K when it is tyrosine phosphorylated at YXXM motifs by other RTKs. Class I phosphoinositide 3-kinase (PI3K) is a heterodimer composed of a p110α catalytic subunit and a p85 regulatory subunit. In un-stimulated cells, PI3K exists in the cytoplasm in an inactive conformation. However, when receptors or adaptor proteins become activated, the two p85 src homology 2 (SH2) domains bind to phosphorylated tyrosine residues in YXXM motifs. As a result, PI3K is recruited to the cell membrane and p110α is released from p85 inhibition, allowing for the phosphorylation of the membrane lipid phosphatidylinositol 4,5-bisphosphate (PIP$_2$) to produce phosphatidylinositol 3,4,5-trisphosphate (PIP$_3$). This leads to the recruitment and activation of several downstream signaling effectors including AKT.

In this study, we examine the molecular mechanism by which MEK inhibition leads to increased PI3K/AKT and RAF/MEK signaling. We provide evidence suggesting that this feedback activation occurs via ERBB3 through loss of an

54

inhibitory ERK-dependent threonine phosphorylation in the conserved JM domains of EGFR and HER2, previously found to regulate to EGFR auto-phosphorylation (Red Brewer et al., 2009). Elucidation of this mechanism provides a greater understanding of the feedback systems regulating these key pathways that drive human cancers, and supports the argument in favor of combining MEK inhibitors with ERBB inhibitors, or PI3K inhibitors, in the clinic.

4.3 Materials and Methods

Cell culture and reagents

The *EGFR* mutant NSCLC cell lines HCC827 (exon19 del), H4006 (exon19 del), and H1975 (L858R/T790M) have been previously characterized (Amann et al., 2005; Engelman et al., 2006b; Engelman et al., 2007b; Turke et al.). The three *HER2* amplified cell lines used in this study included BT-474, a breast cancer cell line (a kind gift from Dr. Carlos L. Arteaga, Vanderbilt University School of Medicine, Nashville, Tennessee), MD-MBA-453 a breast cancer cell line, and NCI-N87 a gastric cancer cell line. The three *KRAS* mutant colorectal cancer cell lines used in this study included SW837, SW1463 and Gp5d cells. Both MD-MBA-453 and NCI-N87 cells, and the three *KRAS* mutant cell lines were provided by the Center for Molecular Therapeutics (Massachusetts General Hospital). HCC827, H4006, H1975, NCI-N87, SW1463, SW837, and Gp5d cell lines were maintained in RPMI 1640 (Cellgro; Mediatech Inc., Herndon, CA) supplemented with 10% FBS. BT-474 and MDA-MB-453 cells were maintained in Dulbecco's Modification of Eagle's Medium (DMEM) (Cellgro; Mediatech Inc., Herndon, CA) supplemented with 10% FBS. CHO-KI cells were purchased from ATCC and maintained in DMEM/F12 supplemented with 10% FBS. All growth medium was supplemented with 100 units/mL penicillin, 100 units/mL streptomycin, and 2 mM glutamine.

AZD6244 (ARRY-142886) was purchased from Selleck Chemicals (Houston, TX) and used at 2uM. Rapamycin (Sigma) was used at 50nM. Gefitinib (American Custom Chemical Corporation), lapatinib (LC Laboratories Woburn, MA), the AKT inhibitor AKT1/2 (Signa-Gen Laboratories), the PI3K inhibitor GDC-0941 (LC Laboratories Woburn, MA), and the IGFR inhibitor NVP-AEW541 (Novartis) were each used at 1μM. All drugs were dissolved in DMSO for cell culture experiments.

Antibodies, Western Blotting, and Immunoprecipitiations

Cells were lysed in an NP-40 containing lysis buffer, separated by SDS/PAGE electrophoresis and transferred to PVDF membranes as previously described (Engelman et al., 2007b; Turke et al., 2010). Immunoblotting was performed according to the antibody manufacturer's recommendations. Antibody binding was detected using enhanced chemiluminescence (PerkinElmer, Waltham, MA). Anti-phospho-Akt (Ser 473 and Thr308), anti-phospho-ERBB-3 (Tyr 1289), anti-phospho-EGFR (Thr 669), anti-phospho-p42/44 MAP kinase (Thr 202 Tyr 204), anti-p42/44 MAP kinase, anti-phospho-MEK1/2 (Ser 217/221), anti-phospho-C-RAF (Ser 338), phospho-GSK3a/B (Ser 21/9), phospho-PRAS40 (Thr 246), phosph-ATP Citrate Lyase (Ser 455), anti-PTEN, anti-phospho-S6 ribosomal protein (Ser 335/236), anti-S6 ribosomal protein, anti-phospho HER2 (Tyr 1211/1222) and anti-phospho-Tyr-100 antibodies were from Cell Signaling Technology (Beverly, MA). Anti-ERBB3, anti-AKT, and anti-EGFR antibodies were purchased from Santa Cruz Biotechnology (Santa Cruz, CA). The phospho-specific EGFR (Tyr1068) antibody was from AbCam (Cambridge, MA). The anti-HER2 antibody was from Oncogene Research Products now Calbiochem (SanDiego, CA). The anti-p85 antibody used for immunoprecipitations was from Millipore (Billerica, MA). Anti-NRDP1 antibody was

purchased from US Biologicals. The Quantikine ELISA Kit for quantification of HRG in HCC827 cell lysates was purchased from R&D Systems (Minneapolis, MN).

For biotin labeling immunoprecipitations, HCC827 cells were washed with PBS and labeled for 1 hour at 4 degrees in the presence of 0.5ug/mL Sulfo-NHS-LC-Biotin (Thermo Scientific) re-suspended in PBS in the presence or absence of AZD6244. Labeling was quenched by washing with 100mM glycine in PBS. Following labeling, cells were returned to media and treated for the indicated number of hours at 37 degrees before lysis. Biotin labeled cell surface proteins were immunoprecipitated with NeutrAvidin Agarose Resins (Thermo Scientific) overnight, separated by SDS page, and immunoblotted to detect the indicated proteins. Transferrin receptor was used as an internal loading control.

PIP$_2$/PIP$_3$ Isolation and Quantification

Following treatment, phospholipids were isolated from cells and PIP$_3$ and PI(4,5)P$_2$ levels were measured using ELISA kits purchased from Echelon (K-2500s and K4500, respectively) according to the manufacturer's instructions.

Xenograft Studies

Xenograft studies were performed in accordance with the standards of the Institutional Animal Care and Use Committee (IACUC) under a protocol approved by the Animal Care and Use Committee of Massachusetts General Hospital. Nude mice (nu/nu; 6-8 weeks old; Charles River Laboratories) were anesthetized using a 2% Isoflurane (Baxter) inhalation oxygen mixture. A suspension of 5x10^6 H1975 cells (in 0.2 ml of PBS) was inoculated subcutaneously into the lower-left quadrant of the flank of each mouse. Once the mean tumor volume reached ~500 mm^3 AZD6244 was administered by oral gavage in 3 doses of 25mg/kg over 30 hours. Tumors were

measured twice weekly using calipers, and volume was calculated using the formula (length x width^2 x 0.52). Mice were monitored daily for body weight and general condition. The experiment was terminated when the mean size of either the treated or control groups reached 2000 mm3 (Faber et al., 2009).

qRT-PCR

RNA was isolated from HCC827 and BT-474 cells using the RNEasy RNA isolation kit (Qiagen) and cDNA was transcribed from 2 µg total RNA with Superscript II Reverse Transcriptase (Invitrogen) and used as a template for subsequent PCR amplifications. The relative copy number for *ERBB3* and *HRG* was determined using quantitative real time PCR using a lightcycler 480 (Roche) as previously described (Faber et al., 2009). The PCR primers and conditions are available upon request.

siRNA and Transient Transfections

ERBB3 s4779 silencer select validated siRNA and silencer negative control siRNA were purchased from Ambion (Austin, TX). Cells were seeded on a 6-well plate for Westen blot or a 6cm plate for FACS in DMEM media without penicillin or streptomycin. Cells were transfected with 50nM siRNA with using HiPerFect Transfection Reagent (Qiagen) according to manufacturer's instructions.

CHO-KI cells were seeded in six-well plates at 50% confluency. Transient transfections were performed with *Trans*IT®-LT1 Transfection Reagent (Mirus Bio LLC, Madison, WI) according to the manufacturer's recommendations. Wild type ERBB3 was co-transfected with an equal ratio of GFP, wild type EGFR, wild type HER2, EGFR T669A or HER2 T677A.

shRNA Constructs, DNA Constructs and Lentiviral Production

The EGFR shRNA hairpin #4705 targeting the 3' UTR (sequence: 5'-CCGG-AGAATGTGGAATACCTAAGG-TTTTG-3') was purchased from Dr. Toshi Shoda (Mass General Hospital, Molecular Profiling Laboratory, Charlestown, MA) in the pLKO-puro vector backbone and has been previously described (Rothenberg et al., 2008). The ERBB3 shRNA hairpin #475 (Engelman et al., 2005), sequence: 5'-CCGG-AATTCTCTACTCTACCATTGCCTC-GAGGCAATGGTAGAGTAGAGAATT-TTTTG-3') was provided by Dr. William Hahn (RNAi Consortium, Boston, MA). The ERBB3 shRNA hairpin was introduced into the inducible tet-on PLKO vector. For the shERBB3 studies, HCC827 cells were infected as previously described (Engelman et al., 2005; Rothenberg et al., 2008) with tet-on PLKO shERBB3 and tet-on PLKO scramble control shRNA (Addgene Cambridge, MA) knockdown vectors and selected in 2 μg/μL puromycin.

The human EGFR (wild type and exon 19del) and HER2 cDNA coding regions were cloned into the pENTR/D-TOPO vector (Invitrogen) and the T669A and T677A mutants were constructed with Quick Change Site-Directed Mutagenesis Kit (Stratagene) according to the manufacturer's instructions and as previously described (Engelman et al., 2006b). All constructs were confirmed by DNA sequencing. EGFR and HER2 wild type, T669A and T677A mutant constructs, and a GFP vector control were cloned into the plenti-IRES-GFP lentiviral vector (Addgene, Cambridge, MA) and infections were performed as described previously (Engelman et al., 2006b).

Flow Cytometry

BT-474 cells were transfected with ERBB3 siRNA (Ambion) for 48 hours and then treated with AZD6244 or GDC-0941 for 48 hours. Following treatment, cells

were collected and stained with propidium iodide (PI) and Annexin V as described

previously (Faber et al., 2006). Cells analyzed using a BD LSR 3 analytical flow

cytometer (BD Biosciences). Percent apoptosis was calculated using the sum of

Annexin V positive and PI/Annexin V double positive cells.

Tandem mass spectrometry (LC/MS/MS)

For targeted mass spectrometry (MS) experiments, EGFR or HER2 proteins

were immunoprecipitated from HCC827 or BT-474 cells that were treated with

AZD6244. Proteins were immunoprecipated overnight using anti-EGFR antibody

(Santa Cruz) or an anti-HER2 antibody, respectively, and were separated using

SDS-PAGE, stained with Coomassie blue, and bands were excised. Samples were

prepared and analyzed by reversed-phase microcapillary/tandem mass spectrometry

(LC/MS/MS) as described previously (Dibble et al., 2009; Egan et al., 2011; Zheng et

al., 2009). Peptide ions representing from EGFR predicted Thr669 phosphorylation

and non-phosphorylated sites were targeted in MS/MS mode for quantitative

analyses using the following ions (Non-PO_4: 678.70, 3+ and 1017.55, 2+, PO_4:

705.36, 3+ and 1057.53, 2+). For the HER2 Thr677 site, the following ions were

used [Non-PO_4: 885.12, 3+; 890.44, 3+(+16 Msx); 895.77, 3+(+32 Msx); PO_4:

911.77, 3+; 917.10, 3+(+16 Msx); 922.43, 3+(+32, 2 Msx)]. MS/MS spectra collected

via CID were searched against the concatenated target and decoy (reversed) Swiss-

Prot protein database using Sequest (Proteomics Browser Software, Thermo

Scientific) with differential modifications for Ser/Thr/Tyr phosphorylation (+79.97) and

differential modification of Met oxidation (+15.99, Msx). Phosphorylated and

unphosphorylated peptide sequences were identified if they initially passed the

following Sequest scoring thresholds against the target database: 1+ ions, Xcorr ≥

2.0 Sf ≥ 0.4, P ≥ 5; 2+ ions, Xcorr ≥ 2.0, Sf ≥ 0.4, P ≥ 5; 3+ ions, Xcorr ≥ 2.60, Sf ≥

0.4, P ≥ 5 against the target protein database with mass accuracy less than 15 ppm.

Manual inspection and determination of the exact sites of phosphorylation was

confirmed using FuzzyIons and GraphMod software (Proteomics Browser Software,

Thermo Scientific). False discovery rates (FDR) of peptide hits (phosphorylated and

non-phosphorylated) were estimated below 1.0% based on reversed database hits.

Relative quantification of phosphorylated peptide signal levels was

performed as described previously (Dibble et al., 2009; Egan et al., ; Zheng et al.,

2009) using the following equations:

$$TIC_{PO4}/(TIC_{PO4}+TIC_{nonPO4}) = Ratio\ of\ phosphopeptide\ signal\ (R_{PO4})$$

These ratios of phosphopeptide signal were then compared to the same

phosphopeptide ratios from the untreated samples according to the following

equation:

$$[(R_{PO4}Treated/R_{PO4}Untreated)-1]\ x\ 100 = \%\ change\ in\ phosphorylation\ upon$$

$$treatment$$

4.4 Results

MEK inhibition leads to activation of ERBB3/PI3K/AKT.

We had previously observed that AKT phosphorylation increased in response

to MEK inhibition in *HER2* amplified and *EGFR* mutant cancers (Faber et al., 2009).

To determine whether this potential feedback is observed in in multiple cancer

models with addiction to EGFR or HER2, we treated a panel of *HER2* amplified or

EGFR mutant cell lines with the MEK inhibitor AZD6244. In each cell line, we

observed a substantial increase in AKT phosphoylation at both S473 and T308

residues, as well as increased phosphorylation of several downstream targets of

AKT including GSK3α, GSK3β, ATP citrate lyase, and PRAS40 (Figure 17A). We

confirmed that the increased phosphorylation of these proteins was indeed a
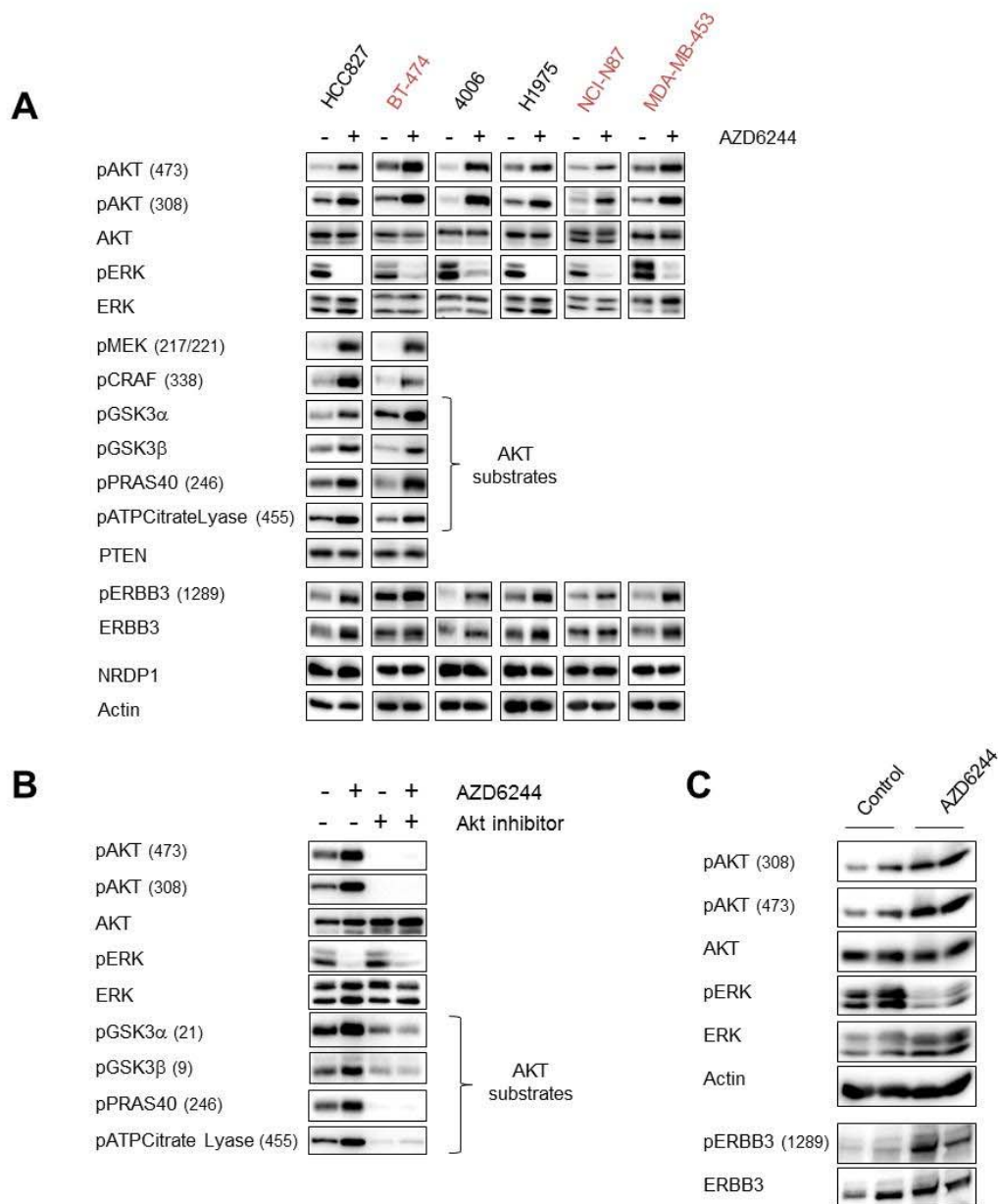
Figure 17. MEK inhibition leads to feedback activation of ERBB3/PI3K/AKT and RAF/MEK signaling. (A) A panel of EGFR-driven (black) or HER2-driven (blue) cell lines were treated with 2µM AZD6244 for 6 hours. Cell lysates were immunoblotted to detect the indicated proteins. **(B)** HCC827 cells were treated with 2µM of AZD6244 or 2µM of an AKT inhibitor or their combination for 6 hours. Cell lysates were immunoblotted to detect the indicated proteins. **(C)** H1975 (EGFR L858R/T790M) xenografts in *nu/nu* mice were treated with three doses of AZD6244 25mg/kg over 30 hours. Mice were sacrificed following treatment and tumors were harvested. Tumor cell lysates were immunoblotted to detect the indicated proteins.

consequence of increased AKT activation, as co-treatment with an allosteric AKT

inhibitor blocked MEK inhibitor induced increases in their phosphorylation (Figure

17B). Of note, we observed that MEK inhibition led to significant up-regulation of

phospho-C-RAF and phospho-MEK (Figure 17A), suggesting the possibility of

activation of a common upstream signaling molecule leading to activation of both

RAF and PI3K signaling. To determine if this feedback mechanism was observed in

vivo as well, we treated an *EGFR*-mutant H1975 (L858R/T790M) xenograft model

with AZD6244 and observed increased phosphorylation of AKT in tumor lysates

(Figure 17C).
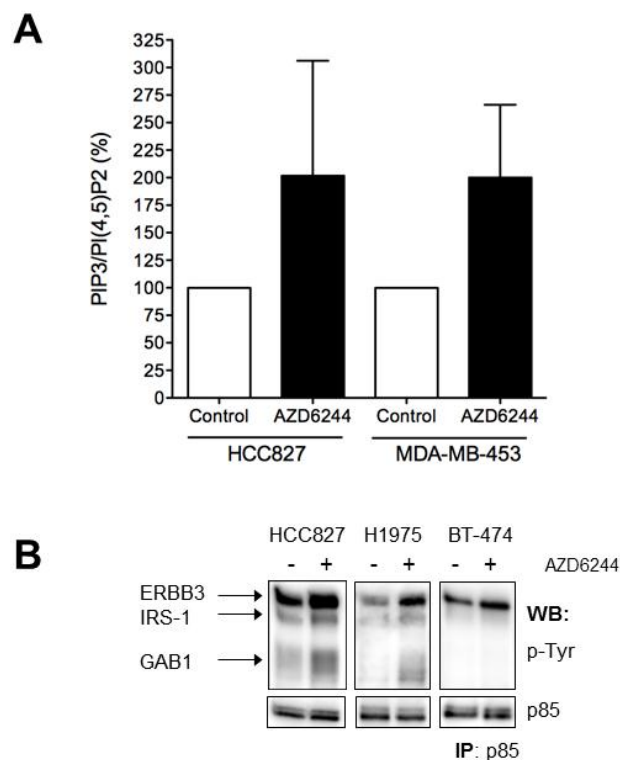
Figure 18. MEK inhibitor-induced feedback increases PI3K signaling and PIP$_3$ production.
(A) HCC827 and MDA-MB-453 cells were treated for 18 hours with 2µM AZD6244. Phospholipids
were isolated from cell lysates and relative PIP$_3$ and PI(4,5)P$_2$ levels were quantified by ELISA.
Each data point represents the mean ±SEM of two independent experiments performed in
triplicate. For normalization, the ratio between PIP$_3$ and PI(4,5)P$_2$ was arbitrarily set to 100%. **(B)**
Cells were treated for 6 hours with 2µM of AZD6244. Cell extracts were immunoprecipitated with
an anti-p85 antibody followed by Western blot with anti-p-Tyr and an anti-p85 antibody.

The increase in AKT phosphorylation suggested that there could be a change in the abundance of PIP$_3$. To directly examine this possibility, we isolated lipids from EGFR-driven HCC827 and HER2-driven MDA-MB-453 cells and quantified PIP$_3$ levels in the presence or absence of a MEK inhibitor. In both cell lines we observed significant increases in PIP$_3$ levels in cells treated with AZD6244 (Figure 18A). The increased amount of PIP$_3$ could be secondary to increased production or decreased degradation. We did not observe any change in expression of the PTEN phosphatase, the 3' phosphatase responsible for de-phosphorylating PIP$_3$ regulation of PI3K signaling (Figure 17A). To determine whether the increases we observed in AKT phosphorylation might be due to increased PI3K activation, we immunoprecipitated the p85 regulatory subunit of PI3K to assess whether there was an increase in the abundance of upstream adaptors. We found that treatment with AZD6244 increased binding of PI3K adaptors including ERBB3 and GAB1 in multiple cell lines, suggesting an increase in PI3K engagement with phospho-tyrosine proteins (Figure 18B). These results are consistent with the notion that MEK inhibition leads to activation of phospho-tyrosine signaling cascades that directly activate PI3K, which in turn increases the abundance of PIP$_3$, ultimately leading to activation of AKT and its downstream substrates.

In EGFR and HER2-driven cell lines, ERBB3 serves as a primary activator of PI3K/AKT signaling (Engelman et al., 2005; Hsieh and Moasser, 2007), and we observed increased ERBB3 binding to PI3K following MEK inhibition (Figure 18B). This led us to investigate whether treatment with a MEK inhibitor also led to increased ERBB3 tyrosine phosphorylation. Indeed, we observed that MEK inhibition substantially increased tyrosine phosphorylated ERBB3 levels (Figure 17A), consistent with the increased binding observed between ERBB3 and PI3K

upon MEK inhibitor treatment (Figure 18B). In some cancer cell lines, we observed

an increase in total ERBB3 along with phospho-ERBB3 (Figure 17A). Of note, we

did not observe a change in expression of the E3-ubiquitin ligase, neuregulin

receptor degradation protein 1 (NRDP1), which has been shown to control the

steady state levels of ERBB3 (Figure 17A) (Carraway, 2010; Diamonti et al., 2002).
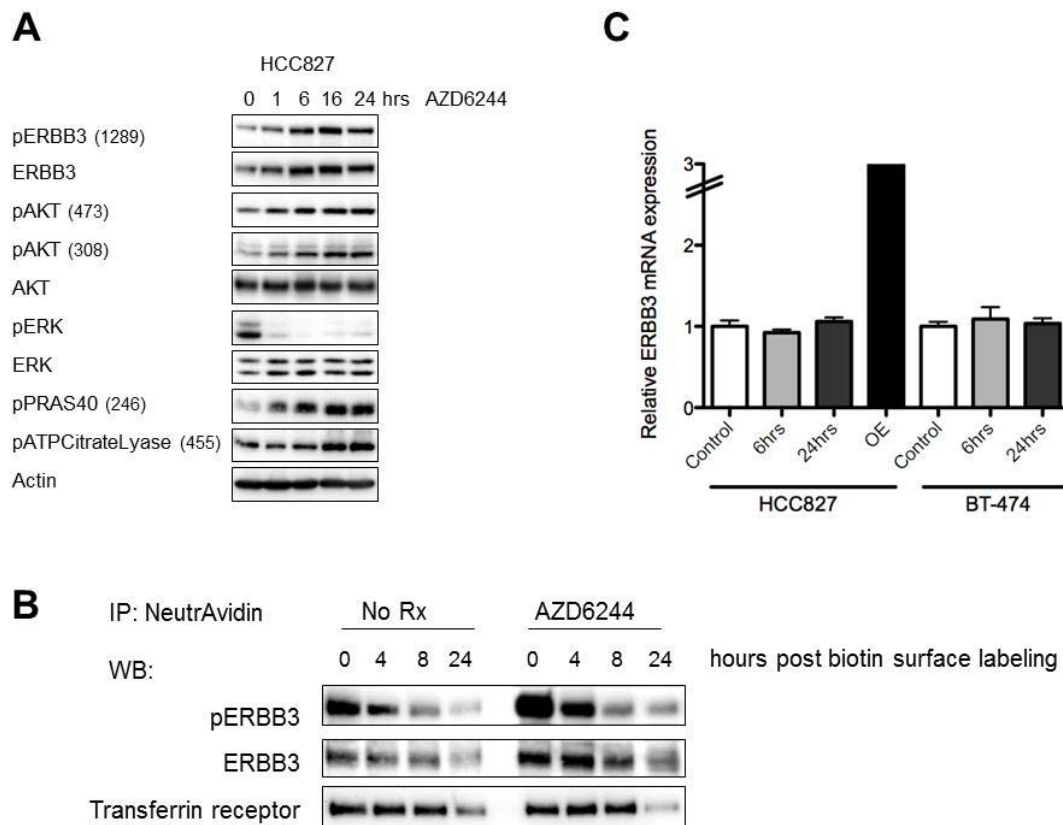
Figure 19. Feedback activation and increased surface localization of ERBB3 is post-transcriptional and occurs within one hour of treatment with AZD6244. (A) HCC827 cells were treated for the indicated number of hours with AZD6244. Cell lysates were immunoblotted to detect the indicated proteins. **(B)** HCC827 cells were treated with DMSO (NoRx) or AZD6244 for 1 hour at 4C degrees during biotin labeling of cell surface proteins. Following labeling, cells were returned to media and treated for the indicated number of hours before lysis. Biotin labeled cell surface proteins were immunoprecipitated with NeutrAvidin beads, separated by SDS page, and immunoblotted to detect the indicated proteins. **(C)** HCC827 or BT-474 cells were treated with AZD6244 for 6 or 24 hours. RNA was collected and transcribed to produce cDNA. ERBB3 cDNA was quantified using qPCR and values were normalized to actin. HCC827 cells significantly over expressing (OE) ERBB3 were used as a positive control. Each data point represents the mean ±SD of three independent experiments.

To assess the kinetics of this feedback response, we treated the *EGFR*-mutant HCC827 cell line with AZD6244 for a time course ranging from 1 to 24 hours. Phosho-ERBB3 and phospho-AKT, as well as activation of downstream substrates, increased after just one hour of MEK inhibition. Feedback activation continued to accumulate over the next several hours, and persisted for 24 hours (Figure 19A). Next, to determine if the feedback activation of ERBB3 occurs on the plasma membrane, we biotin-labeled the surface of HCC827 cells in the presence or absence of AZD6244 and immunoprecipitated these labeled proteins for analysis by Western blot. After just one hour of MEK inhibition during biotin labeling at 4 degrees, surface levels of the activated receptor were significantly elevated (Figure 19B). We also observed increased levels of total ERBB3 on the cell surface following AZD6244 treatment. MEK inhibition did not seem to significantly affect the kinetics of loss of phospho- or total ERBB3 on the cell surface (Figure 19B), suggesting that receptor internalization or cycling was not significantly affected by MEK inhibition.

An increase in total protein levels of ERBB3 and other RTKs via transcriptional up-regulation has been demonstrated as a common mechanism of feedback activation (Chakrabarty et al., 2011; Chandarlapaty et al., 2011). However, the rapid kinetics of MEK feedback on increasing ERBB3 phosphorylation does not favor a transcriptional mechanism for this feedback. To confirm that the increase in phospho and total ERBB3 levels following MEK inhibition was post-transcriptional, we measured ERBB3 mRNA levels by qPCR following treatment with AZD6244 for 6 and 24 hours. As predicted, we did not observe any change in ERBB3 mRNA levels in HCC827 or BT-474 cells treated with AZD6244 (Figure 19C). These data suggest that MEK inhibition leads to increased ERBB3/PI3K/AKT signaling in multiple EGFR

and HER2-driven cancer cell line models, and that this feedback mechanism involves post-transcriptional activation of ERBB3.

Knockdown of ERBB3 abrogates MEK/ERK feedback on AKT and downstream substrates.

To determine if increased phosphorylation of ERBB3 plays a significant role in the activation of AKT following MEK inhibition, we suppressed expression of
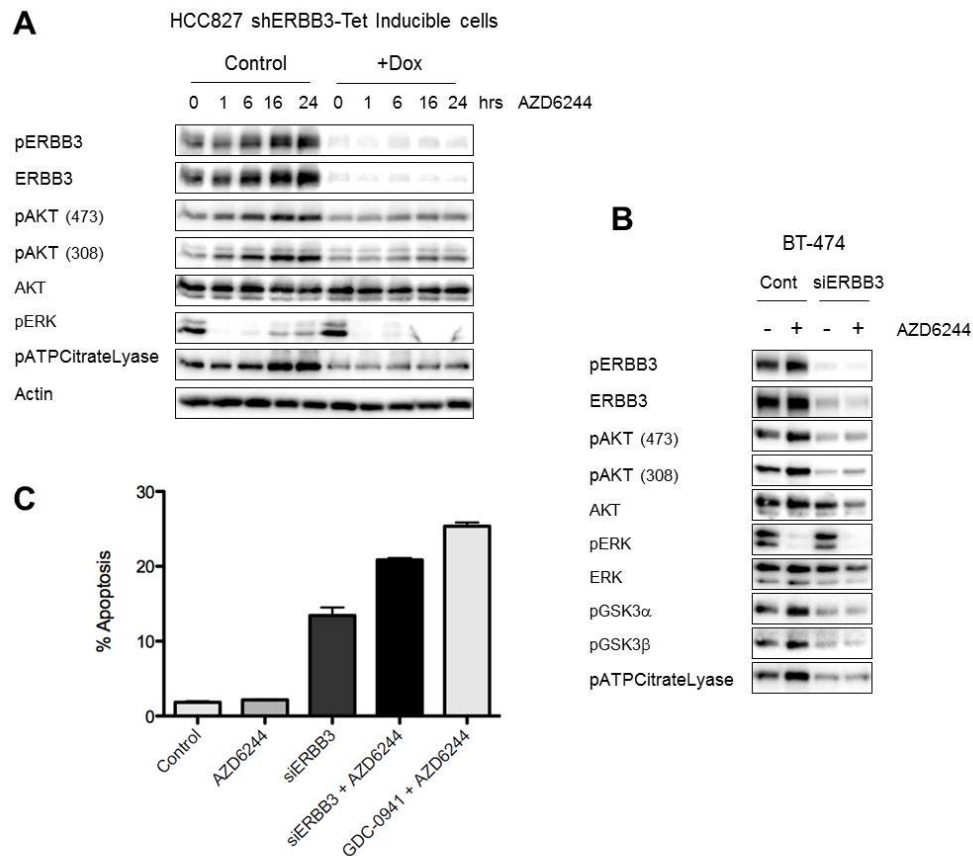
Figure 20. Knockdown of ERBB3 abrogates MEK/ERK feedback on PI3K/AKT signaling. (A) HCC827 cells were infected to express a Tet-inducible shERBB3 hairpin and knockdown was induced with 100ng/mL doxycycline (+Dox) for 48 hours. Following knockdown, cells were treated with AZD6244 for the indicated number of hours. Cell lysates were immunoblotted to detect the indicated proteins. (B) BT-474 cells were transfected with control or ERBB3 targeted siRNA for 48 hours, followed by treatment with AZD6244 for 6 hours. Cell lysates were immunoblotted with the indicated proteins. (C) BT-474 cells were transfected with control or ERBB3 targeted siRNA for 48 hours, followed by treatment with 2µM AZD6244, 1µM of the PI3K inhibitor GDC-0941, or the combination for 48 hours. Cells were collected and stained for propidium iodide and Annexin V to determine the percentage of apoptotic cells (see materials and methods). Each data point represents the mean ±SD of three independent experiments.

ERBB3. In *EGFR*-mutant HCC827 cells we introduced a Tet-inducible shERBB3

hairpin construct. Following treatment with doxycycline there was effective

knockdown of ERBB3, and this abrogated the increase in AKT signaling normally

observed in HCC827 cells following MEK inhibition (Figure 20A). In *HER2* amplified

BT-474 cells we used siRNA to knockdown ERBB3. Similar to our observations in

HCC827 cells, the increase in AKT signaling following MEK inhibition was attenuated

in BT-474 cells lacking ERBB3 expression (Figure 20B). In contrast to HCC827 cells,

we also observed significant down-regulation of basal AKT signaling in BT-474 cells

following ERBB3 knockdown (Figure 20B), which indicates the sole reliance on

ERBB3 for PI3K activation in this *HER2* amplified cancer. In contrast, *EGFR* mutant

cancers also utilize GAB1 to activate PI3K (Figure 18B) (Engelman et al., 2005;

Turke et al., 2010).

We expected that knockdown of ERBB3 would increase the efficacy of MEK

inhibition since it would lead to suppression of PI3K/AKT signaling as well. We used

PI/Annexin staining to assess induction of apoptosis in BT-474 cells following

treatment with a MEK inhibitor alone, ERBB3 siRNA alone, or the combination.

Single agent MEK inhibition did not cause any significant cell death in BT-474 cells

compared to cells grown in media alone; however, knockdown of ERBB3 caused a

modest induction of apoptosis. The addition of the MEK inhibitor to cells treated with

ERBB3 siRNA increased this cell death response, approaching the level of apoptosis

achieved in cells treated with a PI3K inhibitor, GDC-0941, in combination with

AZD6244 (Figure 20C). These data indicate that ERBB3 plays a significant role in

MEK feedback on PI3K/AKT signaling in EGFR and HER2-driven cell lines, and

suggests that combination therapies targeting MEK and PI3K, or MEK and ERBB3,

may block feedback activation of ERBB3/PI3K/AKT signaling and thus be more effective than treatment with a MEK inhibitor alone.

MEK inhibition results in feedback activation of ERBB3 even in KRAS-mutant cell lines with low basal levels of phospho-ERBB3.

We next determined whether MEK feedback on ERBB3 also occurs in other cancers models not addicted to EGFR or HER2. We treated a panel of *KRAS*-mutant cell lines, which have low basal levels of phospho-ERBB3, with AZD6244. Surprisingly, MEK inhibition led to significant activation of ERBB3, but in contrast to the *EGFR* mutant and *HER2* amplified cancers, the increase in ERBB3 activation did not translate to increased AKT signaling (Figure 21A). Similar to the EGFR and HER2 driven models, we also observed feedback up-regulation of phospho-C-RAF and phospho-MEK following MEK inhibition. We suspect that the increase in ERBB3 phosphorylation did not drive PI3K in these models simply because these *KRAS*-mutant cell lines express significantly less EGFR and HER2, resulting in markedly less absolute levels of phospho-ERBB3 compared to those observed in the EGFR and HER2-driven models discussed above (Figure 21B). Thus, the feedback from MEK inhibition to activation of ERBB3 phosphorylation appears to be conserved in many cancer models, but results in increased PI3K/AKT signaling only in cell lines that express sufficient basal levels of phospho-ERBB3.

The feedback that we observe upon MEK inhibition appears to be distinct from a well-described feedback mechanism in which TORC1 inhibition leads to increased expression of the IRS-1 adaptor protein and subsequent up-regulation of IGF-IR/IRS signaling (Carracedo et al., 2008; O'Reilly et al., 2006). In the *KRAS*-mutant cell lines that we analyzed, the IGF-1R/IRS was the main activator of the PI3K/AKT pathway as we have described previously (Figure 21C) (Ebi et al., 2011),
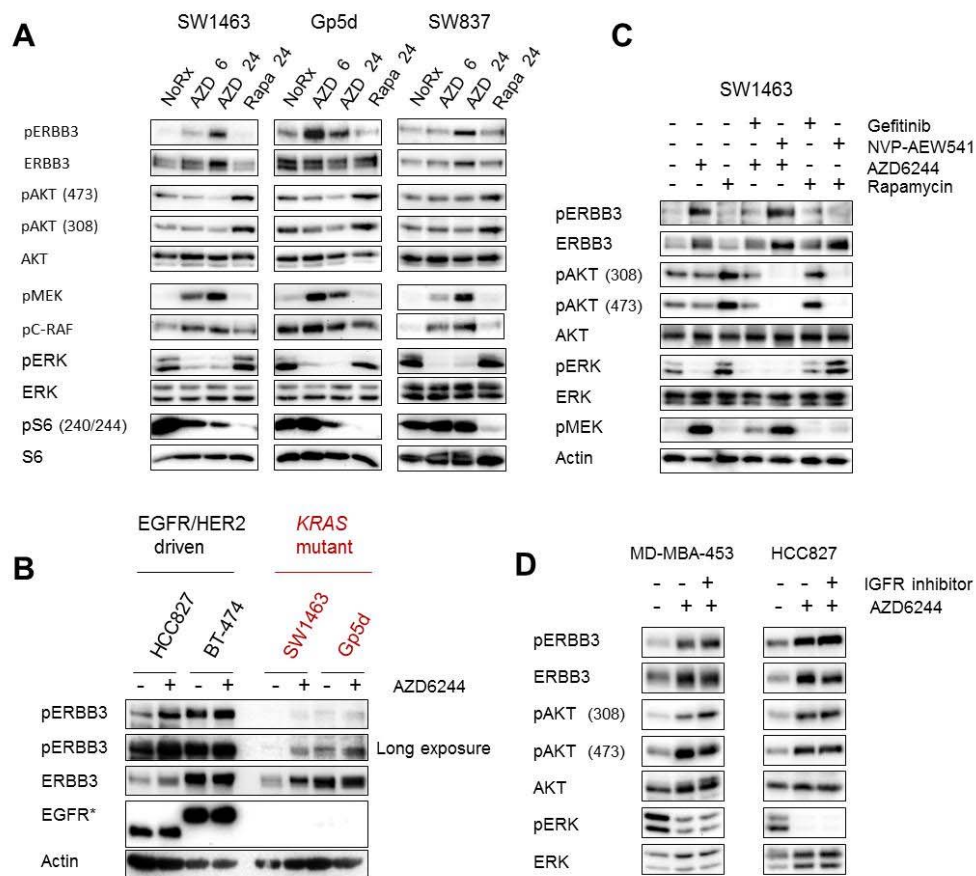
Figure 21. MEK/ERK feedback on ERBB3 occurs in *KRAS*-mutant cell lines and is distinct from TORC1 feedback on IRS-1. **(A)** *KRAS*-mutant cell lines were treated with AZD6244 (AZD) or rapamycin (Rapa) for 6 or 24 hours. Cell lysates were immunoblotted to detect the indicated proteins. **(B)** EGFR or HER2-driven cell lines (black) and *KRAS*-mutant cell lines (red) were treated with AZD6244 for 6 hours. Cell lysates were immunoblotted to detect the indicated proteins. *The antibody used to detect EGFR cross-reacts and detects HER2 in BT-474 cells. **(C)** SW1463 cells were treated with 1µM of the EGFR inhibitor gefitinib or 1µM of the IGFR inhibitor NVP-AEW541, alone or in combination with 2µM AZD6244 or 50nM rapamycin for 24 hours. Cell lysates were immunoblotted to detect the indicated proteins. **(D)** HER2-driven MDA-MB-453 cells or EGFR-driven HCC827 cells were treated with 2µM of AZD6244 alone or in combination with 1µM of the IGFR inhibitor NVP-AEW541 for 16 hours. Cell lysates were immunoblotted to detect the indicated proteins.

and treatment with the mTORC1 inhibitor rapamycin led to feedback activation of AKT signaling that was blocked by co-treatment with the IGF-IR/IR inhibitor, NVP-AEW541 (Figure 21A, C). The MEK inhibitor-induced activation of ERBB3 in the *KRAS* mutant cancers was blocked by gefitinib, but not NVP-AEW541 (Figure 21C). Similarly, NVP-AEW541 did not impair the AZD6244-induced activation of AKT

phosphorylation in the EGFR and HER2-driven cell lines (Figure 21D). Together

these data indicate that feedback activation of ERBB3 following MEK inhibition

occurs in a broad range of cancers, but this only leads to activation of AKT in a

subset of cancers (e.g., *EGFR* mutant lung and *HER2* amplified breast cancers).

Further, the effect of MEK inhibition on ERBB3 is a novel feedback mechanism

distinct from TORC1 feedback on IRS-1. A model describing these findings is shown

in Figure 22.
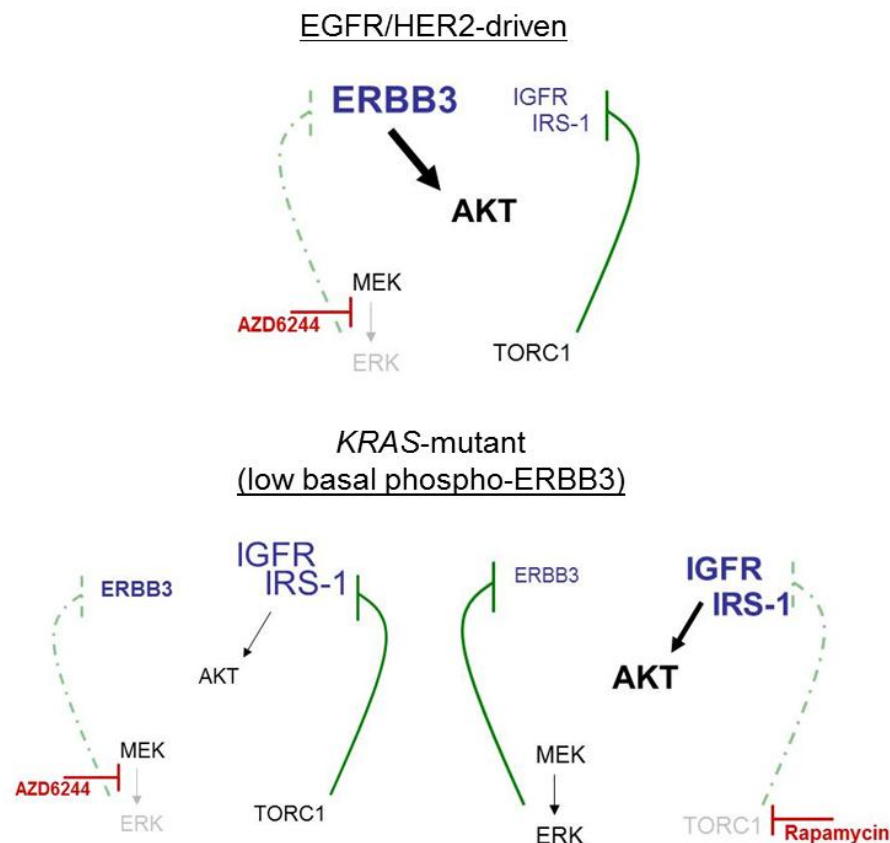
Figure 22. Model of MEK feedback on ERBB3. MEK inhibition leads to feedback activation of ERBB3 in both EGFR/HER2-driven cancers and *KRAS*-mutant cancers with low basal levels of phospho-ERBB3. However, feedback activation of ERBB3 only translates to up-regulation of PI3K/AKT signaling in EGFR/HER2-driven cancers. mTORC1 feedback activation of IGFR/IRS-1 signaling is a distinct feedback mechanism, and in *KRAS*-mutant cancers up-regulation of IGFR/IRS-1 results in activation of downstream PI3K/AKT signaling.

MEK inhibition results in increased tyrosine phosphorylation of EGFR and HER2 due to inhibition of ERK-mediated threonine phosphorylation of these receptors.

Based on these results, we investigated the mechanism by which treatment with the MEK inhibitor leads to increased ERBB3 phosphorylation. We did not observe a change in the expression of HRG ligand protein or mRNA as measured by ELISA and qPCR, respectively (Figure 23A, B). However, we also observed that the
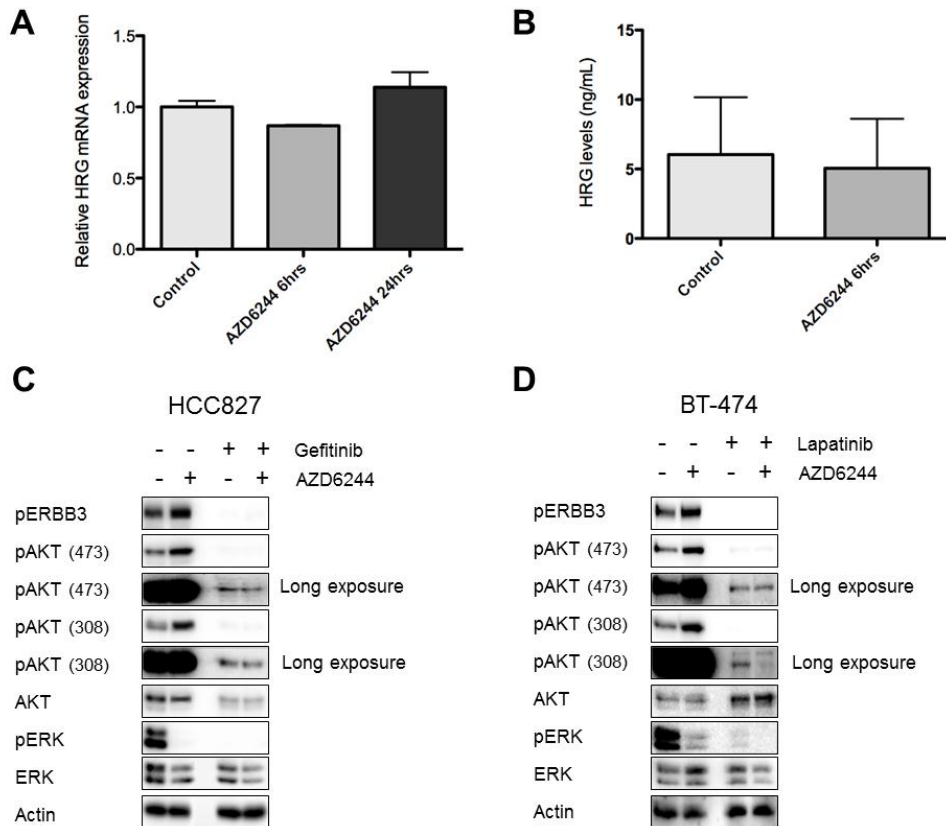
Figure 23. MEK feedback on ERBB3 is dependent on EGFR or HER2 activation and does not affect expression of HRG ligand. (A) HCC827 cells were treated for 6 or 24 hours with AZD6244. RNA was collected and transcribed to produce cDNA. Heregulin (HRG) cDNA was quantified using qPCR and values were normalized to actin. Each data point represents the mean ±SD of three independent experiments. **(B)** HCC827 cells were treated for 6 hours with AZD6244. HRG levels in cell lysates were quantified using an HRG ELISA, each data point represents the mean ±SD of three independent experiments. **(C)** HCC827 cells were treated with 1µM of the EGFR inhibitor gefitinib or 2µM of AZD6244 alone or in combination for 24 hours. **(D)** BT-474 cells were treated with 1µM of the HER2 inhibitor lapatinib or 2µM of AZD6244 alone or in combination for 24 hours. Cell lysates were immunoblotted to detect the indicated proteins.

MEK inhibitor-induced feedback activation of AKT phosphorylation required EGFR

and HER2 kinase activity (Figure 23C, D). Indeed, even in the *KRAS* mutant
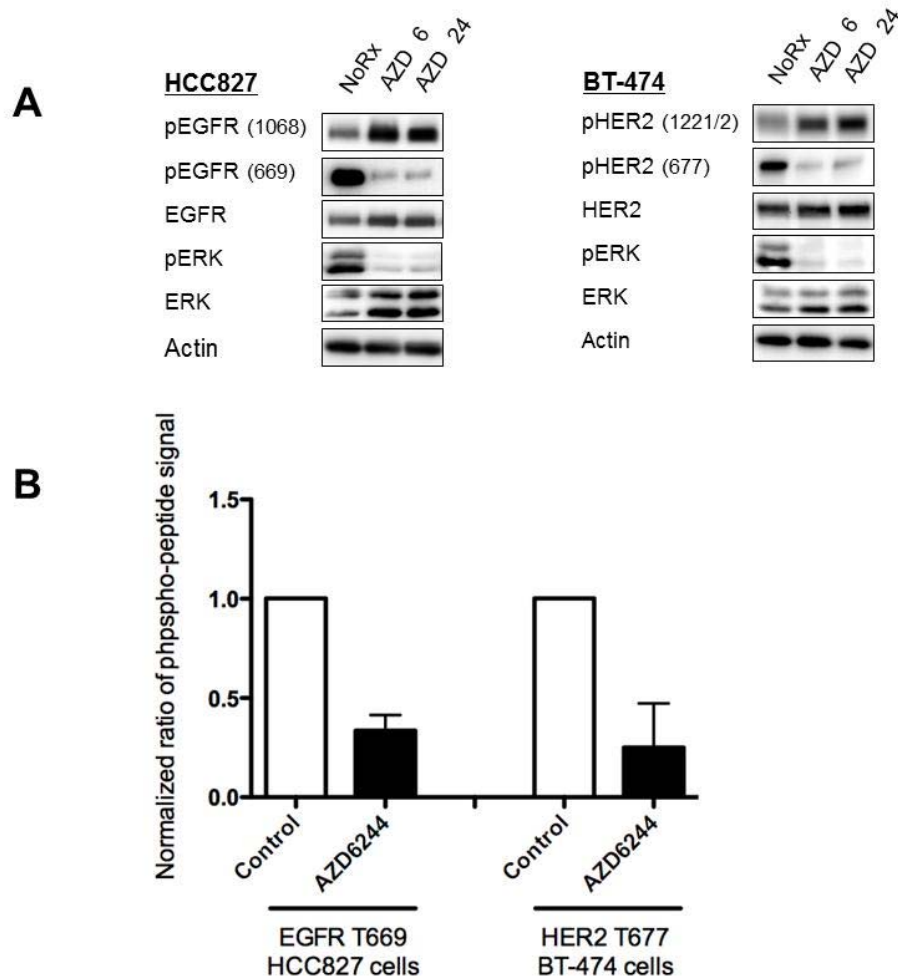
Figure 24. MEK inhibition blocks phosphorylation of a direct ERK target site in the conserved JM domains of EGFR and HER2. (A) HCC827 and BT-474 cells were treated with AZD6244 for 6 or 24 hours. Cell lysates were immunoblotted to detect the indicated proteins. The signal for phospho-HER2 (677) runs at 185kDa and represents a cross reaction from blotting with an anti-phispho-EGFR (669) antibody. (B) HCC827 or BT-474 cells were treated with AZD6244 for 6 hours. EGFR or HER2, respectively, was immunoprecipitated and bands were excised for mass spectrometry analysis of peptide phosphorylation (see materials and methods). Each data point represents the mean ±SD of three independent experiments.

SW1463 cells, MEK feedback on ERBB3 was still dependent on EGFR kinase activity (Figure 21C).

Because inhibition of EGFR and HER2 blocked the effect of MEK feedback activation of ERBB3/PI3K/AKT signaling, we investigated whether MEK inhibition was also directly effecting the activation of EGFR and HER2. We treated HCC827 and BT-474 cells with AZD6244 for 6 or 24 hours and observed increased tyrosine phosphorylation of both EGFR and HER2, indicative of receptor activation (Figure 24A). It has been reported that activation of EGFR involves the formation of an asymmetric dimmer in which the N-terminal lobe of the "receiver/acceptor" kinase interacts with the C-terminal lobe of the "activator/donor" kinase, allowing for tyrosine phosphorylation and activation of both RTKs by the "receiver/acceptor", which has been instilled with kinase activity by the "activator/donor" (Hubbard, 2009). Importantly, formation of the active RTK dimmer is facilitated by stabilizing contacts made between the juxtamembrane (JM) domain of the "receiver/acceptor" and the C-terminal lobe of the "activator/donor" kinase (Hubbard, 2009; Jura et al., 2009; Red Brewer et al., 2009). Threonine 669, a putative MAPK target site, is conserved within the JM domain of EGFR, HER2, and ERBB4 and may regulate dimerization dynamics (Li et al., 2008; Northwood et al., 1991; Red Brewer et al., 2009; Takishima et al., 1991).

Thus, we hypothesized that the MEK-ERK signaling pathway may suppress trans-phosphorylation of ERBB3 by directly phosphorylating EGFR and HER2 in the JM domains. We used tandem mass spectrometry to determine if phosphorylation of this JM domain threonine residue was lost following treatment with AZD6244. We immunoprecipitated the corresponding RTKs from cell treated with AZD6244 and directly analyzed phosphorylation of this conserved threonine residue by targeted

LC/MS/MS. By targeting both the phosphorylated and non-phosphorylated peptide forms, we observed a 66% average decrease in the level of T669 phosphorylation of EGFR, and a 75% decrease in the level of T677 phosphorylation of HER2 upon treatment with AZD6244 (Figure 24B). Antibodies specific to these JM phosphorylation sites confirmed that treatment with AZD6244 led to loss of phosphorylation of T669 of EGFR and the analogous T677 of HER2 (Figure 24A). Together these data indicate that loss of this inhibitory threonine phosphorylation on the JM domains of EGFR and HER2 occurs in our cell line models following MEK inhibition.

Mutation of T669 and T677 abrogates MEK inhibitor-induced suppression of ERBB3 activation.

Based on the results discussed above, we hypothesized that MEK inhibition activates AKT by decreasing ERK1/2 phosphorylation, which in turn blocks an inhibitory threonine phosphorylation on the JM domains of EGFR and HER2, thereby increasing phosphorylation of ERBB3. To test this hypothesis, we expressed wild type ERBB3 with either wild type EGFR or mutant EGFR T669A in CHO-KI cells, which do not express ERBB receptors endogenously. In cells expressing wild type EGFR, MEK inhibition led to feedback activation of phospho-ERBB3 and phosho-EGFR, recapitulating the results we had observed in our panel of cancer cell lines (Figure 25A). However, in contrast, the EGFR T669A mutant led to a basal increase in both EGFR and ERBB3 tyrosine phosphorylation, and this was not augmented by MEK inhibition. As a control, we treated CHO-KI cells expressing the EGFR T669A mutant with 50ng/mL of HRG ligand to induce ERBB3 phosphorylation. In response to HRG stimulation we achieved a further increase in ERBB3 activation (Figure 25A). This indicated that the lack of induction of phospho-ERBB3 in EGFR T669A

75

expressing cells following MEK inhibition was not simply due to the fact that we had

saturated the system with maximum ERBB3 activation. We observed analogous

results in CHO-KI cells expressing wild type ERBB3 in combination with wild type or

the T677A mutant HER2 receptor (Figure 25B). Together these results support the

hypothesis that inhibition of phosphorylation of a conserved threonine residue within
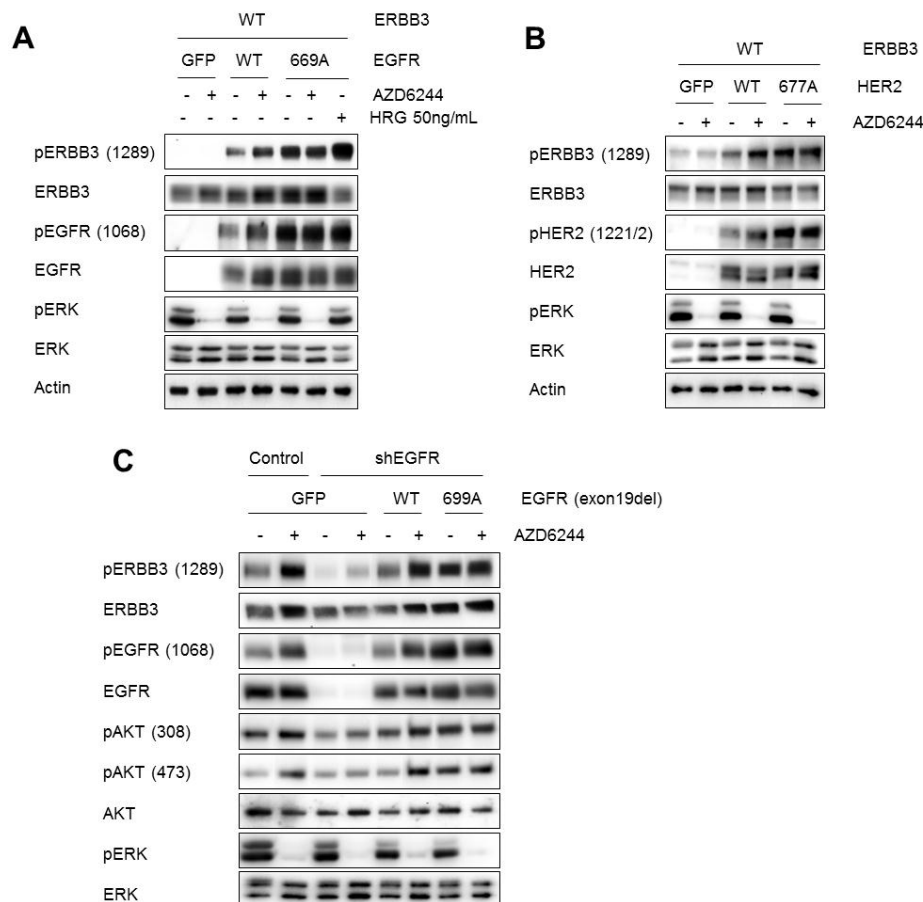
Figure 25. T669A mutation of EGFR or T677A mutation of HER2 blocks MEK feedback activation of ERBB receptors. (A, B) CHO-KI cells were transiently transfected to express wild type ERBB3 in combination with a GFP control, or wild type or mutant *(A)* EGFR or *(B)* HER2. 48 hours post transfection cells were treated with AZD6244 for 90 minutes. Cell lysates were immunoblotted to detect indicated proteins. Cells expressing T669A mutant EGFR were also treated with 50ng/mL HRG ligand for 30 minutes to achieve maximal ERBB3 phosphorylation **(C)** HCC827 cells were infected with a control or shEGFR hairpin, followed by infection with lentiviral vectors expressing GFP, T669 wild type EGFR (exon 19del), or T669A mutant EGFR (exon 19del). Following knockdown and puro selection for 72 hours, cells were treated with AZD6244 for 6 hours. Cell lysates were immunoblotted to detect the indicated proteins.

the JM domains of EGFR and HER2 leads to feedback up-regulation of ERBB

receptor activation (Figure 26).

To confirm that this feedback model explains the activation PI3K signaling in

EGFR mutant cancers, we used an shRNA system to knockdown endogenous

EGFR (which carries an exon 19 deletion) in the *EGFR*-mutant HCC827 (exon

19del) NSCLC cell line and replaced with either EGFR (exon 19del) wild type at

T669, or EGFR (exon 19del) carrying a T669A mutation. Of note, this is the same

cell line in which we determined that EGFR T669 is phosphorylated in MEK-

dependent manner (Figure 24). In parental HCC827 cells, MEK inhibition leads to
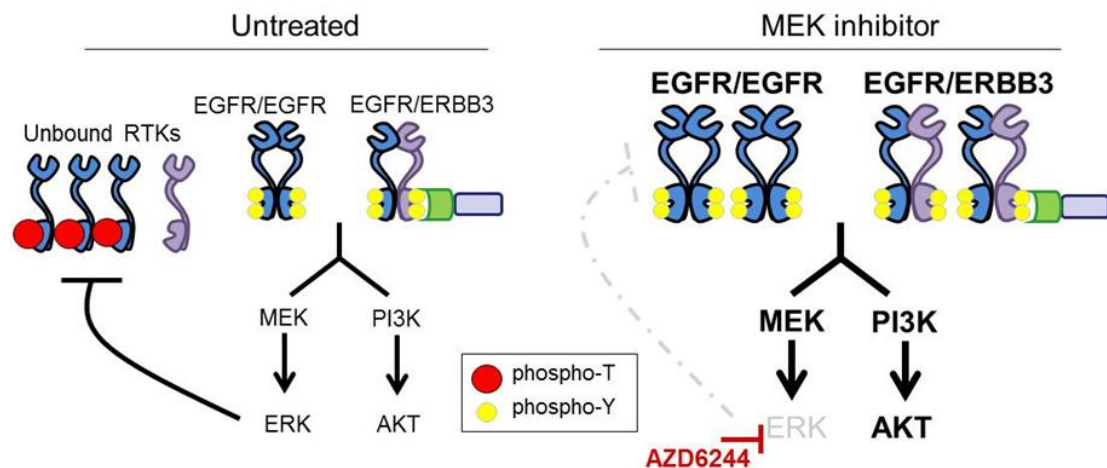
Figure 26. Model of MEK inhibitor-induced feedback on ERBB receptor signaling pathways.
In untreated cells *(left)* EGFR is phosphorylated at T669 *(red circles)*, which partially inhibits tyrosine phosphorylation *(yellow circles)* and activation of EGFR homodimers and EGFR-ERBB3 heterodimers. In the presence of AZD6244 *(right)* ERK is inhibited and T669 phosphorylation is blocked. This results in increased EGFR and ERBB3 tyrosine phosphorylation and up-regulation of downstream signaling pathways.

significant feedback activation ERBB3/PI3K/AKT signaling (Figures 17 and 18), and

when endogenous EGFR was replaced with an EGFR (exon19del) construct wild

type at T669 we saw similar results (Figure 25C). However, replacement with the

EGFR (exon19 del) T669A mutant led to increased tyrosine phosphorylation of both

EGFR and ERBB3 and activation of PI3K/AKT signaling, mimicking the effect of MEK inhibition (Figure 25C). These results demonstrate that the phosphorylation of T669 is necessary for MEK/ERK to suppress EGFR-mediated activation of ERBB3. This supports the hypothesis that ERK feedback on ERBB3/PI3K/AKT and RAF/MEK signaling is mediated though phosphorylation of T669 on EGFR. In our EGFR and HER2-driven cancer cell lines, increased receptor activation translates to increased phosphorylation of ERBB3 and up-regulation of downstream PI3K/AKT signaling.

4.5 Discussion

RAF and MEK inhibitors are currently being developed for treatment of cancers with persistent activation of RAF/MEK/ERK signaling. However, the efficacy of these drugs as single agents has been underwhelming to date. Although there are several potential reasons for this lack of efficacy, feedback activation of parallel oncogenic pathways including PI3K/AKT signaling has been invoked as a potential limitation (Faber et al., 2009; Hoeflich et al., 2009; Mirzoeva et al., 2009). This idea is analogous to the findings that TORC1 inhibitors are limited by feedback activation of PI3K signaling (O'Reilly et al., 2006). In this study, we show that MEK feedback on ERBB receptors occurs in multiple cell line models. We propose a mechanism for this feedback in which MEK inhibition blocks threonine phosphorylation of a direct ERK target site in the conserved JM domains of EGFR and HER2. Phosphorylation of this threonine residue has been shown to impair receptor activation (Red Brewer et al., 2009). Therefore, relief from this negative feedback, through MEK inhibition leads to increased ERBB signaling and activation of downstream effectors including PI3K/AKT signaling.

Our findings suggest that direct phosphorylation of EGFR T669 and HER2 T677 by MEK/ERK signaling suppresses activation of ERBB3. Previous data

suggests that phosphorylation of these residues impairs dimerization and activation

(Li et al., 2008; Red Brewer et al., 2009). Our findings agree with those by Li and

colleagues who expressed EGFR T669A mutant homodimers in CHO-KI cells and

observed no additive effect on tyrosine phosphorylation of this EGFR mutant with the

addition of a MEK inhibitor (Li et al., 2008). In addition to increased ERBB3 tyrosine

phosphorylation, we also observe increased expression of total ERBB3 protein

following MEK inhibition. This increase appears to be post-transcriptional as no

change in ERBB3 mRNA levels was observed following treatment with AZD6244

(Figure 19C). We were unable to definitively determine the mechanism for increased

expression of total ERBB3. We hypothesize that ERBB3 protein levels become

elevated following MEK inhibition because loss of T669/T677 phosphorylation allows

for stronger EGFR-ERBB3 or HER2-ERBB3 dimer formation and increased receptor

stability. Increased ERBB3 expression was not caused by increased tyrosine

phosphorylation of ERBB3. In *KRAS*-mutant SW1463 cells treated with AZD6244 in

combination with an EGFR inhibitor, total ERBB3 levels remained elevated despite

potent inhibition of ERBB3 tyrosine phosphorylation (Figure 21C). Indeed, ERK

phosphorylation of the threonine sites appeared to be necessary for this effect. For

example, expression of the T669A mutant EGFR in both the CHO-KI cells and the

HCC827 cells led to an increase in basal ERBB3 levels, which was not further

increased by the addition of a MEK inhibitor (Figure 25). These results suggest that

increases in ERBB3 protein levels are dependent on EGFR threonine

phosphorylation at residue 669 in the JM domain, and are likely a result of improved

dimerization and receptor stability.

In EGFR and HER2-driven cancers, both the PI3K/AKT and RAF/MEK

signaling pathways are activated by the respective RTKs, and the ERBB3 receptor

scaffold is used as a primary activator of PI3K signaling. HER2-driven cancers have

demonstrated sensitivity to single agent PI3K inhibitors; however single agent MEK inhibitors or alternative therapeutic strategies that do not block phosphorylation of AKT are largely ineffective in inducing apoptosis (Brachmann et al., 2009; Serra et al., 2008; She et al., 2008). In contrast, EGFR-driven cancers require inhibition of both PI3K/AKT signaling and RAF/MEK signaling for induction of cell death (Faber et al., 2009). In this study, we show that feedback up-regulation of ERBB3 occurs in multiple *EGFR* mutant and *HER2* amplified cell line models and that this response translates to activation of downstream PI3K/AKT signaling. Our data provides mechanistic insights into the previous findings that MEK feedback on AKT is dependent on ERBB signaling in human gastric cells (Yoon et al., 2009). These results suggest that combining MEK inhibitors with either ERBB inhibitors, or PI3K inhibitors, may be effective therapeutic strategies in the clinic. Furthermore, although there are currently no approved therapies targeting ERBB3, pre-clinical development of anti-ERBB3 antibodies is underway and our data points to the possible utility of combining these therapeutic antibodies with MEK inhibitors to block feedback activation of AKT in multiple cancer models.

Interestingly, we also observed feedback activation of ERBB3 following MEK inhibition in *KRAS*-mutant cancers that express low basal levels of phosphor-ERBB3 and therefore do not use ERBB3 to activate PI3K. This observation suggests that MEK feedback on ERBB3 occurs in a broad range of cancers, regardless of dependence on ERBB signaling, and highlights another potential complication for patients treated exclusively with inhibitors of the RAF/MEK/ERK pathway. For example, in *KRAS*-mutant or *BRAF*-mutant cancers that initially respond to single agent RAF or MEK inhibitors, chronic inhibition of this pathway may lead to activation of EGFR or HER2 and the development of a dependence on these pathways that was not present before treatment. Therefore, these data suggest a possible

mechanism of acquired resistance to single agent RAF or MEK inhibitors.

Chapter 5- General Discussion

5.1 Summary of Results

In this thesis my colleagues and I describe a novel resistance mechanism in multiple EGFR-driven NSCLC models in which expression of HGF ligand leads to activation of MET signaling in the absence of *MET* amplification. In these models, activation of MET via ligand leads to maintenance of GAB1/PI3K/AKT signaling as well as MEK/ERK signaling despite sustained EGFR inhibition, and treatment with a combination of an EGFR inhibitor and a MET inhibitor is necessary to restore sensitivity in the presence of HGF. Further, we show that *MET* amplification preexists in a small subpopulation of the parental HCC827 NSCLC cell line, and that selection of these *MET* amplified cells in the presence of an EGFR inhibitor consistently leads to the development of *MET* amplification as a resistance mechanism. Further, we showed that the presence of HGF ligand dramatically accelerated the kinetics of selection of preexisiting *MET* amplified cells. Transient exposure to HGF allowed cells to become stably resistant and ligand-independent after just two weeks of treatment with an EGFR inhibitor.

We also performed analysis of paired tumor samples from NSCLC patients with acquired resistance to gefitinib and found that detection of preexisting *MET* amplified cells in gefitinib sensitive pre-treatment samples allowed us to predict whether a patient would develop *MET* amplification following treatment with an EGFR inhibitor in the clinic. High HGF expression levels also correlated significantly with gefitinib resistance in NSCLC patient samples. Together, these results suggest the utility of using a combination of a MET inhibitor and an EGFR inhibitor in patients with high HGF expression levels, as well as in treatment naïve patients with preexisting subpopulations of *MET* amplified cells.

PI3K/AKT and MEK/ERK signaling cascades are intricately connected by an array of feedback loops that regulate flux through these pathways. In this thesis my colleagues and I describe a feedback loop in which MEK inhibition leads to activation of ERBB3/PI3K/AKT signaling. We present a novel mechanism for this effect in which treatment with a MEK inhibitor blocks direct ERK phosphorylation of a conserved threonine residue in the juxtamembrane domains of EGFR and HER2. Loss of this inhibitory threonine phosphorylation leads to increased RTK activation and up-regulation of downstream effectors including increased ERBB3 phosphoryation, PIP_3 production and phosphorylation of AKT and its substrates. This feedback occurs in multiple cell line models, including *KRAS*-mutant cancers, regardless of whether ERBB3 normally drives PI3K/AKT signaling. In pre-clinical studies, single agent MEK inhibitors have been shown to be less effective in cases where treatment leads to up-regulation of AKT phosphorylation (Hoeflich et al., 2009; Mirzoeva et al., 2009) and these cancers may be more effectively treated with a combination of a MEK inhibitor and a PI3K inhibitor or RTK inhibitor. Of note, in cancers that do not use ERBB receptors to drive PI3K/AKT signaling, chronic treatment with a MEK inhibitor may lead these cells to become dependent on EGFR or HER2 and shift to use ERBB signaling to maintain PI3K activation and other downstream effectors as mechanisms of survival.

5.2 PI3K/AKT and RAF/MEK/ERK Signaling in Cancer[4]

The importance of PI3K/AKT and MEK/ERK signaling for cancer cell survival, growth, proliferation and metabolism has been well established (Davies et al., 2002; Engelman, 2009; Montagut and Settleman, 2009; Samuels et al., 2004). In many

---

[4] Excerpts and figures from this section were published in Yang, et al. *Cancer Research* September 2011.

cases, targeted therapies are effective when treatment leads to down-regulation of both of these central oncogenic pathways (Engelman et al., 2008; Faber et al., 2009), and conversely the development of resistance is commonly associated with reactivation of one or both of these pathways. However, it is still unclear why in some cancers single agent inhibitors are effective; e.g., *HER2* amplified breast cancers tend to respond to treatment with a PI3K inhibitor alone (Faber et al., 2010; Ihle et al., 2009; Serra et al., 2008; She et al., 2008), and *BRAF* mutant cancers often respond to single agent BRAF or MEK inhibition (Flaherty et al., 2010; McDermott et al., 2007; Solit et al., 2006). In other cancer models including *EGFR* mutant NSCLC, it is often necessary to inhibit both PI3K/AKT and MEK/ERK signaling in order to achieve growth arrest and apoptosis (Faber et al., 2009). It has been suggested that cancer cells become most dependent on those pathways that regulate mTORC1 in a particular model, and in some cases one pathway is predominant while in others both PI3K and MEK/ERK seem to drive mTORC1 signaling and downstream effectors (Ebi et al., 2011; O'Brien et al., 2010). As discussed above, when we consider the use of both MEK inhibitors and PI3K inhibitors as single agents it will be critically important to be aware of the complex feedback networks that link these two pathways, as inhibition of a single effector often leads to up-regulation of a parallel pathway.

Because of the well-established role for PI3K/AKT signaling in human cancers, there is an increased effort to identify activators of PI3K in order to inform the most effective treatment strategies. In some cancers, PI3K is activated by direct mutation, but more commonly it is activated by mutation or amplification of upstream receptor tyrosine kinases. In collaboration with Dr. John Asara (BIDMC Mass Spectrometry Core Facility, Boston, MA) my colleagues and I developed and validated a systematic method to determine which RTK signaling cascades activate

PI3K in certain cancers (Yang et al., 2011). Traditional techniques often involve immunoprecipiation of the p85 regulatory subunit of PI3K followed by repeated Western blotting for co-immunoprecipitating adaptors. However, this approach is relatively time consuming, non-quantitative, and requires specific antibodies for each candidate activator of PI3K.

Our group recently identified a quantitative tandem mass spectrometry (LC/MS/MS) approach that identifies upstream activators of PI3K both *in vitro* and *in vivo* (Yang et al., 2011). We validated this method in a number of systems including
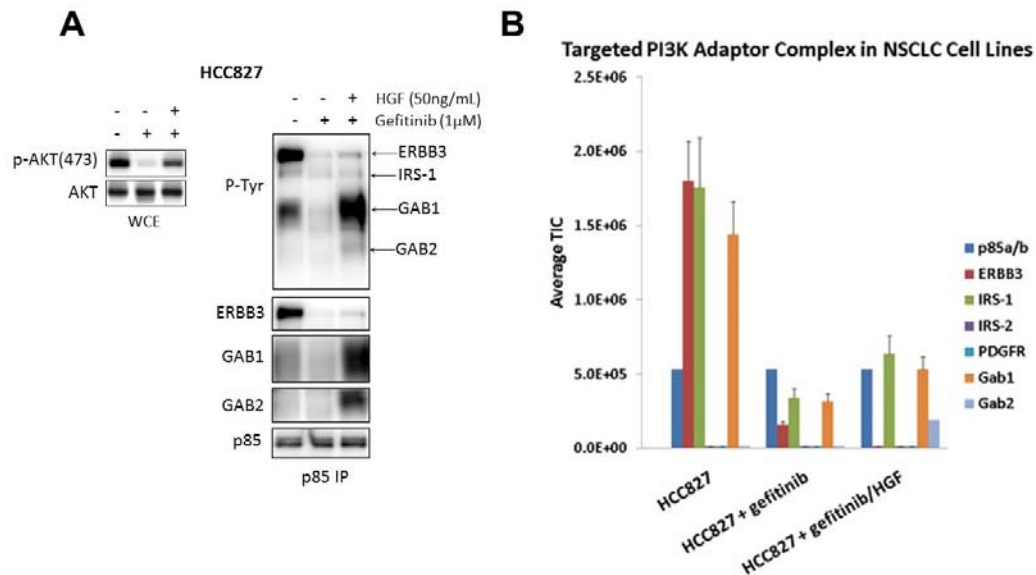
Figure 27. Targeted Mass Spectrometry to identify activators of PI3K in HCC827 cells. (A) HCC827 cells were treated in the absence or presence of gefitinib (1μM) and HGF (50 ng/mL) for 6 hours. Whole cell extracts *(left)* were probed with the indicated antibodies. Extracts were subjected to a p85 IP *(right)*, and the IP was probed with the indicated antibodies. **(B)** The quantitative output of targeted MS approach in HCC827cells subjected to the indicated conditions. Cells were treated with the indicated drugs and ligands for 6 hours before lysis. The relative signal level of each detected adaptor (normalized for p85 levels) is shown.

a human cancer cell line with acquired gefitinib resistance mediated through IGFR signaling, an ALK-driven NSCLC xenograft model which uses IRS-1 and IRS-2 to activated PI3K, and a cell line model in which we identified the presence of an

E454K mutation in the p110α subunit of PI3K. We also tested this approach in the

HCC827 cell line treated with gefitinib and HGF ligand and showed that HGF

treatment rescues GAB1 and GAB2, but not ERBB3, binding to PI3K (Figure 27).

Having an efficient high throughput method to assess activators of this pathway will

be useful in helping to guide the selection of tyrosine kinase inhibitors for

personalized therapies.

5.3 Biomarkers and Personalized Medicine[5]

With the development of molecular targeted therapies, cancer biology has

begun to transition towards personalized medicine. This new field uses diagnostic

tests to identify the specific genes, proteins and pathways driving a particular cancer

with the goal of determining individualized treatment strategies for each patient.

Ultimately, distinguishing individual patients based on the genetic and molecular

characteristics of their tumors will allow us to design and conduct more efficient

clinical trials leading to faster, less costly drug approvals, and better therapeutic

options for patients. Further, prospectively identifying which patients are likely to

respond to a particular targeted therapy will reduce unnecessary toxicities incurred

by patients who are unlikely to receive any benefit from treatment.   The future of

personalized medicine will continue to improve as more targets are identified, new

therapies are designed and approved, and more efficient diagnostics become part of

standard clinical practice.

Numerous genetic and molecular biomarkers have already been identified to

determine which patients will respond to specific targeted cancer therapies. The

EGFR tyrosine kinase inhibitors gefitinib and erlotinib were the first targeted

---

[5] Excerpts and figures from this section were published in Sequist, et al., *Science Translational Med,* March 2011.

therapies to be approved for the treatment of NSCLC. During the course of their clinical development, it has become clear that the substantial clinical benefit associated with EGFR TKIs is limited to a distinct subset of patients harboring *EGFR* activating mutations (Paez et al., 2004; Pao et al., 2004). A phase III clinical trial performed in treatment naïve patients with pulmonary adenocarcinoma and published in 2009 in the New England Journal of Medicine showed that gefitinib provided a modest clinical benefit as compared to carboplatin-palcitaxel chemotherapy (Mok et al., 2008). However, when patients treated with gefitinib were separated according to *EGFR* mutational status, those with *EGFR* activating mutations had an objective response rate of 71.2%, whereas *EGFR* wild-type patients with an objective response rate of 1.1%. Further, progression free survival was significantly longer in the mutation-positive subgroup treated with gefitinib compared to chemotherapy, but surprisingly, the opposite was true in the *EGFR* wild-type subgroup and these patients had significantly poorer outcomes when treated with gefitinib (Mok et al., 2008). These results suggest that *EGFR* mutational status is a critical biomarker for gefitinib response in NSCLC.

Additional biomarkers have also been validated to predict responsiveness to EGFR targeted therapies. *KRAS* mutation as well as *PTEN* deletion and *PIK3CA* mutation have all been correlated with poor response to RTK targeted therapies (Berns et al., 2007; Engelman et al., 2006b; Ludovini et al., 2011; Yamasaki et al., 2007). Faber et al. recently showed that expression levels of the pro-apoptotic protein BIM predict responsiveness to targeted therapies in multiple cancer models (Faber et al., 2011). The presence of preexisiting T790M mutant *EGFR* has previously been show to predict the development of gefitinib resistance (Inukai et al., 2006). Finally, the data presented in this thesis suggest that high levels of the HGF ligand correlate with a lack of responsiveness and a tendency to develop resistance

to EGFR targeted therapies, and that preexistence of a small sub-population of *MET* amplified cells is a predictive biomarker for the development of *MET* amplification as a resistance mechanism to EGFR TKIs (Turke et al., 2010).

The identification of biomarkers to predict whether a drug is hitting its target in patients, and to quickly determine after initial treatment whether a patient is likely to respond to a specific targeted therapy, will also be useful. It has recently been suggested that the phosphorylation status of the S6 ribosomal protein, a downstream effector of mTORC1, will be an informative biomarker to predict whether or not a patient will respond to a given targeted therapy. For example, in breast cancer models treated with single agent PI3K inhibitors, a decrease in S6 phosphorylation has been shown to significantly correlate with sensitivity and tumor regressions (O'Brien et al., 2010).

As the number of biomarkers predicting responsiveness to targeted therapies grows, there is an increasing need for improved diagnostic techniques and frequent analysis of cancers as they evolve during treatment. It will be essential for the future of personalized cancer medicine that efficient and cost effective diagnostic tests become the standard or care and that protocols are updated to encourage analysis of tumors both before treatment and as frequently as reasonably possible over the course of disease progression.

Our group recently published a study in collaboration with Dr. Lecia Sequist (Massachusetts General Hospital, Boston, MA) assessing the clinical progression at the molecular level of 37 NSCLC patients with *EGFR* activating mutations, initially exhibiting sensitivity but ultimately acquiring resistance to gefitinib (Sequist et al., 2011). Repeat biopsies of recurrent disease sites were performed over the course of disease as part of routine clinical care and molecular analyses were performed to assess the prevalence of established biomarkers and to identify new mechanisms of

resistance. As predicted, known mechanisms of resistance including *EGFR* T790M

mutation and the development of *MET* amplification were observed, and in three

patients serial biopsies revealed that genetic mechanisms of resistance were lost in

the absence of continued selective pressure of EGFR inhibitor treatment and such

cancers were sensitive to a second round of treatment with EGFR inhibitors.

Surprisingly, five resistant tumors transitioned from NSCLC to small-cell lung cancer

(SCLC) and responded to standard SCLC treatments, and some resistant cancers

showed unexpected genetic changes including *EGFR* amplification and mutations in

the *PIK3CA* gene (Sequist et al., 2011).

In the laboratory, my colleagues and I observed a different phenotypic

transformation when using the H1975 (L858R/T790M) lung adenocarcinoma cell line

to model acquired resistance to an EGFR inhibitor. The cell line was made resistant

to the irreversible EGFR inhibitor, PF00299804, to which it was initially sensitive

(Figure 28A). The resistant cell line (H1975 Resistant) did not acquire *MET*

amplification, but did show an increased copy number of the *EGFR* T790M allele,

consistent with previous reports (Ercan et al., 2010). In addition, it underwent a

marked histological change and developed a spindle-like morphology (Figure 28B).

Assessment of E-cadherin and vimentin expression confirmed that the resistant cell

line had undergone an epithelial-to-mesenchymal transition (EMT) (Figure 28C).

EMT describes a cancer cell that loses its epithelial morphology and develops a

more spindle-like mesenchymal morphology; this histological change is often

associated with a shift in expression of specific proteins (for example, loss of E-

cadherin and gain of vimentin) and a more invasive phenotype. In contrast,

HCC827GR cells that had developed *MET* amplification upon resistance to an EGFR

TKI (Engelman et al., 2007b) did not undergo an EMT (Figure 28C).
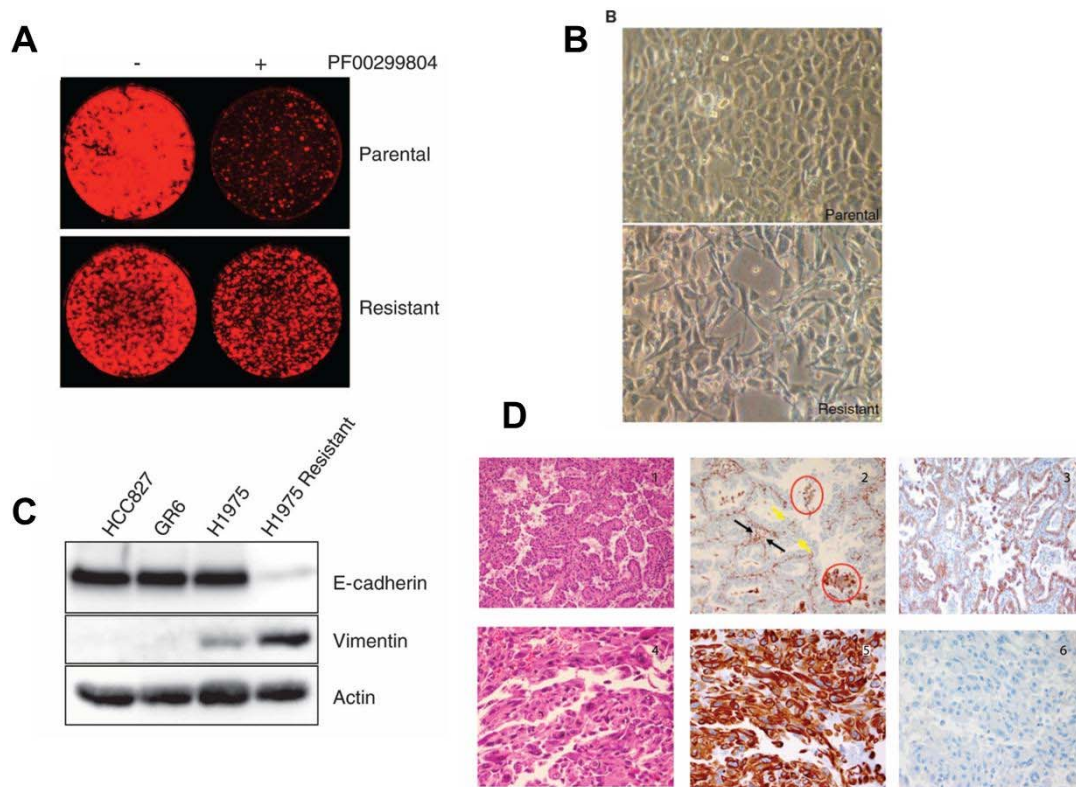
Figure 28. EMT and acquired resistance. (A) H1975 cells were cultured in the presence of the irreversible EGFR inhibitor PF00299804 until drug resistance developed, as demonstrated by Syto60 viability assays. **(B)** Images of the parental and drug-resistant H1975 cells by bright-field microscopy demonstrate that the resistant cells have developed a spindle-like morphology. **(C)** Parental and resistant H1975 cells were lysed and probed with antibodies against E-cadherin, vimentin, and actin, revealing loss of E-cadherin expression and gain of vimentin expression among drug-resistant H1975 cells. For comparison, HCC827 cells and the derived HCC827 GR6 cell line (HCC827 cells that acquired resistance to gefitinib via *MET* amplification), which does not undergo an EMT, are shown. **(D)** Example of a case whose drug resistant tumor shows evidence of an EMT (*top*, pretreatment specimens; *bottom*, drug resistant post-treatment specimens). H&E staining *(left);* staining for vimentin *(middle);* staining for E-cadherin *(right)*. The vimentin-positive areas in panel 2 include alveolar macrophages (red circles), inflammatory and stromal cells in fibrovascular cores (black arrows), but not tumor cells lining papillary structures (yellow arrows).

This finding supported previous observations that cancer cell lines undergoing an EMT have intrinsic resistance to EGFR inhibitors (Frederick et al., 2007; Fuchs et al., 2008; Rho et al., 2009; Thomson et al., 2005). This prompted us to analyze paired tissue samples from seven patients with unknown mechanisms of resistance for the development of mesenchymal features and changes in vimentin and E-cadherin expression. Three of the seven resistant specimens had phenotypic changes consistent with a mesenchymal appearance at the time of TKI resistance.

Further analyses confirmed that two of these three post-treatment specimens had acquired vimentin expression and lost E-cadherin expression compared to their pre-treatment counterparts, supporting an EMT (Figure 28D).

Overall, this study of the progression of *EGFR* mutant cancers as they become resistant to first line targeted therapies underscores the importance of repeatedly assessing cancers throughout the course of the disease. Of note, there were no major biopsy related complications observed during this study. In fact, evidence from three patients with multiple biopsies over the course of their disease suggests that both tumor genotype and phenotype may evolve dynamically under the selective pressure of targeted therapies. Therefore, repeat tumor biopsies after the development of resistance should be performed whenever practical to provide current knowledge of the genetic and histological properties of a tumor and allow clinicians to identify the best treatment options for individual patients.

5.4 Combination Therapies[6]

As we continue to identify more and more biomarkers and targets in oncology and develop a collection of targeted therapies, acquired resistance remains a significant and pervasive limitation to longer-term success in the clinic. In an effort to combat resistance, numerous combination therapies are being explored. Notably, combinations of specific PI3K inhibitors or dual PI3K/mTOR inhibitors with MEK inhibitors have been extensively tested in the laboratory (Engelman et al., 2008; Faber et al., 2009; Wong et al., 2010) and are beginning to enter clinical trials. Both MET inhibitors and IGFR inhibitors are being combined with EGFR inhibitors in the clinic. These combination RTK targeted therapies may be useful either as first line

---

[6] Excerpts and figures from this section were published in Turke, et al., *Clinical Cancer Research,* July 2010.

treatments in a subset of patients, or in patients with acquired resistance to gefitinib. Multiple HGF and ERBB3 targeted therapies are also under development and may be tested in combination with RTK inhibitors or therapies targeting downstream effectors.

Several criteria are important to consider in the context of combination therapies. First, when targeted therapies are combined in the clinic, significant side effects and toxicities become a concern, particularly when relatively high doses of an inhibitor are necessary to achieve target inhibition. Second, it is debated whether combination therapies should be given sequentially or simultaneously, and whether each drug should be given at a moderate dose at regular intervals or at a high pulsed dose less frequently (Shah et al., 2008). Finally, it has been suggested that successful therapies often lead to both growth arrest as well as apoptosis of cancer cells. To this point, preliminary studies in our laboratory and others have begun to explore the use of drugs designed to induce a cell death response (e.g., cytotoxic chemotherapies, or pro-apoptotic protein mimetics) in combination with targeted therapies shown to induce a cytostatic effect.

In a recent commentary (Turke and Engelman, 2010) we discuss the need for more rigorous criteria for defining whether a drug or combination of drugs is effective in pre-clinical cancer models. Many laboratory studies define sensitivity to a specific drug according to its ability to decrease growth *in vitro*. Indeed, several studies use IC_{50} values as the primary mode to define sensitivity. This measure provides a quick and robust readout that facilitates comparisons across a large panel of cancer models, and although such assays identify the cell lines whose growth is impacted by the drug, it remains less clear if such data will faithfully predict which cancers will respond to specific targeted therapies in a clinical setting. For example, these data may identify cancer cell lines that grow more slowly in response to drug. However, in

the clinic, this finding may still amount to disease progression, not tumor shrinkage. Of note, recent studies correlate responsiveness to PI3K inhibitors and MEK *in vivo* with the induction of cell death (Brachmann et al., 2009; Faber et al., 2009). Thus, future efforts to discover clinically useful biomarkers may benefit from implementation of more stringent laboratory criteria for "sensitivity", including effects on both cell proliferation and apoptosis.

5.5 Concluding Remarks

Over the past decade there has been a decrease in overall cancer incidence and death rates for both men and women in the United States. This is largely due to decreases in lung, prostate and colorectal cancer in men and breast and colorectal cancer in women (Jemal et al., 2010). These effects have been mediated primarily through increased prevention, e.g., the identification tobacco smoke as a carcinogen; and through better methods for early detection, e.g., the development of prostate specific antigen (PSA) testing, PAP smears, and mammograms. In addition, we are rapidly gaining a comprehensive understanding of the signaling pathways and molecular mechanisms that drive cancer cells, and this information has begun to translate into the development and approval of successful targeted therapies.

Despite progress in reducing cancer incidence and mortality rates and improving survival, 1 in 4 deaths in the United Sates are still due to cancer (Jemal et al., 2010). It will remain important for at-risk patients to continue to undergo preventative screening, and for researchers to continue to identify new carcinogens and methods for early detection. However, despite these measures, cancer will continue to occur in a large percentage of individuals and the demand for effective therapies will continue to exist in oncology. Overall, there is still a need for the identification of new targets and mechanisms of resistance, and the development of

better drugs and diagnostics with more effective treatment regimens. For example, in our recent study of gefitinib resistant NSCLC patients, no cause of resistance was identified for 30% percent of patients analyzed (Sequist et al., 2011). Further, there is still a significant unmet need for therapeutics targeting non-kinases including RAS and ERBB3, as well as drugs mediating the apoptotic response. Perhaps most importantly, we need a better understanding of the genetics and molecular biology of each unique tumor in order to effectively stratify and treat individual patients and move towards personalized cancer medicine.

Bibliography

Amann, J., Kalyankrishna, S., Massion, P. P., Ohm, J. E., Girard, L., Shigematsu, H., Peyton, M., Juroske, D., Huang, Y., Stuart Salmon, J*., et al.* (2005). Aberrant epidermal growth factor receptor signaling and enhanced sensitivity to EGFR inhibitors in lung cancer. Cancer Res *65*, 226-235.

Asahina, H., Yamazaki, K., Kinoshita, I., Sukoh, N., Harada, M., Yokouchi, H., Ishida, T., Ogura, S., Kojima, T., Okamoto, Y*., et al.* (2006). A phase II trial of gefitinib as first-line therapy for advanced non-small cell lung cancer with epidermal growth factor receptor mutations. Br J Cancer *95*, 998-1004.

Balak, M. N., Gong, Y., Riely, G. J., Somwar, R., Li, A. R., Zakowski, M. F., Chiang, A., Yang, G., Ouerfelli, O., Kris, M. G*., et al.* (2006). Novel D761Y and common secondary T790M mutations in epidermal growth factor receptor-mutant lung adenocarcinomas with acquired resistance to kinase inhibitors. Clin Cancer Res *12*, 6494-6501.

Baselga, J. (2001a). Clinical trials of Herceptin(trastuzumab). Eur J Cancer *37 Suppl 1*, S18-24.

Baselga, J. (2001b). The EGFR as a target for anticancer therapy--focus on cetuximab. Eur J Cancer *37 Suppl 4*, S16-22.

Bazell, R. (1998). The Making of Herceptin, a Revolutionary Treatment for Breast Cancer (New York: Random House).

Bean, J., Brennan, C., Shih, J. Y., Riely, G., Viale, A., Wang, L., Chitale, D., Motoi, N., Szoke, J., Broderick, S*., et al.* (2007). MET amplification occurs with or without T790M mutations in EGFR mutant lung tumors with acquired resistance to gefitinib or erlotinib. Proc Natl Acad Sci U S A *104*, 20932-20937.

Berns, K., Horlings, H. M., Hennessy, B. T., Madiredjo, M., Hijmans, E. M., Beelen, K., Linn, S. C., Gonzalez-Angulo, A. M., Stemke-Hale, K., Hauptmann, M*., et al.* (2007). A functional genetic approach identifies the PI3K pathway as a major determinant of trastuzumab resistance in breast cancer. Cancer Cell *12*, 395-402.

Brachmann, S. M., Hofmann, I., Schnell, C., Fritsch, C., Wee, S., Lane, H., Wang, S., Garcia-Echeverria, C., and Maira, S. M. (2009). Specific apoptosis induction by the dual PI3K/mTor inhibitor NVP-BEZ235 in HER2 amplified and PIK3CA mutant breast cancer cells. Proc Natl Acad Sci U S A *106*, 22299-22304.

Brugge, J., Hung, M. C., and Mills, G. B. (2007). A new mutational AKTivation in the PI3K pathway. Cancer Cell *12*, 104-107.

Cantley, L. C. (2002). The phosphoinositide 3-kinase pathway. Science *296*, 1655-1657.

Carpten, J. D., Faber, A. L., Horn, C., Donoho, G. P., Briggs, S. L., Robbins, C. M., Hostetter, G., Boguslawski, S., Moses, T. Y., Savage, S*., et al.* (2007). A transforming mutation in the pleckstrin homology domain of AKT1 in cancer. Nature *448*, 439-444.

Carracedo, A., Baselga, J., and Pandolfi, P. P. (2008). Deconstructing feedback-signaling networks to improve anticancer therapy with mTORC1 inhibitors. Cell Cycle *7*, 3805-3809.

Carraway, K. L., 3rd (2010). E3 ubiquitin ligases in ErbB receptor quantity control. Semin Cell Dev Biol *21*, 936-943.

Chakrabarty, A., Sanchez, V., Kuba, M. G., Rinehart, C., and Arteaga, C. L. (2011). Breast Cancer Special Feature: Feedback upregulation of HER3 (ErbB3) expression and activity attenuates antitumor effect of PI3K inhibitors. Proc Natl Acad Sci U S A.

Chandarlapaty, S., Sawai, A., Scaltriti, M., Rodrik-Outmezguine, V., Grbovic-Huezo, O., Serra, V., Majumder, P. K., Baselga, J., and Rosen, N. (2011). AKT inhibition relieves feedback suppression of receptor tyrosine kinase expression and activity. Cancer Cell *19*, 58-71.

Christensen, J. G., Schreck, R., Burrows, J., Kuruganti, P., Chan, E., Le, P., Chen, J., Wang, X., Ruslim, L., Blake, R*., et al.* (2003). A selective small molecule inhibitor of c-Met kinase inhibits c-Met-dependent phenotypes in vitro and exhibits cytoreductive antitumor activity in vivo. Cancer Res *63*, 7345-7355.

Davies, H., Bignell, G. R., Cox, C., Stephens, P., Edkins, S., Clegg, S., Teague, J., Woffendin, H., Garnett, M. J., Bottomley, W*., et al.* (2002). Mutations of the BRAF gene in human cancer. Nature *417*, 949-954.

Demetri, G. D., von Mehren, M., Blanke, C. D., Van den Abbeele, A. D., Eisenberg, B., Roberts, P. J., Heinrich, M. C., Tuveson, D. A., Singer, S., Janicek, M*., et al.* (2002). Efficacy and safety of imatinib mesylate in advanced gastrointestinal stromal tumors. N Engl J Med *347*, 472-480.

Der, C. J., Krontiris, T. G., and Cooper, G. M. (1982). Transforming genes of human bladder and lung carcinoma cell lines are homologous to the ras genes of Harvey and Kirsten sarcoma viruses. Proc Natl Acad Sci U S A *79*, 3637-3640.

Diamonti, A. J., Guy, P. M., Ivanof, C., Wong, K., Sweeney, C., and Carraway, K. L., 3rd (2002). An RBCC protein implicated in maintenance of steady-state neuregulin receptor levels. Proc Natl Acad Sci U S A *99*, 2866-2871.

Dibble, C. C., Asara, J. M., and Manning, B. D. (2009). Characterization of Rictor phosphorylation sites reveals direct regulation of mTOR complex 2 by S6K1. Mol Cell Biol *29*, 5657-5670.

Doll, R., and Hill, A. B. (1950). Smoking and carcinoma of the lung; preliminary report. Br Med J *2*, 739-748.

Druker, B. J., Sawyers, C. L., Kantarjian, H., Resta, D. J., Reese, S. F., Ford, J. M., Capdeville, R., and Talpaz, M. (2001). Activity of a specific inhibitor of the BCR-ABL tyrosine kinase in the blast crisis of chronic myeloid leukemia and acute lymphoblastic leukemia with the Philadelphia chromosome. N Engl J Med *344*, 1038-1042.

Ebi, H., Corcoran, R. B., Singh, A., Chen, Z., Song, Y., Lifshits, E., Ryan, D., Meyerhardt, J., Benes, C., Settleman, J*., et al.* (2011). Receptor tyrosine kinases exert dominant control over PI3K signaling in human KRAS mutant colorectal cancers. Journal of Clinical Investigation *in press*.

Egan, D. F., Shackelford, D. B., Mihaylova, M. M., Gelino, S., Kohnz, R. A., Mair, W., Vasquez, D. S., Joshi, A., Gwinn, D. M., Taylor, R*., et al.* Phosphorylation of ULK1 (hATG1) by AMP-activated protein kinase connects energy sensing to mitophagy. Science *331*, 456-461.

Engelman, J. A. (2009). Targeting PI3K signalling in cancer: opportunities, challenges and limitations. Nat Rev Cancer *9*, 550-562.

Engelman, J. A., Chen, L., Tan, X., Crosby, K., Guimaraes, A. R., Upadhyay, R., Maira, M., McNamara, K., Perera, S. A., Song, Y*., et al.* (2008). Effective use of PI3K and MEK inhibitors to treat mutant Kras G12D and PIK3CA H1047R murine lung cancers. Nat Med *14*, 1351-1356.

Engelman, J. A., and Janne, P. A. (2008). Mechanisms of acquired resistance to epidermal growth factor receptor tyrosine kinase inhibitors in non-small cell lung cancer. Clin Cancer Res *14*, 2895-2899.

Engelman, J. A., Janne, P. A., Mermel, C., Pearlberg, J., Mukohara, T., Fleet, C., Cichowski, K., Johnson, B. E., and Cantley, L. C. (2005). ErbB-3 mediates phosphoinositide 3-kinase activity in gefitinib-sensitive non-small cell lung cancer cell lines. Proc Natl Acad Sci U S A *102*, 3788-3793.

Engelman, J. A., Luo, J., and Cantley, L. C. (2006a). The evolution of phosphatidylinositol 3-kinases as regulators of growth and metabolism. Nat Rev Genet *7*, 606-619.

Engelman, J. A., Mukohara, T., Zejnullahu, K., Lifshits, E., Borras, A. M., Gale, C. M., Naumov, G. N., Yeap, B. Y., Jarrell, E., Sun, J*., et al.* (2006b). Allelic dilution obscures detection of a biologically significant resistance mutation in EGFR-amplified lung cancer. J Clin Invest *116*, 2695-2706.

Engelman, J. A., and Settleman, J. (2008). Acquired resistance to tyrosine kinase inhibitors during cancer therapy. Curr Opin Genet Dev *18*, 73-79.

Engelman, J. A., Zejnullahu, K., Gale, C. M., Lifshits, E., Gonzales, A. J., Shimamura, T., Zhao, F., Vincent, P. W., Naumov, G. N., Bradner, J. E*., et al.* (2007a). PF00299804, an irreversible pan-ERBB inhibitor, is effective in lung cancer models with EGFR and ERBB2 mutations that are resistant to gefitinib. Cancer Res *67*, 11924-11932.

Engelman, J. A., Zejnullahu, K., Mitsudomi, T., Song, Y., Hyland, C., Park, J. O., Lindeman, N., Gale, C. M., Zhao, X., Christensen, J., *et al.* (2007b). MET amplification leads to gefitinib resistance in lung cancer by activating ERBB3 signaling. Science *316*, 1039-1043.

Ercan, D., Zejnullahu, K., Yonesaka, K., Xiao, Y., Capelletti, M., Rogers, A., Lifshits, E., Brown, A., Lee, C., Christensen, J. G., *et al.* (2010). Amplification of EGFR T790M causes resistance to an irreversible EGFR inhibitor. Oncogene *29*, 2346-2356.

Faber, A. C., Corcoran, R. B., Ebi, H., Sequist, L., Waltman, B. A., Chung, E., Incio, J., Digumarthy, S., Pollack, S. F., Song, Y., *et al.* (2011). BIM Expression in Treatment-Naive Cancers Predicts Responsiveness to Kinase Inhibitors. Cancer Discovery *4*.

Faber, A. C., Dufort, F. J., Blair, D., Wagner, D., Roberts, M. F., and Chiles, T. C. (2006). Inhibition of phosphatidylinositol 3-kinase-mediated glucose metabolism coincides with resveratrol-induced cell cycle arrest in human diffuse large B-cell lymphomas. Biochem Pharmacol *72*, 1246-1256.

Faber, A. C., Li, D., Song, Y., Liang, M. C., Yeap, B. Y., Bronson, R. T., Lifshits, E., Chen, Z., Maira, S. M., Garcia-Echeverria, C., *et al.* (2009). Differential induction of apoptosis in HER2 and EGFR addicted cancers following PI3K inhibition. Proc Natl Acad Sci U S A *106*, 19503-19508.

Faber, A. C., Wong, K. K., and Engelman, J. A. (2010). Differences underlying EGFR and HER2 oncogene addiction. Cell Cycle *9*, 851-852.

Farber, S., and Diamond, L. K. (1948). Temporary remissions in acute leukemia in children produced by folic acid antagonist, 4-aminopteroyl-glutamic acid. N Engl J Med *238*, 787-793.

Flaherty, K. T., Puzanov, I., Kim, K. B., Ribas, A., McArthur, G. A., Sosman, J. A., O'Dwyer, P. J., Lee, R. J., Grippo, J. F., Nolop, K., and Chapman, P. B. (2010). Inhibition of mutated, activated BRAF in metastatic melanoma. N Engl J Med *363*, 809-819.

Frederick, B. A., Helfrich, B. A., Coldren, C. D., Zheng, D., Chan, D., Bunn, P. A., Jr., and Raben, D. (2007). Epithelial to mesenchymal transition predicts gefitinib resistance in cell lines of head and neck squamous cell carcinoma and non-small cell lung carcinoma. Mol Cancer Ther *6*, 1683-1691.

Fuchs, B. C., Fujii, T., Dorfman, J. D., Goodwin, J. M., Zhu, A. X., Lanuti, M., and Tanabe, K. K. (2008). Epithelial-to-mesenchymal transition and integrin-linked kinase mediate sensitivity to epidermal growth factor receptor inhibition in human hepatoma cells. Cancer Res *68*, 2391-2399.

Gorre, M. E., Mohammed, M., Ellwood, K., Hsu, N., Paquette, R., Rao, P. N., and Sawyers, C. L. (2001). Clinical resistance to STI-571 cancer therapy caused by BCR-ABL gene mutation or amplification. Science *293*, 876-880.

Guertin, D. A., and Sabatini, D. M. (2007). Defining the role of mTOR in cancer. Cancer Cell *12*, 9-22.

Guix, M., Faber, A. C., Wang, S. E., Olivares, M. G., Song, Y., Qu, S., Rinehart, C., Seidel, B., Yee, D., Arteaga, C. L., and Engelman, J. A. (2008). Acquired resistance to EGFR tyrosine kinase inhibitors in cancer cells is mediated by loss of IGF-binding proteins. J Clin Invest *118*, 2609-2619.

Hellman, A., Zlotorynski, E., Scherer, S. W., Cheung, J., Vincent, J. B., Smith, D. I., Trakhtenbrot, L., and Kerem, B. (2002). A role for common fragile site induction in amplification of human oncogenes. Cancer Cell *1*, 89-97.

Hoeflich, K. P., O'Brien, C., Boyd, Z., Cavet, G., Guerrero, S., Jung, K., Januario, T., Savage, H., Punnoose, E., Truong, T.*, et al.* (2009). In vivo antitumor activity of MEK and phosphatidylinositol 3-kinase inhibitors in basal-like breast cancer models. Clin Cancer Res *15*, 4649-4664.

Hofmann, W. K., Komor, M., Wassmann, B., Jones, L. C., Gschaidmeier, H., Hoelzer, D., Koeffler, H. P., and Ottmann, O. G. (2003). Presence of the BCR-ABL mutation Glu255Lys prior to STI571 (imatinib) treatment in patients with Ph+ acute lymphoblastic leukemia. Blood *102*, 659-661.

Hsieh, A. C., and Moasser, M. M. (2007). Targeting HER proteins in cancer therapy and the role of the non-target HER3. Br J Cancer *97*, 453-457.

Huang, C. H., Mandelker, D., Schmidt-Kittler, O., Samuels, Y., Velculescu, V. E., Kinzler, K. W., Vogelstein, B., Gabelli, S. B., and Amzel, L. M. (2007). The structure of a human p110alpha/p85alpha complex elucidates the effects of oncogenic PI3Kalpha mutations. Science *318*, 1744-1748.

Huang, J., and Manning, B. D. (2008). The TSC1-TSC2 complex: a molecular switchboard controlling cell growth. Biochem J *412*, 179-190.

Hubbard, S. R. (2009). The juxtamembrane region of EGFR takes center stage. Cell *137*, 1181-1183.

Ihle, N. T., Lemos, R., Jr., Wipf, P., Yacoub, A., Mitchell, C., Siwak, D., Mills, G. B., Dent, P., Kirkpatrick, D. L., and Powis, G. (2009). Mutations in the phosphatidylinositol-3-kinase pathway predict for antitumor activity of the inhibitor PX-866 whereas oncogenic Ras is a dominant predictor for resistance. Cancer Res *69*, 143-150.

Inoue, A., Suzuki, T., Fukuhara, T., Maemondo, M., Kimura, Y., Morikawa, N., Watanabe, H., Saijo, Y., and Nukiwa, T. (2006). Prospective phase II study of gefitinib for chemotherapy-naive patients with advanced non-small-cell lung cancer with epidermal growth factor receptor gene mutations. J Clin Oncol *24*, 3340-3346.

Inukai, M., Toyooka, S., Ito, S., Asano, H., Ichihara, S., Soh, J., Suehisa, H., Ouchida, M., Aoe, K., Aoe, M.*, et al.* (2006). Presence of epidermal growth

factor receptor gene T790M mutation as a minor clone in non-small cell lung cancer. Cancer Res *66*, 7854-7858.

Janne, P. A., Borras, A. M., Kuang, Y., Rogers, A. M., Joshi, V. A., Liyanage, H., Lindeman, N., Lee, J. C., Halmos, B., Maher, E. A*., et al.* (2006). A rapid and sensitive enzymatic method for epidermal growth factor receptor mutation screening. Clin Cancer Res *12*, 751-758.

Janne, P. A., Schellens, J. H., Engelman, J. A., Eckhardt, S. G., Millham, R., Denis, L. J., Britten, C. D., Wong, S. G., Boss, D. S., and Camidge, D. R. (2008). Preliminary activity and safety results from a phase I clinical trial of PF-00299804, an irreversible pan-HER inhibitor, in patients (pts) with NSCLC. Journal of Clinical Oncology *26*, ASCO #8027.

Jemal, A., Siegel, R., Xu, J., and Ward, E. (2010). Cancer statistics, 2010. CA Cancer J Clin *60*, 277-300.

Jura, N., Endres, N. F., Engel, K., Deindl, S., Das, R., Lamers, M. H., Wemmer, D. E., Zhang, X., and Kuriyan, J. (2009). Mechanism for activation of the EGF receptor catalytic domain by the juxtamembrane segment. Cell *137*, 1293-1307.

Katayama, R., Khan, T. M., Benes, C., Lifshits, E., Ebi, H., Rivera, V. M., Shakespeare, W. C., Iafrate, A. J., Engelman, J. A., and Shaw, A. T. (2011). Therapeutic strategies to overcome crizotinib resistance in non-small cell lung cancers harboring the fusion oncogene EML4-ALK. Proc Natl Acad Sci U S A *108*, 7535-7540.

Kim, D. H., Sarbassov, D. D., Ali, S. M., King, J. E., Latek, R. R., Erdjument-Bromage, H., Tempst, P., and Sabatini, D. M. (2002). mTOR interacts with raptor to form a nutrient-sensitive complex that signals to the cell growth machinery. Cell *110*, 163-175.

Kobayashi, S., Boggon, T. J., Dayaram, T., Janne, P. A., Kocher, O., Meyerson, M., Johnson, B. E., Eck, M. J., Tenen, D. G., and Halmos, B. (2005). EGFR mutation and resistance of non-small-cell lung cancer to gefitinib. N Engl J Med *352*, 786-792.

Kosaka, T., Yatabe, Y., Endoh, H., Yoshida, K., Hida, T., Tsuboi, M., Tada, H., Kuwano, H., and Mitsudomi, T. (2006). Analysis of epidermal growth factor receptor gene mutation in patients with non-small cell lung cancer and acquired resistance to gefitinib. Clin Cancer Res *12*, 5764-5769.

Lee, J. Y., Engelman, J. A., and Cantley, L. C. (2007). Biochemistry. PI3K charges ahead. Science *317*, 206-207.

Li, J., Yen, C., Liaw, D., Podsypanina, K., Bose, S., Wang, S. I., Puc, J., Miliaresis, C., Rodgers, L., McCombie, R*., et al.* (1997). PTEN, a putative protein tyrosine phosphatase gene mutated in human brain, breast, and prostate cancer. Science *275*, 1943-1947.

Li, X., Huang, Y., Jiang, J., and Frank, S. J. (2008). ERK-dependent threonine phosphorylation of EGF receptor modulates receptor downregulation and signaling. Cell Signal *20*, 2145-2155.

Ludovini, V., Bianconi, F., Pistola, L., Chiari, R., Minotti, V., Colella, R., Giuffrida, D., Tofanetti, F. R., Siggillino, A., Flacco, A.*, et al.* (2011). Phosphoinositide-3-kinase catalytic alpha and KRAS mutations are important predictors of resistance to therapy with epidermal growth factor receptor tyrosine kinase inhibitors in patients with advanced non-small cell lung cancer. J Thorac Oncol *6*, 707-715.

Lynch, T. J., Bell, D. W., Sordella, R., Gurubhagavatula, S., Okimoto, R. A., Brannigan, B. W., Harris, P. L., Haserlat, S. M., Supko, J. G., Haluska, F. G.*, et al.* (2004). Activating mutations in the epidermal growth factor receptor underlying responsiveness of non-small-cell lung cancer to gefitinib. N Engl J Med *350*, 2129-2139.

Maehama, T., and Dixon, J. E. (1998). The tumor suppressor, PTEN/MMAC1, dephosphorylates the lipid second messenger, phosphatidylinositol 3,4,5-trisphosphate. J Biol Chem *273*, 13375-13378.

Maheswaran, S., Sequist, L. V., Nagrath, S., Ulkus, L., Brannigan, B., Collura, C. V., Inserra, E., Diederichs, S., Iafrate, A. J., Bell, D. W.*, et al.* (2008). Detection of mutations in EGFR in circulating lung-cancer cells. N Engl J Med *359*, 366-377.

Malumbres, M., and Barbacid, M. (2003). RAS oncogenes: the first 30 years. Nat Rev Cancer *3*, 459-465.

Manning, B. D., and Cantley, L. C. (2007). AKT/PKB signaling: navigating downstream. Cell *129*, 1261-1274.

McDermott, U., Sharma, S. V., Dowell, L., Greninger, P., Montagut, C., Lamb, J., Archibald, H., Raudales, R., Tam, A., Lee, D.*, et al.* (2007). Identification of genotype-correlated sensitivity to selective kinase inhibitors by using high-throughput tumor cell line profiling. Proc Natl Acad Sci U S A *104*, 19936-19941.

Miller, C. T., Lin, L., Casper, A. M., Lim, J., Thomas, D. G., Orringer, M. B., Chang, A. C., Chambers, A. F., Giordano, T. J., Glover, T. W., and Beer, D. G. (2006). Genomic amplification of MET with boundaries within fragile site FRA7G and upregulation of MET pathways in esophageal adenocarcinoma. Oncogene *25*, 409-418.

Mirzoeva, O. K., Das, D., Heiser, L. M., Bhattacharya, S., Siwak, D., Gendelman, R., Bayani, N., Wang, N. J., Neve, R. M., Guan, Y.*, et al.* (2009). Basal subtype and MAPK/ERK kinase (MEK)-phosphoinositide 3-kinase feedback signaling determine susceptibility of breast cancer cells to MEK inhibition. Cancer Res *69*, 565-572.

Mok, T., Wu, Y., and Thongprasert, S. (2008). Phase III, randomized, open label, first-line study of gefitinib vs. carboplatin/paclitaxel in clinically selected patients with advanced non-small cell lung cancer (IPASS). Annals of Oncology *19*.

Montagut, C., and Settleman, J. (2009). Targeting the RAF-MEK-ERK pathway in cancer therapy. Cancer Lett *283*, 125-134.

Mukherjee, S. (2010). The Emperor of All Maladies, (New York: Scribner).

Mukohara, T., Engelman, J. A., Hanna, N. H., Yeap, B. Y., Kobayashi, S., Lindeman, N., Halmos, B., Pearlberg, J., Tsuchihashi, Z., Cantley, L. C.*, et al.* (2005). Differential effects of gefitinib and cetuximab on non-small-cell lung cancers bearing epidermal growth factor receptor mutations. J Natl Cancer Inst *97*, 1185-1194.

Northwood, I. C., Gonzalez, F. A., Wartmann, M., Raden, D. L., and Davis, R. J. (1991). Isolation and characterization of two growth factor-stimulated protein kinases that phosphorylate the epidermal growth factor receptor at threonine 669. J Biol Chem *266*, 15266-15276.

O'Brien, C., Wallin, J. J., Sampath, D., Guhathakurta, D., Savage, H., Punnoose, E. A., Guan, J., Berry, L., Prior, W. W., Amler, L. C.*, et al.* (2010). Predictive Biomarkers of Sensitivity to the Phosphatidylinositol 3' Kinase Inhibitor GDC-0941 In Breast Cancer Preclinical Models. Clin Cancer Res.

O'Hare, T., Shakespeare, W. C., Zhu, X., Eide, C. A., Rivera, V. M., Wang, F., Adrian, L. T., Zhou, T., Huang, W. S., Xu, Q.*, et al.* (2009). AP24534, a pan-BCR-ABL inhibitor for chronic myeloid leukemia, potently inhibits the T315I mutant and overcomes mutation-based resistance. Cancer Cell *16*, 401-412.

O'Reilly, K. E., Rojo, F., She, Q. B., Solit, D., Mills, G. B., Smith, D., Lane, H., Hofmann, F., Hicklin, D. J., Ludwig, D. L.*, et al.* (2006). mTOR inhibition induces upstream receptor tyrosine kinase signaling and activates Akt. Cancer Res *66*, 1500-1508.

Ogino, A., Kitao, H., Hirano, S., Uchida, A., Ishiai, M., Kozuki, T., Takigawa, N., Takata, M., Kiura, K., and Tanimoto, M. (2007). Emergence of epidermal growth factor receptor T790M mutation during chronic exposure to gefitinib in a non small cell lung cancer cell line. Cancer Res *67*, 7807-7814.

Ono, M., Hirata, A., Kometani, T., Miyagawa, M., Ueda, S., Kinoshita, H., Fujii, T., and Kuwano, M. (2004). Sensitivity to gefitinib (Iressa, ZD1839) in non-small cell lung cancer cell lines correlates with dependence on the epidermal growth factor (EGF) receptor/extracellular signal-regulated kinase 1/2 and EGF receptor/Akt pathway for proliferation. Mol Cancer Ther *3*, 465-472.

Paez, J. G., Janne, P. A., Lee, J. C., Tracy, S., Greulich, H., Gabriel, S., Herman, P., Kaye, F. J., Lindeman, N., Boggon, T. J.*, et al.* (2004). EGFR mutations in lung cancer: correlation with clinical response to gefitinib therapy. Science *304*, 1497-1500.

Pao, W., Miller, V., Zakowski, M., Doherty, J., Politi, K., Sarkaria, I., Singh, B., Heelan, R., Rusch, V., Fulton, L.*, et al.* (2004). EGF receptor gene mutations are common in lung cancers from "never smokers" and are associated with sensitivity of tumors to gefitinib and erlotinib. Proc Natl Acad Sci U S A *101*, 13306-13311.

Pao, W., Miller, V. A., Politi, K. A., Riely, G. J., Somwar, R., Zakowski, M. F., Kris, M. G., and Varmus, H. (2005). Acquired resistance of lung adenocarcinomas to gefitinib or erlotinib is associated with a second mutation in the EGFR kinase domain. PLoS Med *2*, e73.

Parada, L. F., Tabin, C. J., Shih, C., and Weinberg, R. A. (1982). Human EJ bladder carcinoma oncogene is homologue of Harvey sarcoma virus ras gene. Nature *297*, 474-478.

Paz-Ares, L., Sanchez, J., Garcia-Velasco, A., Massuti, B., Lopez-Vivanco, G., Provencio, M., Montes, A., Isla, D., Amador, M. L., and Rossel, R. (2006). A prospective phase II trial of erlotinib in advanced non-small cell lung cancer (NSCLC) patients (p) with mutations in the tyrosine kinase (TK) domain of the epidermal growth factor receptor (EGFR). Journal of Clinical Oncology *24*, ASCO #7020.

Red Brewer, M., Choi, S. H., Alvarado, D., Moravcevic, K., Pozzi, A., Lemmon, M. A., and Carpenter, G. (2009). The juxtamembrane region of the EGF receptor functions as an activation domain. Mol Cell *34*, 641-651.

Rho, J. K., Choi, Y. J., Lee, J. K., Ryoo, B. Y., Na, II, Yang, S. H., Kim, C. H., and Lee, J. C. (2009). Epithelial to mesenchymal transition derived from repeated exposure to gefitinib determines the sensitivity to EGFR inhibitors in A549, a non-small cell lung cancer cell line. Lung Cancer *63*, 219-226.

Riely, G. J. (2008). Second-generation epidermal growth factor receptor tyrosine kinase inhibitors in non-small cell lung cancer. J Thorac Oncol *3*, S146-149.

Roche-Lestienne, C., Lai, J. L., Darre, S., Facon, T., and Preudhomme, C. (2003). A mutation conferring resistance to imatinib at the time of diagnosis of chronic myelogenous leukemia. N Engl J Med *348*, 2265-2266.

Roche-Lestienne, C., Soenen-Cornu, V., Grardel-Duflos, N., Lai, J. L., Philippe, N., Facon, T., Fenaux, P., and Preudhomme, C. (2002). Several types of mutations of the Abl gene can be found in chronic myeloid leukemia patients resistant to STI571, and they can pre-exist to the onset of treatment. Blood *100*, 1014-1018.

Rothenberg, S. M., Engelman, J. A., Le, S., Riese, D. J., 2nd, Haber, D. A., and Settleman, J. (2008). Modeling oncogene addiction using RNA interference. Proc Natl Acad Sci U S A *105*, 12480-12484.

Rusch, V., Baselga, J., Cordon-Cardo, C., Orazem, J., Zaman, M., Hoda, S., McIntosh, J., Kurie, J., and Dmitrovsky, E. (1993). Differential expression of

the epidermal growth factor receptor and its ligands in primary non-small cell lung cancers and adjacent benign lung. Cancer Res *53*, 2379-2385.

Samuels, Y., Wang, Z., Bardelli, A., Silliman, N., Ptak, J., Szabo, S., Yan, H., Gazdar, A., Powell, S. M., Riggins, G. J*., et al.* (2004). High frequency of mutations of the PIK3CA gene in human cancers. Science *304*, 554.

Schellens, J. H., Britten, C. D., Camidge, D. R., Boss, D., Wong, S., Diab, S., Guo, F., Maguire, R. P., Letrent, S. P., and Eckhardt, S. G. (2007). First-in-human study of the safety, tolerability, pharmacokinetics (PK), and pharmacodynamics (PD) of PF-00299804, a small molecule irreversible pan-HER inhibitor in patients with advanced cancer. Journal of Clinical Oncology *25*, ASCO #3599.

Schoeberl, B., Faber, A. C., Li, D., Liang, M. C., Crosby, K., Onsum, M., Burenkova, O., Pace, E., Walton, Z., Nie, L*., et al.* (2010). An ErbB3 antibody, MM-121, is active in cancers with ligand-dependent activation. Cancer Res *70*, 2485-2494.

Sequist, L. V., Martins, R. G., Spigel, D., Grunberg, S. M., Spira, A., Janne, P. A., Joshi, V. A., McCollum, D., Evans, T. L., Muzikansky, A*., et al.* (2008). First-line gefitinib in patients with advanced non-small-cell lung cancer harboring somatic EGFR mutations. J Clin Oncol *26*, 2442-2449.

Sequist, L. V., Waltman, B. A., Dias-Santagata, D., Digumarthy, S., Turke, A. B., Fidias, P., Bergethon, K., Shaw, A. T., Gettinger, S., Cosper, A. K*., et al.* (2011). Genotypic and histological evolution of lung cancers acquiring resistance to EGFR inhibitors. Sci Transl Med *3*, 75ra26.

Serra, V., Markman, B., Scaltriti, M., Eichhorn, P. J., Valero, V., Guzman, M., Botero, M. L., Llonch, E., Atzori, F., Di Cosimo, S*., et al.* (2008). NVP-BEZ235, a dual PI3K/mTOR inhibitor, prevents PI3K signaling and inhibits the growth of cancer cells with activating PI3K mutations. Cancer Res *68*, 8022-8030.

Serra, V., Scaltriti, M., Prudkin, L., Eichhorn, P. J., Ibrahim, Y. H., Chandarlapaty, S., Markman, B., Rodriguez, O., Guzman, M., Rodriguez, S*., et al.* (2011). PI3K inhibition results in enhanced HER signaling and acquired ERK dependency in HER2-overexpressing breast cancer. Oncogene *30*, 2547-2557.

Shah, N. P., Kasap, C., Weier, C., Balbas, M., Nicoll, J. M., Bleickardt, E., Nicaise, C., and Sawyers, C. L. (2008). Transient potent BCR-ABL inhibition is sufficient to commit chronic myeloid leukemia cells irreversibly to apoptosis. Cancer Cell *14*, 485-493.

Shah, N. P., Nicoll, J. M., Nagar, B., Gorre, M. E., Paquette, R. L., Kuriyan, J., and Sawyers, C. L. (2002). Multiple BCR-ABL kinase domain mutations confer polyclonal resistance to the tyrosine kinase inhibitor imatinib (STI571) in chronic phase and blast crisis chronic myeloid leukemia. Cancer Cell *2*, 117-125.

Sharma, S. V., Bell, D. W., Settleman, J., and Haber, D. A. (2007). Epidermal growth factor receptor mutations in lung cancer. Nat Rev Cancer *7*, 169-181.

She, Q. B., Chandarlapaty, S., Ye, Q., Lobo, J., Haskell, K. M., Leander, K. R., DeFeo-Jones, D., Huber, H. E., and Rosen, N. (2008). Breast tumor cells with PI3K mutation or HER2 amplification are selectively addicted to Akt signaling. PLoS One *3*, e3065.

Shih, C., and Weinberg, R. A. (1982). Isolation of a transforming sequence from a human bladder carcinoma cell line. Cell *29*, 161-169.

Slamon, D. J., Clark, G. M., Wong, S. G., Levin, W. J., Ullrich, A., and McGuire, W. L. (1987). Human breast cancer: correlation of relapse and survival with amplification of the HER-2/neu oncogene. Science *235*, 177-182.

Smolen, G. A., Sordella, R., Muir, B., Mohapatra, G., Barmettler, A., Archibald, H., Kim, W. J., Okimoto, R. A., Bell, D. W., Sgroi, D. C*., et al.* (2006). Amplification of MET may identify a subset of cancers with extreme sensitivity to the selective tyrosine kinase inhibitor PHA-665752. Proc Natl Acad Sci U S A *103*, 2316-2321.

Solit, D. B., Garraway, L. A., Pratilas, C. A., Sawai, A., Getz, G., Basso, A., Ye, Q., Lobo, J. M., She, Y., Osman, I*., et al.* (2006). BRAF mutation predicts sensitivity to MEK inhibition. Nature *439*, 358-362.

Stehelin, D., Varmus, H. E., Bishop, J. M., and Vogt, P. K. (1976). DNA related to the transforming gene(s) of avian sarcoma viruses is present in normal avian DNA. Nature *260*, 170-173.

Takishima, K., Griswold-Prenner, I., Ingebritsen, T., and Rosner, M. R. (1991). Epidermal growth factor (EGF) receptor T669 peptide kinase from 3T3-L1 cells is an EGF-stimulated "MAP" kinase. Proc Natl Acad Sci U S A *88*, 2520-2524.

Tamura, K., Okamoto, I., Kashii, T., Negoro, S., Hirashima, T., Kudoh, S., Ichinose, Y., Ebi, N., Shibata, K., Nishimura, T*., et al.* (2008). Multicentre prospective phase II trial of gefitinib for advanced non-small cell lung cancer with epidermal growth factor receptor mutations: results of the West Japan Thoracic Oncology Group trial (WJTOG0403). Br J Cancer *98*, 907-914.

Thomson, S., Buck, E., Petti, F., Griffin, G., Brown, E., Ramnarine, N., Iwata, K. K., Gibson, N., and Haley, J. D. (2005). Epithelial to mesenchymal transition is a determinant of sensitivity of non-small-cell lung carcinoma cell lines and xenografts to epidermal growth factor receptor inhibition. Cancer Res *65*, 9455-9462.

Turke, A. B., and Engelman, J. A. (2010). PIKing the right patient. Clin Cancer Res *16*, 3523-3525.

Turke, A. B., Zejnullahu, K., Wu, Y. L., Song, Y., Dias-Santagata, D., Lifshits, E., Toschi, L., Rogers, A., Mok, T., Sequist, L*., et al.* (2010). Preexistence and

clonal selection of MET amplification in EGFR mutant NSCLC. Cancer Cell *17*, 77-88.

Wong, K. K., Engelman, J. A., and Cantley, L. C. (2010). Targeting the PI3K signaling pathway in cancer. Curr Opin Genet Dev *20*, 87-90.

Wynder, E. L., and Graham, E. A. (1950). Tobacco smoking as a possible etiologic factor in bronchiogenic carcinoma; a study of 684 proved cases. J Am Med Assoc *143*, 329-336.

Yamasaki, F., Johansen, M. J., Zhang, D., Krishnamurthy, S., Felix, E., Bartholomeusz, C., Aguilar, R. J., Kurisu, K., Mills, G. B., Hortobagyi, G. N., and Ueno, N. T. (2007). Acquired resistance to erlotinib in A-431 epidermoid cancer cells requires down-regulation of MMAC1/PTEN and up-regulation of phosphorylated Akt. Cancer Res *67*, 5779-5788.

Yang, X., Turke, A. B., Qi, J., Song, Y., Rexer, B. N., Miller, T. W., Janne, P. A., Arteaga, C. L., Cantley, L. C., Engelman, J. A., and Asara, J. M. (2011). Using Tandem Mass Spectrometry in Targeted Mode to Identify Activators of Class IA PI3K in Cancer. Cancer Res.

Yano, S., Wang, W., Li, Q., Matsumoto, K., Sakurama, H., Nakamura, T., Ogino, H., Kakiuchi, S., Hanibuchi, M., Nishioka, Y.*, et al.* (2008). Hepatocyte growth factor induces gefitinib resistance of lung adenocarcinoma with epidermal growth factor receptor-activating mutations. Cancer Res *68*, 9479-9487.

Yeh, T. C., Marsh, V., Bernat, B. A., Ballard, J., Colwell, H., Evans, R. J., Parry, J., Smith, D., Brandhuber, B. J., Gross, S.*, et al.* (2007). Biological characterization of ARRY-142886 (AZD6244), a potent, highly selective mitogen-activated protein kinase kinase 1/2 inhibitor. Clin Cancer Res *13*, 1576-1583.

Yoon, Y. K., Kim, H. P., Han, S. W., Hur, H. S., Oh do, Y., Im, S. A., Bang, Y. J., and Kim, T. Y. (2009). Combination of EGFR and MEK1/2 inhibitor shows synergistic effects by suppressing EGFR/HER3-dependent AKT activation in human gastric cancer cells. Mol Cancer Ther *8*, 2526-2536.

Yun, C. H., Mengwasser, K. E., Toms, A. V., Woo, M. S., Greulich, H., Wong, K. K., Meyerson, M., and Eck, M. J. (2008). The T790M mutation in EGFR kinase causes drug resistance by increasing the affinity for ATP. Proc Natl Acad Sci U S A *105*, 2070-2075.

Zhang, H., Berezov, A., Wang, Q., Zhang, G., Drebin, J., Murali, R., and Greene, M. I. (2007). ErbB receptors: from oncogenes to targeted cancer therapies. J Clin Invest *117*, 2051-2058.

Zhao, L., and Vogt, P. K. (2008). Helical domain and kinase domain mutations in p110alpha of phosphatidylinositol 3-kinase induce gain of function by different mechanisms. Proc Natl Acad Sci U S A *105*, 2652-2657.

Zheng, B., Jeong, J. H., Asara, J. M., Yuan, Y. Y., Granter, S. R., Chin, L., and Cantley, L. C. (2009). Oncogenic B-RAF negatively regulates the tumor suppressor LKB1 to promote melanoma cell proliferation. Mol Cell *33*, 237-247.

Zhou, W., Ercan, D., Chen, L., Yun, C. H., Li, D., Capelletti, M., Cortot, A. B., Chirieac, L., Iacob, R. E., Padera, R.*, et al.* (2009). Novel mutant-selective EGFR kinase inhibitors against EGFR T790M. Nature *462*, 1070-1074.

Zhou, W., Ercan, D., Janne, P. A., and Gray, N. S. (2011). Discovery of selective irreversible inhibitors for EGFR-T790M. Bioorg Med Chem Lett *21*, 638-643.

Zou, H. Y., Li, Q., Lee, J. H., Arango, M. E., McDonnell, S. R., Yamazaki, S., Koudriakova, T. B., Alton, G., Cui, J. J., Kung, P. P.*, et al.* (2007). An orally available small-molecule inhibitor of c-Met, PF-2341066, exhibits cytoreductive antitumor efficacy through antiproliferative and antiangiogenic mechanisms. Cancer Res *67*, 4408-4417.